Thesis report 2011

Candidate:

Behzad Rahimi Sharefi

Title:

Modeling for Control of Hydropower Systems

Telemark University College
 Faculty of Technology
Kjølnes
3914 Porsgrunn
Norway

Telemark University College
Faculty of Technology
M.Sc. Programme

THESIS FMH606

Students: **Behzad Rahimi Sharefi**

Project title: **Modeling for Control of Hydropower Systems**

Signatures: . . . . . .

Number of pages: **172**

Keywords: **Hydropower, Hydroelectricity, Water Hammer, Finite Volumes Method, Simulation and Modeling of Dynamic Systems, Power System Dynamics**

Supervisor: **Bernt Lie** sign.: . . . . . .

2nd Supervisor: sign.: . . . . . .

Censor: sign.: . . . . . .

External partner: sign.: . . . . . .

Availability: Open

Archive approval (supervisor signature)**:** sign.: . . . . . **Date :** . . . . . .

Abstract:

Modeling of a high-head hydropower generation unit is considered in this work. It's been shown how to use the "Finite Volume Method" and MATLAB to simulate the behavior of a penstock when elasticity of the penstock walls and compressibility of the water is taken into account. The best options for the ODE solver which is used in MATLAB are examined. Then the simulation model thus obtained is validated using available charts for pressure rise in case of uniform gate closure. Available models for the other parts of the waterway (inelastic) are extended to include an interface to the elastic penstock model. It's shown how to input the data from performance charts of Francis turbines into MATLAB and develop an interpolation function. The whole waterway model (with both elastic and inelastic penstock sub-models) is simulated in MATLAB using a classic controller for a given time-varying active-power-consuming turbine load. Simulation is also carried out with constant turbine load and time varying reference signal for the guide vanes opening. Models for the synchronous generator is studied and applied to the whole hydropower generation unit considering the inelastic penstock model. Synchronous operation of the hydropower generation unit is then simulated when generator is connected to an infinite bus.

Table of Contents

List of Figures and Tables

Preface

I would like to thank Professor Bernt Lie, Professor Bjørn Glemmestad and Wenjing Zhou for their help and support during this work. Part of the work in Chapter 3 is done with help and cooperation of Wenjing Zhou.

Due to the lack of complete data from real plants, validation of simulations in this work was not possible by comparing to real plant operations data. However in the simulations of the water hammer effect, the amounts of pressure rises were compared to the charts available in the literature. Due to the lack of time, implementing of an advanced controller which had been considered as an option in the thesis task description was not possible. However model of a classic controller was used to simulate the whole plant.

Nomenclature

Symbol	Description	Units
$\dot{m}$	Mass flow rate	[Kg/sec]
p	Pressure	[Pa]
P	Index referring to the penstock	
L_P	Penstock length	[m]
A_P	Cross-section area of penstock with inelastic walls (constant through the whole length of the penstock)	$[m^2]$
p_i	Water pressure along the penstock at location $X = X_i$	[Pa]
ρ_i	Water density along the penstock at location $X = X_i$ as a function of pressure p_i	$[Kg/m^3]$
$A_{P,i}$	Cross-section area of penstock with elastic walls at location $X = X_i$ as a function of water pressure p_i inside the penstock at that location.	$[m^2]$
A_P^{atm}	Cross-section area of penstock with elastic walls when pressure inside and outside of the penstock is equal to atmospheric pressure, i.e. empty penstock (constant through the whole length of the penstock)	$[m^2]$
p^{atm}	Atmospheric pressure	[Pa]
ρ^{atm}	Water density at atmospheric pressure	$[Kg/m^3]$
CV_{2i+1}	Control volume enclosed between penstock cross-sections at	$[m^3]$

Symbol	Description	Units
	locations X_{2i} and X_{2i+2} for applying mass conservation rule (for i=1,…,N-1)	
CV_{2i+2}	Control volume enclosed between penstock cross-sections at locations X_{2i+1} and X_{2i+3} for applying momentum conservation rule (for i=1,…,N-1)	$[m^3]$
V	Volume	$[m^3]$
HWDI	Index referring to the interface variables between elastic penstock and head water system. "HW" refers to head water, "D" refers to "at downstream of HW" and "I" indicates that the variable is **an input to HW system**.	
HWDO	Index referring to the interface variables between elastic penstock and head water system. "HW" refers to head water, "D" refers to "at downstream of HW" and "I" indicates that the variable is **an output from the HW system**.	
TWUI	Index referring to the interface variables between elastic penstock and tail water system. "TW" refers to tail water, "U" refers to "at the upstream of TW" and "I" indicates that the variable is **an input to TW system**.	
TWUO	Index referring to the interface variables between elastic penstock and tail water system. "TW" refers to tail water, "U" refers to "at the upstream of TW" and "I" indicates that the variable is **an output from the TW system**.	
β_P^{total}	total compressibility due to water compressibility and pipe shell elasticity	$[Pa^{-1}]$

Symbol	Description	Units
β_P^{eq}	equivalent compressibility due to the pipe shell elasticity	$[Pa^{-1}]$
β	Compressibility of water	$[Pa^{-1}]$
$\dot{m}_{P,i}$	Mass flow rate through a cross-section of penstock at location $X = X_i$ (in direction of increasing "i" or simply X direction.)	$[Kg/sec]$
$v_{P,i}$	Velocity of water along penstock wall at location $X = X_i$ (in direction of increasing "i" or simply X direction.)	$[m/sec]$
$F_{p,2i+2}$	The force acting on the water column inside the control volume CV_{2i+2} due to pressure difference at both ends	[N]
$F_{G,2i+2}$	The gravity force acting on the water column inside the control volume CV_{2i+2}	[N]
$F_{F,2i+2}$	The friction force acting on the water column inside the control volume CV_{2i+2}	[N]
ξ_{2i+2}	A friction factor. Friction force applying on the control volume CV_{2i+2} is given by $\xi_{2i+2}v_{P,2i+2}$	[N.sec/m]
f	Fanning friction factor	[-]
$\Pi_{P,2i+2}$	Internal perimeter of the penstock cross section at $X = X_{2i+2}$	[m]
P_t^h	Hydraulic power available for conversion by turbine	[W]
$\dot{m}_t$	Mass flow rate of water through turbine	[Kg/sec]
Δp_t	Pressure drop across turbine inlet and outlet	[Pa]
P_t^m	Mechanical output power of the turbine	[W]

Symbol	Description	Units
η_t	Efficiency of the turbine	[-]
H_n (H_t)	Turbine head	[m] or [%]
Q_t	Turbine volumetric discharge	$[m^3/sec]$ or [%]
Y_{GV}	Guide vanes opening	[% or degrees]
ω_m	Turbine mechanical rotation speed	$[rad/sec]$
N_s	Turbine Specific Speed	[-]
N_{td}	Turbine design speed	[rpm]
ω_m^{design}	Turbine design speed	[Rad/sec]
P_{td}	Turbine design power	[kW]
H_{td}	Turbine design head	[m]
η_{td}	Turbine efficiency at design head and rated power and discharge	[-]
H^{eq} and Q^{e}	Equivalent head and discharge as defined in Section 2.2.2	[m] and $[m^3/sec]$
H	Head (in some cases through the report is used as values of turbine head)	[m]
Q	Volumetric flow rate (in some cases through the report is used as values of turbine discharge)	$[m^3/sec]$
C	Index indicating that property belongs to conduit	

Symbol	Description	Units
S	Index indicating that property belongs to surge shaft	
lS	Length of the water column in the surge shaft	[m]
a, b, c	Index which refers to one of the stator coils	[-]
F, D, Q	Index which refers to one of the rotor coils. "F" is the coil in which the field (magnetizing) current flows. "D" and "Q" are the damper windings.	[-]
L_x	Self-inductance of the coil "x" where x refers to one of the indices a, b, c, F, D and Q.	[H]
L_{xy}	Mutual inductance between the "x" and "y" coils where x and y refer to the indices a, b, c, F, D and Q. The equality $L_{xy} = L_{yx}$ always holds.	[H]
n_P	Number of the poles of the generator	[-]
f_m	Rotation frequency of the rotor	[Hz]
f_e	Frequency of induced voltage in the stator coils ($f_e = N_P f_m/2$)	[Hz]
ω_m	Rotor rotation angular speed ($\omega_m = 2\pi f_m$)	[rad/sec]
ω_e	Angular speed of the induced voltage in the stator coils ($\omega_e = 2\pi f_e$)	[rad/sec]
θ_m and θ_e	The rotor angle $\theta_r(t) = \omega_r t + \theta_r(0)$ is the rotor position measured in a reference frame fixed to the stator. The rotor electrical angle $\theta_e(t)$ is defined by $\theta_e(t) = \omega_e t + \theta_e(0) = N_P\theta_m(t)/2$. The initial angle $\theta_r(0)$ depends on the measuring	[rad]

Symbol	Description	Units
	points on the rotor and the stator and is usually chosen in such a way that the open circuit terminal voltage of the "a" stator coils becomes proportional to $\sin\theta_e(t)$.	
L_S	Average value of any of the quantities L_a , L_b and L_c taken over the rotor electrical angle (θ_e) values between 0 and π [rad].	[H]
M_S	Absolute value of the average of any of the quantities L_{ab}, L_{ac} and L_{bc} taken over the rotor electrical angle (θ_e) values between 0 and π [rad].	[H]
L_M	Absolute value of maximum deviation of any of the quantities L_a , L_b , L_c , L_{ab}, L_{ac} and L_{bc} from their average value when the rotor electrical angle (θ_e) varies between 0 and π [rad].	[H]
M_F	Absolute value of maximum of any of the quantities L_{aF} , L_{bF} , L_{cF} when the rotor electrical angle (θ_e) varies between 0 and 2π [rad].	[H]
M_D	Absolute value of maximum of any of the quantities L_{aD} , L_{bD} , L_{cD} when the rotor electrical angle (θ_e) varies between 0 and 2π [rad].	[H]
M_Q	Absolute value of maximum of any of the quantities L_{aQ} , L_{bQ} , L_{cQ} when the rotor electrical angle (θ_e) varies between 0 and 2π [rad].	[H]

Chapter 1 Introduction

1.1 Background

Hydropower systems are extensively studied in the literature. Some of the literature in this field or at least some of their references dates back at 1920's. In 1992 IEEE published a paper in which various models for hydropower generation units existing at that time was gathered in one place (IEEE, 1992). An enormous effort has been taken recently for advanced modeling, optimization and control of hydropower production units (Kishor, 2007).

A high head hydropower generation unit typically consists of reservoir, waterway (head-race tunnel, surge shaft, penstock, turbine case and draft tube, and tale-race), turbine, and generator. The overall system is highly non-linear and its controller is usually designed for stability and best performance at the best-efficiency operating point using a linearized model. For having a stable operation and acceptable performance at the other operating points it may be necessary to change the controller parameters when the operating point of the system changes.

It is important to be able to model and simulate the system as accurately as possible. With an accurate model, a designed controller can be tested more reliably for stability and performance in different operating points. Different models with different degrees of complexity have been published (Kishor, 2007). The simple models consider rigid penstock walls with incompressible water column in the penstock. A more accurate model can be obtained if a penstock with elastic walls and compressible water column in the penstock is considered. Such a penstock can be modeled by two nonlinear partial differential equations. These equations can be linearized and solved by the Method of Characteristics (MOC) (Warnick, 1984). Numerical methods can also be used for solving these equations. Some software solutions such as WHAMO (WHAMO, 1998) and Hydro-Plant Library (Modelon, 2010) are available for numerical simulations.

In Telemark University College a research group is established to study around hydropower. In this direction some projects and theses are defined and done previously like (Shresta, 2010) and (Thoresen, 2010). A Phd student is currently working on the subject of modeling and control of hydropower plants. This Thesis is also about the modeling of the hydropower systems.

1.2 Task Description

The complete task description of this thesis is included in the Appendix I. For fulfillment of the tasks, a complete model for the hydropower generation unit is introduced which takes the compressibility of the water and elasticity of the penstock walls into account. It is shown how to enter data available in the performance charts of the Francis turbine into MATLAB and make an interpolation function for estimation of the turbine head and efficiency. The penstock model is validated by the charts available in the literature. A classic controller is used to show the closed loop operation of the introduced models and finally it is shown how to include the synchronous generator with voltage control loop in the overall model and simulate the whole system. (Due to lack of time the generator is only simulated with the inelastic model)

Due to the lack of complete data from real plants, validation of simulations in this work was not possible by comparing to real plant operations data. Also because of time shortage, implementing of an advanced controller which had been considered as an option in the thesis task description was not possible.

1.3 Structure of the report

The report has two main chapters:

Chapter 1 includes the models and simulations of the hydraulic system. In Section 2.1 penstock model with considering compressibility and elasticity effects has been studied. In section 2.2 Francis turbine, similarity laws and turbine performance charts are discussed. In Section 2.3 models available for other parts of the waterway are extended to include an interface part to elastic penstock. In Section 2.4 a classic controller is introduced to use with closed loop simulations. In Section 2.5.1 the elastic penstock model is validated against available charts and finally in Section 2.5.2 the closed loop system (without generator) is simulated for both cases of the waterway with an inelastic penstock and the waterway with elastic penstock. (Elastic penstock in this report refers to the model of penstock with considering water compressibility and elasticity of penstock walls.)

Chapter 3 is devoted to study of the synchronous generator. In sections 3.1.1 to 3.1.3 structure of a multi-pole salient poles generator is discussed. In section 3.1.4 the self and mutual inductances of various windings in the machine are studied. Sections 3.1.5 to 3.1.7 the Park's transform and machine equations in the rotor reference frame are discussed. The power term in the swing

equation which is relevant to the generator active power is discussed in Section 3.1.8. In Sections 3.1.9 to 3.1.11 available simplified models for the synchronous generator are introduced and it is shown how to relate the variables of these models to the network variables through the “phasors” concept. Finally a generator connected to an infinite bus is simulated with the waterway model (without elasticity).

Relevant simulations and discussions necessary for each chapter are included in the same chapter. No separate results chapter is included. Only a short conclusion will be given in the Chapter 4.

MATLAB code of the simulations in this report is included in the Appendix III.

Chapter 2 The Hydraulic System

The hydraulic system in a high-head hydropower plant will be modeled in this chapter. This system consists of all the components in the waterway plus the turbine and its auxiliaries. The interface of this system with the electrical parts of the plant is the turbine-generator shaft. The turbine-generator shaft rotating speed and the mechanical output power of the turbine are the quantities which are needed to be controlled within this system. However measurement of the turbine mechanical output power is easier if it's done indirectly by measuring the electric active power delivered at the generator terminals and dividing it by the generator efficiency or alternatively, by estimation given the guide vanes opening and the current gross head of the plant.

Governing equations for water flow inside the tunnels and pipes (head-water, penstock and tail-water) are an important part of the hydraulic system model. In the Section 2.1 a general model for the penstock will be derived. This model assumes compressible water and elastic penstock walls. Models for the head-water and tail-water tunnels and surge-shaft are similar to the penstock but usually there's no need to consider compressible water and elastic walls for these models due to the lower pressures. Simpler model for the penstock is also available by neglecting the compressibility and elasticity effects. Models for Francis turbine are discussed in the section 2.2. In the section 2.3 differential equations governing the whole head-water system (reservoir, head-water tunnel, surge-shaft and an interface part to the elastic penstock model) and the whole tail-water system (interface to the elastic penstock model, turbine, draft tube, tail-water tunnel and reservoir) will be summarized. The turbine controller model which will be used for simulations throughout this report is given in the section 2.4. Finally in the section 2.5 simulation results of the hydraulic system, with turbine output mechanical power considered as a constant disturbance, for the both cases of elastic penstock and inelastic penstock will be included.

2.1 General Penstock Model

2.1.1 Introduction

Having a model for hydropower station which is as complete as possible is very important. It's true because simulation of the controller performance in a wide range of operating points becomes possible. For this purpose all the nonlinearities, delays and dominant higher order effects (like higher order differential equations) shall be considered in the model. In this section a model for the penstock will be derived which considers effects of compressibility of the water and elasticity of penstock walls. "Finite volume method" (Versteeg & Malalasekera, 1995) of computational fluid dynamics (CFD) will be used to derive a set of ordinary differential equations as the penstock model.

2.1.2 Problem Definition

Compressible water flow inside a penstock with elastic walls is governed by a partial differential equation (Warnick, 1984) (Lie, 2011). This PDE is obtained by applying the mass and momentum conservation laws to a 1D infinitely small control volume along the penstock axis. (Parmakian, 1963). Solving such equation numerically needs both temporal and spatial discretization. Software such as WHAMO (US Army Corps of Engineers, 1998) which is a tool for simulation of water flow in pipe networks uses a finite difference scheme for discretizing the governing differential equations. In this scheme, the partial derivative terms in the differential equations are replaced by their equivalent "difference relations" and so the differential equations turn into difference equations. There is an alternative scheme reffered to as the "finite volume method" or simply "FVM" which is more straight forward. This method (applied to a 1D problem such as fluid flow in a pipe) avoids the partial differential equations from the beginning by dividing the whole pipe volume into several control volumes along the pipe axis and then applying conservation laws to derive two differential equations for each control volume: One of the equations is an exact representation of the conservation of mass (continuity equation) and the other one is an exact representation of the conservation of momentum (Versteeg & Malalasekera, 1995). "Advantage of FVM is that the discredited governing equations retain their physical

interpretation, rather than possibly distorting the physics due to numerical discrimination of each derivative term." (Chung, 2002)

The idea of control volumes in FVM is better described by refering to the Figure (2-1). The whole penstock length is devided into 2N equal segments. The first segment is between the locations $X_1$and X_2 and the last segment is located between X_{2N} and X_{2N+1}. It's possible to define the volume determined by each two adjacent pipe segments located between X_{2i+1} and X_{2i+3} (i=1,…,N-2) as a control volume for application of both mass and momentum conservation laws, but this can cause the discretized momentum equations have unrealistic behaviour for spatially oscillating pressures (Versteeg & Malalasekera, 1995). The solution to this possible problem which is suggested in that reference is to use a so called "staggered grid". Stggered grid for the penstock in the Figure (2-1) means to define the volume determined by each couple of pipe segments located between X_{2i+1} and X_{2i+3} (for i=1,…,N-2) as a control volume for application of the momentum conservation and define the volume determined by each couple of pipe segments located between X_{2i} and X_{2i+2} (for i=1,…,N-1) as a control volume for application of the mass conservation.

The state variables along the pipe which usually appear in the literature of CFD is mass density and velocity of fluid particles. In this report however it's been decided to use static pressure and mass flow rate as the state variables. The later variables are more interesting than the former ones in a hydropower application. In addition, choosing the mass flow rate as the state has the advantage that in the steady-state condition mass flow rate in the whole waterway of the plant will be the same (surge shaft level will be constant in the steady-state condition and hence mass flow rate in the conduit and penstock will also be the same). Hence determining the steady-state value of the states will be much easier. In (Lie, 2011) it is shown that a one to one relation exists between water static pressure and mass density. Later in this report it will be shown that there's also a one to one relation between water velocity and mass flow rate at a particular location along the penstock.

The state "pressure" will be considered spatially constant along the whole length of a control volume for mass conservation and the state "mass flow rate" will be treated as being spatially constant along the whole length of a control volume for application of the momentum conservation. In (Versteeg & Malalasekera, 1995) alternatively "density" and "velocity" is

considered to be spatially constant inside the control volume. These states are indicated at the center of their related control volumes in Figure (2-1). Pressures are shown by bold dots and mass flow rates are shown by bold arrows. The differential equations governing these states will be introduced in the section 2.1.4. Cross-section area of penstock when pressure inside and outside of the penstock is equal to the atmospheric pressure (e.g. when the penstock is empty) will be considered constant throughout this report. Amount of variations of penstock cross-section area due to water pressure inside the penstock will be discussed in the next section.

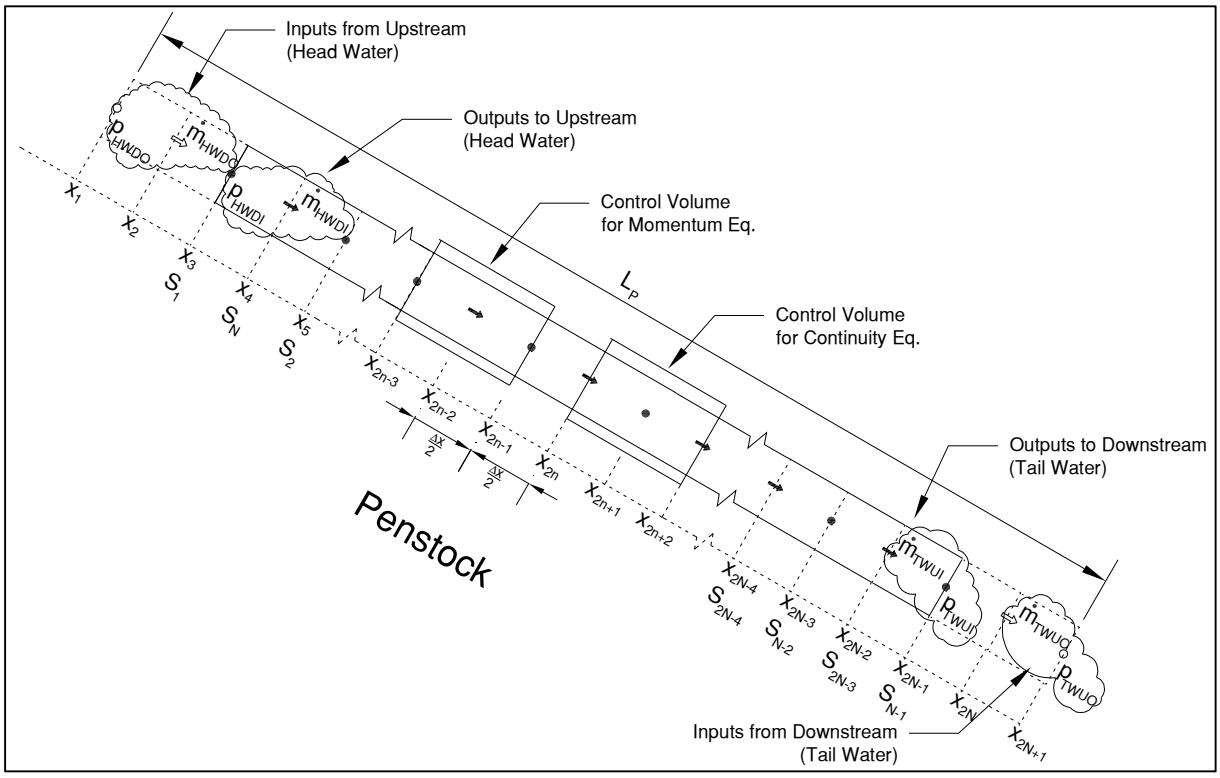

Figure (2-1) Control Volumes for Application of Mass and Momentum Conservation Laws in a Penstock

The pressure and mass flow rate variables at locations X_1, X_2, X_{2N} and X_{2N+1} are shown with hollow dots and arrows. This means that these variables will not be governed by penstock equations. They will be determined by head/tail water system models and will be treated as inputs in the penstock model. States of the penstock model at locations X_3, X_4, X_{2N-2} and X_{2N-1}will be available as outputs to the neighboring systems (head/tail water). They are named after their neighboring systems:

HWDI: Input to the head water system

HWDO: Output from the head water system

TWUI: Input to the tail water system

TWUO: Output from the tail water system

2.1.3 Water Density and Pipe Cross-Section Area as a Function of Pressure

Relationship between water density and pressure is given in (Lie, 2011). Compressibility β for fluids is defined as:

$$\beta = \frac{1}{\rho}\frac{\partial \rho}{\partial p} \tag{2-1}$$

Where ρ stands for density and p stands for pressure

ρ =	Density	$[Kg/m^3]$
p =	Pressure	[Pa]
β =	Compressibility	$[Pa^{-1}]$

If p^{atm} and ρ^{atm} withstand for atmospheric pressure and water density at atmospheric pressure respectively, the following formula can be used to calculate fluid density at other pressures:

$$\rho = \rho^{atm} e^{\beta(p - p^{atm})} \tag{2-2}$$

A typical value of the water compressibility is $\beta = 4.5 \times 10^{-10}$ [1/Pa] which can be considered constant at the range of pressures and temperatures which occur in a hydropower application.

Relationship for changes in the pipe inner radius (ΔR) and changes in the pipe cross-section area (ΔA) against difference in the inside and outside pressure of the pipe (Δp) is given in (Parmakian, 1963) for a pipe which is anchored against longitudinal movement:

$$\frac{\Delta A}{A} = 2\,\frac{\Delta R}{R} = \frac{D(1-\mu^2)}{eE}\;\Delta p \tag{2-3}$$

Where

R =	Pipe inner radius	[m]
D =	Pipe inner diameter	[m]
A =	Pipe cross-section area	[m]
e =	Pipe thickness	[m]
E =	Young's Modulus of Elasticity	[Pa]
μ =	Poisson's ratio	[-]

Here new parameters can be defined as "equivalent compressibility due to the pipe shell elasticity" and "total compressibility due to water compressibility and pipe shell elasticity":

$$\beta_P^{eq} = \frac{1}{A}\frac{\partial A}{\partial p} = \frac{D(1-\mu^2)}{eE} \quad (\text{Equivalent compressibility } [\text{Pa}^{-1}])$$
$$\beta_P^{total} = \beta_P^{eq} + \beta \quad (\text{Total compressibility } [\text{Pa}^{-1}]) \tag{2-4}$$

Speed of sound in water inside the pipe is related to β_P^{total} as follows: (Parmakian, 1963)

$$Speed\ of\ sound = \frac{1}{\sqrt{\rho\,\beta_P^{total}}} \tag{2-5}$$

Illustrative values for β_P^{total} can be calculated having the speed of sound in the water inside a particular pipe. Illustrative values for speed of sound inside various pipes can be found in the same reference. As another example, the following calculations give an illustrative value for

fiberglass pipes series SN10000, DN1400 and PN32 manufactured by Fibrelogic Pipe Systems Pty Ltd[1]. According to datasheet of this manufacturer, stiffness of the pipe is defined by:

$$S = \frac{Ee^3}{12D^3} \qquad [N/m \text{ per metre length of pipe}] \tag{2-6}$$

Specifications of the selected pipe are:

$S = 10000\ [N/m/m]$ (SN10000 series of pipes)

$D = 1.388\ [m]$

$e = 0.0227\ [m]$

$\mu = 0.22$ to 0.29

Using (2-4) and (2-6) with a Poisson's ratio $\mu = 0.29$ will result in:

$$E = \frac{12\,S\,D^3}{e^3} = \frac{12 \times 10000 \times 1.388^3}{0.0227^3} = 2.74329 \times 10^{10}\ [Pa]$$

$$\beta_P^{eq} = \frac{1}{A}\frac{\Delta A}{\Delta p} = \frac{D(1-\mu^2)}{eE} = \frac{1.388 \times (1-0.29^2)}{0.0227 \times 2.74329 \times 10^{10}} = 2.04 \times 10^{-9}\ [Pa^{-1}]$$

Speed of sound in water inside this pipe calculated using (2-5) will be equal to 633 [m/sec].

Similar of the Equation (2-2) can be written for the cross-section area (A) and the product (A×ρ):

$$A = A^{atm} e^{\beta_P^{eq}(p-p^{atm})}$$
$$A \times \rho = A^{atm} \rho^{atm} e^{\beta_P^{total}(p-p^{atm})} \tag{2-7}$$

Where

A^{atm} = Cross section area of the pipe when pressures inside and outside of the pipe both are equal to p^{atm}. $[m^2]$

[1] Datasheet available at the following web address (accessed 06.2011):
http://www.fibrelogic.com/pdfs/Fibrelogic Flowtite Engineering Guidelines DES M-004.pdf

Now it's interesting to know how much error will be involved if someone uses a linear approximation for the exponential functions in (2-2) and (2-7):

$$\text{Max percentage of error} = \frac{e^{\beta_P^{total}(p-p^{atm})} - 1 - \beta_P^{total}(p-p^{atm})}{e^{\beta_P^{total}(p-p^{atm})}}$$

If $\text{Max}\left(\beta_P^{total}\right) = 10^{-9}\ [\text{Pa}^{-1}]$ and $\text{Max}\,(p-p^{atm}) = 10^{7}\ [\text{Pa}]$, then maximum percentage of error will be:

$$\text{Max percentage of error} = 0.005\%$$

So in the range of pressures and elasticity applicable in hydropower one can easily assume that values of A, ρ or the product $A \times \rho$ linearly change with pressure.

$$\begin{aligned} \rho &\approx \rho^{atm}[1+\beta(p-p^{atm})] \\ A &\approx A^{atm}\left[1+\beta_P^{eq}(p-p^{atm})\right] \\ A\times\rho &\approx A^{atm}\rho^{atm}\left[1+\beta_P^{total}(p-p^{atm})\right] \end{aligned} \qquad (2\text{-}8)$$

2.1.4 Governing Equations

In this section governing differential equations for (compressible) water flow inside the penstock with elastic walls will be formulated by:

- Applying the mass conservation law for the control volumes each enclosed between penstock cross-sections at locations X_{2i} and X_{2i+2} (for i=1,…,N-1) which results in N-1 ordinary differential equations for the "pressure" states.
- Applying the momentum conservation law for the control volumes each enclosed between penstock cross-sections at locations X_{2i+1} and X_{2i+3} (for i=1,…,N-2) which results in N-2 ordinary differential equations for the "mass flow rate" states.

Continuity Equation

Continuity equations by applying the mass conservation rule to the control volumes CV_{2i+1} enclosed between penstock cross-sections at locations X_{2i} and X_{2i+2} (for i=1,…,N-1) will be given in this section.

Mass conservation law simply states that the rate of change of the fluid mass inside the control volume with time is equal to the rate of mass flow into the control volume with time. In CFD this fact usually is stated by the following equation which is applicable to a fluid element. A fluid element is the smallest volume in which fluid retains its macroscopic properties. (Versteeg & Malalasekera, 1995)

$$\frac{\partial \rho}{\partial t} + \nabla.(\rho \mathbf{v}) = 0 \qquad (2\text{-}9)$$

Where

ρ =	Density of the fluid as a function of the location with Cartesian coordinates (x,y,z) and the time t	[Kg/m^3]
$\mathbf{v}$ =	Velocity vector field as a function of the location (x,y,z) and the time t	[m/sec]
$\nabla.(\rho \mathbf{v})$ =	Divergence of the vector field $\rho \mathbf{v}$	[Kg/m3/sec]

It can be shown that integrating (2-9) inside the control volume CV_{2i+1} enclosed between penstock cross-sections at locations X_{2i} and X_{2i+2} (for i=1,…,N-1) will result in the same statement as the mass conservation law for that control volume but one should be very careful when evaluating the volume integrals and applying the Gauss' theorem[2] to the divergence term because those boundries of the control volume which coinside with the penstock walls are moving with pressure and hence are moving with time.

The mass of water inside the control volume $CV_{2i+1}$is given by the following relation:

[2] http://en.wikipedia.org/wiki/Divergence_theorem (accessed 06.2011)

$$m_{2i+1} = \int_{x=x_{2i}}^{x_{2i+2}} \rho_{2i+1} A_{P,2i+1} dX = \rho_{2i+1} A_{P,2i+1} \Delta x \qquad (2\text{-}10)$$

Remember from section 2.1.2 that pressure and hence density and cross section area are considered **spatially** constant inside the control volume. In (2-10) these values are set to be equal to their value at the central location X_{2i+1}.

It's of great importance for the later analysis that the value of $A \times \rho$ at the boundaries of the control volume for continuity be considered equal to the mean value of that function in the two adjacent control volumes (Bold dotes shown in the Figure (2-2)).

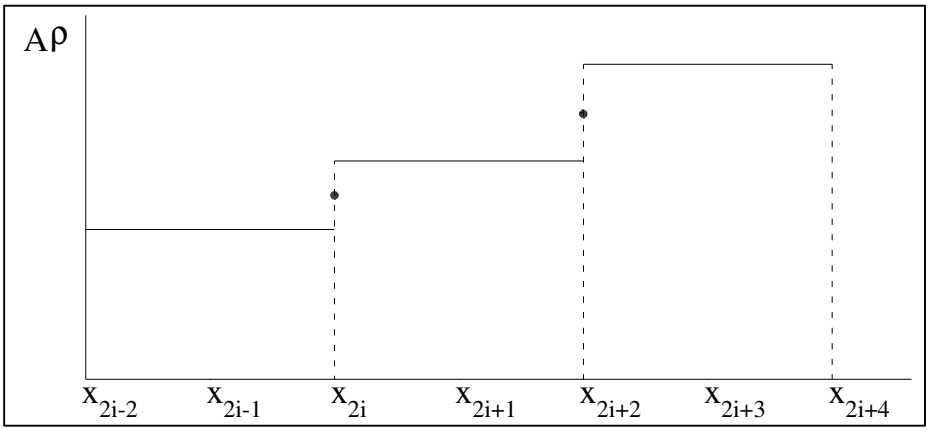

Figure (2-2) Values of the Product A×ρ Inside the Control Volumes for Mass Conservation and at the Boundary Points of the Control Volumes

So applying mass conservation to (2-10) will result in the following differential equation for the control volume CV_{2i+1}:

$$\Delta x \frac{d}{dt}\left(\rho_{2i+1} A_{P,2i+1}\right) = \dot{m}_{2i} - \dot{m}_{2i+2} \quad (i = 1, \dots, N-1) \qquad (2\text{-}11)$$

Where

$\dot{m}_{2i}$ = Mass flow rate into the control volume CV_{2i+1} at location X_{2i} (according to the conventional flow direction shown in the Figure (2-1)) [Kg/sec]

$\dot{m}_{2i+2}$ = Mass flow rate out of the control volume CV_{2i+1} at location X_{2i+2} (according to the conventional flow direction shown in the Figure (2-1)) [Kg/sec]

As discussed in section 2.1.2 it is of interest to represent the Equation (2-11) in terms of the pressure inside the control volume. According to the discussion in Section Chapter 12.1.2, cross-section area of penstock only changes with pressure ($\left(\partial A_{P,2i+1}/\partial X\right) = 0$). So by also using (2-8) the derivative term in (2-11) can be written as the following:

$$\begin{aligned}\frac{d}{dt}\left(A_{P,2i+1}\rho_{2i+1}\right) &= \frac{d}{dp_{2i+1}}\left(A_{P,2i+1}\rho_{2i+1}\right)\ \frac{dp_{2i+1}}{dt} \\ &= \beta_P^{total} A_P^{atm}\rho^{atm}\ \frac{dp_{2i+1}}{dt}\end{aligned} \qquad (2\text{-}12)$$

From (2-11) and (2-12) **the final form of the continuity equations** will be as follows:

$$\Delta x\ \beta_P^{total} A_P^{atm}\rho^{atm}\ \frac{dp_{2i+1}}{dt} = \dot{m}_{2i} - \dot{m}_{2i+2} \quad (i = 1, \dots, N-1) \qquad (2\text{-}13)$$

Momentum Equations

A preliminary form of the momentum equations will be given in this section. The final form of the momentum equations will be given in the next subsection (The Upwind Difference Scheme).

Momentum conservation for the control volume CV_{2i+2} enclosed between penstock cross-sections at locations X_{2i+1} and X_{2i+3} (for i=1,…,N-2) states that rate of change (with time) of the momentum (in the X direction i.e. conventional direction of the water flow) of the water flowing inside the control volume at a particular time t is equal to the rate of the net momentum flowing into the control volume by mass transport at boundary surfaces $X = X_{2i+1}$ and $X = X_{2i+3}$ plus sum of the forces that apply to the water column inside the control volume at the X direction along the penstock axis at that time.

Like the mass conservation case, there is an equation which is applicable to a fluid element: (Versteeg & Malalasekera, 1995)

$$\frac{\partial}{\partial t}(\rho v) + \nabla.(\rho v \mathbf{v}) = -\frac{\partial p}{\partial x} + S_{M_X} \qquad (2\text{-}14)$$

Where

$v =$	Component of the velocity vector field **v** in the X direction as a function of the location (x,y,z) and the time t	[m/sec]
$p =$	Pressure as a function of the location (x,y,z) and the time t	[Pa]
$S_{M_X} =$	Body forces (friction/viscous and gravity) per unit volume in the X direction	[N/m^3]

It can be shown that integration of the above equation over the control volume CV_{2i+2} will result in the momentum conservation statement above. Again one should be careful in performing the volume integration and shall consider movement of those boundaries of the control volume which coincide with the penstock wall.

Amount of momentum of the water column in the control volume CV_{2i+2} is as follows:

$$\text{Momentum of the water Column} =$$

$$\int_{CV_{2i+2}} v\, dm = \int_{CV_{2i+2}} v\,(A\,\rho\, dX) = \int_{CV_{2i+2}} (v\,A\,\rho)\, dX = \int_{CV_{2i+2}} \dot{m}\, dX = \dot{m}_{P,2i+2}\Delta x \qquad (2\text{-}15)$$

In deriving the above relation it's being assumed that mass flow rate in X direction inside the control volume is spatially constant (as mentioned in Section 2.1.2) and equal to $\dot{m}_{2i+2}$. This assumption is indicated in Figure (2-3). By this assumption velocity throughout the control volume will be piecewise constant because the product A×ρ is assumed to be piecewise constant between X_{2i+1} and X_{2i+3} (see Figure (2-2)). The velocity at X_{2i+2} can be considered equal to $\dot{m}_{P,2i+2}/(A_{P,2i+2}\rho_{2i+2})$.

Net momentum in the X direction along the penstock which is flowing into the control volume CV_{2i+2} due to mass transport is equal to:

$$\dot{m}_{P,2i+1}v_{P,2i+1} - \dot{m}_{P,2i+3}v_{P,2i+3} \tag{2-16}$$

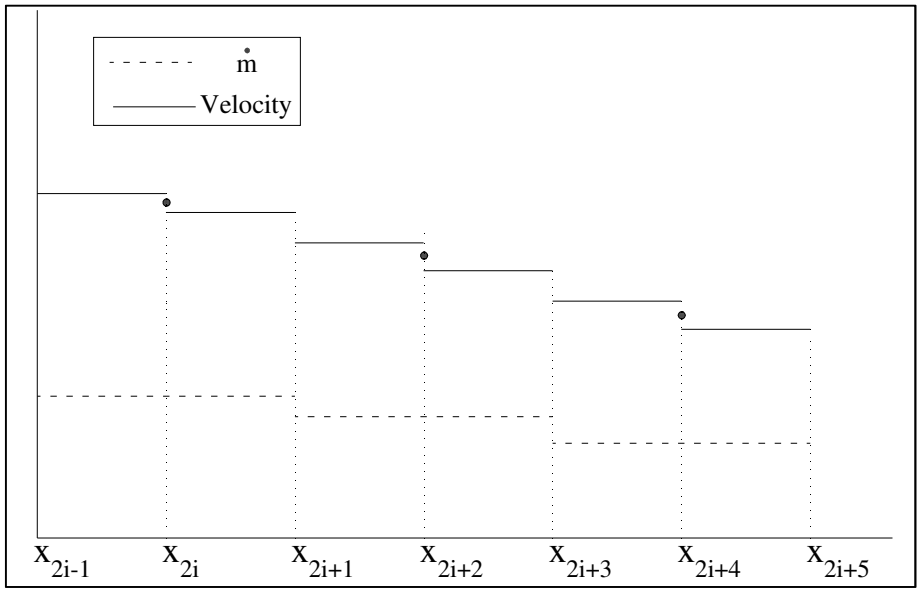

Figure (2-3) Variations of Mass Flow Rate and Velocity inside Control Volumes for Momentum

Forces that act on the water column are due to pressure difference between locations X_{2i+1} and X_{2i+3}, weight of the water column and friction between water and penstock wall. Amount of the force due to pressure difference at locations X_{2i+1} and X_{2i+3} is given in the following relation:

$$F_{p,2i+2} = A_{P,2i+2}\,(p_{2i+1} - p_{2i+3}) \tag{2-17}$$

Relations giving the amount of gravity and friction forces for the water column inside control volume CV_{2i+2} are as follows:

$$F_{G,2i+2} \cong \Delta x\, A_{P,2i+2}\, \rho_{2i+2}\, g \sin\theta$$
$$F_{F,2i+2} = \xi_{2i+2} v_{P,2i+2} \tag{2-18}$$

Where

$F_{G,2i+2}$= Gravity force applied to the control volume [N]

$F_{F,2i+2}=$	Friction force applied to the control volume	[N]
$\xi_{2i+2}=$	A friction coefficient of the control volume (always negative) given by the following formula: $\xi_{2i+2} = -\frac{1}{2} f_P \, \Delta x \, \Pi_{P,2i+2} \, \rho_{2i+2} \, \mathrm{sign}(v_{P,2i+2}) \, v_{P,2i+2}$	[N.sec/m]
$f_P =$	Fanning friction factor	[-]
$\Pi_{P,2i+2} =$	Internal perimeter of the penstock cross section at $X = X_{2i+2}$	[m]

Average of the product A×ρ is used in the relation for gravity force and average velocity is used in the relation for friction.

Now the momentum conservation law can be formulated for the control volume CV_{2i+2} using (2-15) to (2-18):

$$\Delta x \frac{d\dot{m}_{P,2i+2}}{dt} = \dot{m}_{P,2i+1} v_{P,2i+1} - \dot{m}_{P,2i+3} v_{P,2i+3} + F_{p,2i+2} + F_{G,2i+2} + F_{F,2i+2} \qquad (2\text{-}19)$$

This is not the final form of the momentum equations. Before obtaining the final form, this question shall be answered: What shall be substituted for values of $\dot{m}_P$ and v_P at locations X_{2i+1} and X_{2i+3}? **Answer to this question and final form of the momentum equations are given in the next subsection (The upwind difference scheme).**

The Upwind Difference Scheme

For determining values of $\dot{m}_P$ and v_P at locations X_{2i+1} and X_{2i+3}, it's necessary to rewrite (2-19) in terms of $(dv_{P,2i+2}/dt)$:

$$\frac{d\dot{m}_{P,2i+2}}{dt} = \frac{d}{dt}\left(A_{P,2i+2}\ \rho_{2i+2}\ v_{P,2i+2}\right)$$

$$= A_{P,2i+2}\ \rho_{2i+2}\ \frac{d\ v_{P,2i+2}}{dt} + v_{P,2i+2}\ \frac{d}{dt}\left(A_{P,2i+2}\ \rho_{2i+2}\right) \qquad (2\text{-}20)$$

$$= A_{P,2i+2}\ \rho_{2i+2}\ \frac{d\ v_{P,2i+2}}{dt} + v_{P,2i+2}\ \frac{d}{dt}\left(\frac{A_{P,2i+1}\ \rho_{2i+1} + A_{P,2i+3}\ \rho_{2i+3}}{2}\right)$$

By substituting the terms of the form $d(A_P\ \rho)/dt$ from (2-11) into (2-20) the following relation will be concluded:

$$\frac{d\dot{m}_{P,2i+2}}{dt} = A_{P,2i+2}\ \rho_{2i+2}\ \frac{d\ v_{P,2i+2}}{dt} + v_{P,2i+2}\ \left(\frac{\dot{m}_{P,2i} - \dot{m}_{P,2i+4}}{2\ \Delta x}\right) \qquad (2\text{-}21)$$

By substituting (2-21) into (2-19), the continuity equation in the form of differential equation for $v_{P,2i+2}$ will be obtained as follows:

$$\Delta x\ A_{P,2i+2}\ \rho_{2i+2}\ \frac{d\ v_{P,2i+2}}{dt} + \left(\frac{\dot{m}_{P,2i} - \dot{m}_{P,2i+4}}{2} - \xi_{2i+2}\right)\ v_{P,2i+2} + \dot{m}_{P,2i+3}v_{P,2i+3} - \dot{m}_{P,2i+1}v_{P,2i+1} = F_{G,2i+2} + F_{P,2i+2} \qquad (2\text{-}22)$$

In Equation (2-22) values of v_P and $\dot{m}_P$ at X_{2i+1} and X_{2i+3} shall be determined. One possibility known as Central Differences Scheme (Versteeg & Malalasekera, 1995) could be as follows:

$$\dot{m}_{P,2i+1} = \frac{\dot{m}_{P,2i} + \dot{m}_{P,2i+2}}{2}\ ,\ v_{P,2i+1} = \frac{v_{P,2i} + v_{P,2i+2}}{2}$$
$$\dot{m}_{P,2i+3} = \frac{\dot{m}_{P,2i+2} + \dot{m}_{P,2i+4}}{2}\ ,\ v_{P,2i+3} = \frac{v_{P,2i+2} + v_{P,2i+4}}{2} \qquad (2\text{-}23)$$

In this case (2-22) can be re-written as follows:

$$\Delta x\ A_{P,2i+2}\ \rho_{2i+2}\ \frac{d\ v_{P,2i+2}}{dt} + a'_{2i+2}\ v_{P,2i+2} = a'_{2i}v_{P,2i} + a'_{2i+4}\ v_{P,2i+4} + F_{G,2i+2} + F_{p,2i+2} \qquad (2\text{-}24)$$

Where

$$a'_{2i} = \frac{\dot{m}_{P,2i} + \dot{m}_{P,2i+2}}{4}$$

$$a'_{2i+2} = \frac{\dot{m}_{P,2i} - \dot{m}_{P,2i+4}}{4} - \xi_{2i+2}$$

$$a'_{2i+2} = -\frac{\dot{m}_{P,2i+2} + \dot{m}_{P,2i+4}}{4}$$

It can be shown that at inviscid flows with large Peclet numbers the above choice does not guarantee stability of the variables. (Versteeg & Malalasekera, 1995) One sufficient condition for (2-22) to have a stable answer for steady-state velocity values in case of known pressures is (the same reference):

1. All the three coefficients a'_{2i} , a'_{2i+2} and a'_{2i+4} should be positive
2. The following condition shall be satisfied:

$$\frac{a'_{2i} + a'_{2i+4}}{a'_{2i+2}} \begin{cases} \leq 1 & \text{for all } i = 1,2,\dots,N-2 \\ < 1 & \text{at least for one } i = 1,2,\dots,N-2 \end{cases} \qquad (2\text{-}25)$$

When the system reaches the steady state condition, all $\dot{m}$ values become equal and the first condition obviously isn't satisfied in (2-24).

One solution known as "Upwind Difference Scheme" is available to the above problem. In this solution the values of v_P and $\dot{m}_P$ at X_{2i+1} and X_{2i+3} for use with (2-22) are determined as below:

$$\dot{m}_{P,2i+1} = \frac{\dot{m}_{P,2i} + \dot{m}_{P,2i+2}}{2} \quad , \quad \dot{m}_{P,2i+3} = \frac{\dot{m}_{P,2i+2} + \dot{m}_{P,2i+4}}{2}$$

$$\text{If } \dot{m}_{P,2i} + \dot{m}_{P,2i+2} \geq 0 \Rightarrow v_{P,2i+1} = v_{P,2i} \text{ and } v_{P,2i+3} = v_{P,2i+2} \qquad (2\text{-}26)$$

$$\text{If } \dot{m}_{P,2i+2} + \dot{m}_{P,2i+4} \leq 0 \Rightarrow v_{P,2i+1} = v_{P,2i+2} \text{ and } v_{P,2i+3} = v_{P,2i+4}$$

Then a'_{2i}, a'_{2i+2} and a'_{2i+4} in (2-24) will be given by the following table:

	if $\dot{m}_{P,2i} + \dot{m}_{P,2i+2} \geq 0$	if $\dot{m}_{P,2i+2} + \dot{m}_{P,2i+4} \leq 0$
a'_{2i+2}	$\frac{\dot{m}_{P,2i} + \dot{m}_{P,2i+2}}{2} - \xi_{2i+2}$	$-\frac{\dot{m}_{P,2i+2} + \dot{m}_{P,2i+4}}{2} - \xi_{2i+2}$
a'_{2i}	$\frac{\dot{m}_{P,2i} + \dot{m}_{P,2i+2}}{2}$	0
a'_{2i+4}	0	$-\frac{\dot{m}_{P,2i+2} + \dot{m}_{P,2i+4}}{2}$

So the coefficients will always be nonnegative and the following condition will be satisfied:

$$\frac{a'_{2i} + a'_{2i+4}}{a'_{2i+2}} < 1 \quad \text{(in presence of friction)}$$

The relation (2-24) with the coefficients determined by the upwind differences will make the final form of the momentum equation. It's desirable to change back (2-24) as an ODE in terms of $\left(d\dot{m}_{P,2i+2}/dt\right)$. Using (2-19) and (2-26) **the final form of the momentum equations** will be obtained as follows:

$$\Delta x \frac{d\dot{m}_{P,2i+2}}{dt} + a_{2i+2}^{\{2i+2\}} v_{P,2i+2} = a_{2i}^{\{2i+2\}} v_{P,2i} + a_{2i+4}^{\{2i+2\}} v_{P,2i+4} + F_{G,2i+2} + F_{p,2i+2} \quad \text{(2-27)}$$

(i=1,2,….,N-2)

Where $a_{2i}^{\{2i+2\}}$, $a_{2i+2}^{\{2i+2\}}$ and $a_{2i+4}^{\{2i+2\}}$ are obtained from the following table:

	if $\dot{m}_{P,2i} + \dot{m}_{P,2i+2} \geq 0$	if $\dot{m}_{P,2i+2} + \dot{m}_{P,2i+4} \leq 0$
$a_{2i+2}^{\{2i+2\}}$	$\frac{\dot{m}_{P,2i+2} + \dot{m}_{P,2i+4}}{2} - \xi_{2i+2}$	$-\frac{\dot{m}_{P,2i} + \dot{m}_{P,2i+2}}{2} - \xi_{2i+2}$
$a_{2i}^{\{2i+2\}}$	$\frac{\dot{m}_{P,2i} + \dot{m}_{P,2i+2}}{2}$	0

(2-28)

$a_{2i+4}^{\{2i+2\}}$	0	$-\frac{\dot{m}_{P,2i+2}+\dot{m}_{P,2i+4}}{2}$

$F_{G,2i+2}$, $F_{p,2i+2}$ and ξ_{2i+2} are given in (2-17) and (2-18).

2.1.5 Summary Penstock Model

In this section penstock model will be summarized based on the equations developed in the previous section, but before that, some definitions shall be made:

The state vector: The state vector of the penstock $\mathbf{S} \in \mathcal{R}^{2N-3}$ (where N is number of the pipe segments with equal length of Δx along the penstock) contains pressures at the center of the control volumes CV_{2i+1} (control volumes located between X_{2i} and X_{2i+2} for i=1, 2, …, N-1) and mass flow rates at the center of the control volumes CV_{2i+2} (control volumes located between X_{2i+1} and X_{2i+3} for i=1, 2, …, N-2) as shown in the Figure (2-1):

$$\mathbf{S}\left(\in \mathcal{R}^{2N-3}\right) = \begin{bmatrix}\mathbf{p}\\ \dot{\mathbf{m}}\end{bmatrix}$$

$$\mathbf{p}\left(\in \mathcal{R}^{N-1}\right) = [p_{P,3}(=p_{HWDI}) \quad p_{P,5} \quad p_{P,7} \quad \cdots \quad p_{P,2N-3} \quad p_{P,2N-1}(=p_{TWUI})]^T \tag{2-29}$$

$$\dot{\mathbf{m}}\left(\in \mathcal{R}^{N-2}\right) = [\dot{m}_{P,4}(=\dot{m}_{HWDI}) \quad \dot{m}_{P,6} \quad \dot{m}_{P,8} \quad \cdots \quad \dot{m}_{P,2N-4} \quad \dot{m}_{P,2N-2}(=\dot{m}_{TWUI})]^T$$

Extended pressure and mass flow rate vectors: These vectors are the same as p and ṁ defined above except that they include input pressures and mass flow rates from the neighboring systems (Head water and tail water):

$$\begin{aligned}\mathbf{p_{ext}}\left(\in \mathcal{R}^{N+1}\right) = [&p_{P,1}(=p_{HWDO}) \quad p_{P,3}(=p_{HWDI}) \quad p_{P,5} \quad p_{P,7} \quad \cdots\\ &p_{P,2N-3} \quad p_{P,2N-1}(=p_{TWUI}) \quad p_{P,2N+1}(=p_{TWUO})]^T\\ \dot{\mathbf{m}}_{\mathbf{ext}}\left(\in \mathcal{R}^{N}\right) = [&\dot{m}_{P,2}(=\dot{m}_{HWDO}) \quad \dot{m}_{P,4}(=\dot{m}_{HWDI}) \quad \dot{m}_{P,6} \quad \dot{m}_{P,8} \quad \cdots\\ &\dot{m}_{P,2N-4} \quad \dot{m}_{P,2N-2}(=\dot{m}_{TWUI}) \quad \dot{m}_{P,2N}(=\dot{m}_{TWUO})]^T\end{aligned} \tag{2-30}$$

$\boldsymbol{\mathcal{F}}_{\mathbf{p}}$, $\boldsymbol{\mathcal{F}}_{\dot{\mathbf{m}}}$, $\boldsymbol{\mathcal{F}}_{\mathbf{p\_ext}}$ and $\boldsymbol{\mathcal{F}}_{\dot{\mathbf{m}}\mathbf{\_ext}}$: The vector $\boldsymbol{\mathcal{F}}_{\mathbf{p\_ext}}$ contains the products (area × density) at the center of the control volumes CV_{2i+1} (i=1,2, …, N-1) as well as at the end points (X_1 and X_{2N+1}). The vector $\boldsymbol{\mathcal{F}}_{\dot{\mathbf{m}}\mathbf{\_ext}}$ contains the products (area × density) at the center of the control volumes CV_{2i+2} (i=1,2, …, N-2) as well as at the end points (X_2 and X_{2N}).

$$\boldsymbol{\mathcal{F}}_{\mathbf{p\_ext}}\left(\in \mathcal{R}^{N+1}\right) = [A_{P,1} \times \rho_1 \quad A_{P,3} \times \rho_3 \quad \dots \quad A_{P,2N-1} \times \rho_{2N-1} \quad A_{P,2N+1} \times \rho_{2N+1}]^T$$

$$\boldsymbol{\mathcal{F}}_{\dot{\mathbf{m}}\_ext}\left(\in \mathcal{R}^{N}\right) = [A_{P,2} \times \rho_2 \quad A_{P,4} \times \rho_4 \quad \dots \quad A_{P,2N-2} \times \rho_{2N-2} \quad A_{P,2N} \times \rho_{2N}]^T$$

Since penstock is going to connect to systems with incompressible water and inelastic walls models, it's easier to consider the same conditions (incompressible water and inelastic walls) at locations X_1, X_2, X_{2N} and X_{2N+1}. Then $\boldsymbol{\mathcal{F}}_{\mathbf{p\_ext}}$ and $\boldsymbol{\mathcal{F}}_{\dot{\mathbf{m}}\_ext}$ will be as follows**:**

$$\boldsymbol{\mathcal{F}}_{\mathbf{p\_ext}} = \left[A_P^{atm} \times \rho^{atm} \quad \boldsymbol{\mathcal{F}}_{\mathbf{p}}^{\boldsymbol{T}} \quad A_P^{atm} \times \rho^{atm}\right]^T$$

$$\boldsymbol{\mathcal{F}}_{\dot{\mathbf{m}}\_ext} = \left[A_P^{atm} \times \rho^{atm} \quad \boldsymbol{\mathcal{F}}_{\dot{\mathbf{m}}}^{\boldsymbol{T}} \quad A_P^{atm} \times \rho^{atm}\right]^T$$

Where (2-31)

$$\boldsymbol{\mathcal{F}}_{\mathbf{p}}\left(\in \mathcal{R}^{N-1}\right) = [A_{P,3} \times \rho_3 \quad \dots \quad A_{P,2N-1} \times \rho_{2N-1}]^T$$

$$\boldsymbol{\mathcal{F}}_{\dot{\mathbf{m}}}\left(\in \mathcal{R}^{N-2}\right) = [A_{P,4} \times \rho_4 \quad \dots \quad A_{P,2N-2} \times \rho_{2N-2}]^T$$

As a consequence of considering incompressible water and inelastic walls at locations X_1, X_2, X_{2N} and X_{2N+1}, $\mathbf{p_{ext}}$ (including p_{HWI} and p_{TWI}) defined in (2-30) will not be used anymore and $\mathbf{p}$ defined in (2-29) is enough in the penstock model.

Vectors containing velocities and cross-section areas at the center of the control volumes CV_{2i+2} (i=1,2, …, N-2) as well as at the end points (X_2 and X_{2N}):

$$\mathbf{A}_{\dot{\mathbf{m}}\mathbf{\_ext}}(\in \mathcal{R}^{N}) = [A_P^{atm} \quad \mathbf{A}_{\dot{\mathbf{m}}}^{T} \quad A_P^{atm}]^T$$

$$\mathbf{A}_{\dot{\mathbf{m}}}(\in \mathcal{R}^{N-2}) = [A_{P,4} \quad A_{P,6} \quad \dots \quad A_{P,2N-2}]^T \qquad (2\text{-}32)$$

(Area at locations X_2 and X_{2N} is considered not changing with pressure i.e. inelastic walls)

$$\mathbf{v_{\dot{m}\_ext}}(\in \mathcal{R}^{N}) = [v_{P,2} \quad v_{P,4} \quad \cdots \quad v_{P,2N-2} \quad v_{P,2N}]^{T}$$

Vectors containing densities and pipe perimeters at center of the control volumes CV_{2i+2} (i=1, 2, …, N-2):

$$\boldsymbol{\rho}_{\dot{\mathbf{m}}}(\in \mathcal{R}^{N-2}) = [\rho_4 \quad \rho_6 \quad \cdots \quad \rho_{2N-2}]^{T}$$
$$\boldsymbol{\Pi}_{\dot{\mathbf{m}}}(\in \mathcal{R}^{N-2}) = [\Pi_{P,4} \quad \Pi_{P,6} \quad \cdots \quad \Pi_{P,2N-2}]^{T} \tag{2-33}$$

Vectors containing densities and cross-section areas at the center of the control volumes CV_{2i+1} (i=1,2, …, N-1):

$$\boldsymbol{\rho}_{\mathbf{p}}(\in \mathcal{R}^{N-1}) = [\rho_3 \quad \rho_5 \quad \cdots \quad \rho_{2N-1}]^{T}$$
$$\mathbf{A_p}(\in \mathcal{R}^{N-1}) = [A_{P,3} \quad A_{P,5} \quad \cdots \quad A_{P,2N-1}]^{T} \tag{2-34}$$

Pressure at the center of the control volumes CV_{2i+2} (i=1,2, …, N-2):

$$\mathbf{p}_{\dot{\mathbf{m}}}(\in \mathcal{R}^{N-2}) = [p_{P,4} \quad p_{P,6} \quad \cdots \quad p_{P,2N-2}]^{T} \tag{2-35}$$

Gravity and pressure gradient forces acting on the control volumes CV_{2i+2} (i=1,2, …, N-2):

$$\mathbf{F_{G,\dot{m}}}(\in \mathcal{R}^{N-2}) = [F_{G,4} \quad F_{G,6} \quad \cdots \quad F_{G,2N-2}]^{T}$$
$$\mathbf{F_{p,\dot{m}}}(\in \mathcal{R}^{N-2}) = [F_{p,4} \quad F_{p,6} \quad \cdots \quad F_{p,2N-2}]^{T} \tag{2-36}$$

Vector of friction coefficients for the control volumes CV_{2i+2} (i=1,2, …, N-2):

$$\boldsymbol{\xi}_{\dot{\mathbf{m}}}(\in \mathcal{R}^{N-2}) = [\xi_4 \quad \xi_6 \quad \cdots \quad \xi_{2N-2}]^{T} \tag{2-37}$$

The matrix for coefficients of velocities in the momentum equations: This matrix includes the time varying coefficients of the velocity terms in (2-27) and with relations given in (2-28):

$$\boldsymbol{\mathcal{A}}_{\dot{\mathbf{m}}}\left[\in \mathcal{R}^{(\mathrm{N}-2)\times 3}\right] = \begin{bmatrix} -a_4^{\{4\}} & a_2^{\{4\}} & a_6^{\{4\}} \\ -a_6^{\{6\}} & a_4^{\{6\}} & a_8^{\{6\}} \\ \vdots & \vdots & \vdots \\ -a_{2N-4}^{\{2N-4\}} & a_{2N-6}^{\{2N-4\}} & a_{2N-2}^{\{2N-4\}} \\ -a_{2N-2}^{\{2N-2\}} & a_{2N-4}^{\{2N-2\}} & a_{2N}^{\{2N-2\}} \end{bmatrix} \tag{2-38}$$

Now a step by step procedure can be defined for calculation of time derivative of the state vector **S**. This procedure is summarized in Table (2-1).

Table (2-1) Summary Penstock Model

1.

Input N, **S,** $\dot{\mathrm{m}}_{\mathrm{HWDO}}$ and $\dot{\mathrm{m}}_{\mathrm{TWUO}}$ (Elements of S and the other three variables defines in Figure (2-1)

2.

$\mathbf{p} = \mathbf{S}(1\colon \mathrm{N}-1)$ and $\dot{\mathbf{m}} = \mathbf{S}(\mathrm{N}\colon 2\mathrm{N}-3)$

3.

$\dot{\mathbf{m}}_{\mathbf{ext}} = [\dot{\mathrm{m}}_{\mathrm{HWDO}} \quad \dot{\mathbf{m}}^{\mathrm{T}} \quad \dot{\mathrm{m}}_{\mathrm{TWUO}}]^{\mathrm{T}}$

4. Vector form of continuity equations given in (2-13):

$$\frac{\mathrm{d}\mathbf{p}}{\mathrm{dt}} = \left(\Delta \mathrm{x}\, \beta_P^{total} \mathrm{A_P^{atm}} \rho^{\mathrm{atm}}\right) \backslash [\dot{\mathbf{m}}_{\mathbf{ext}}(1\colon \mathrm{N}-1) - \dot{\mathbf{m}}_{\mathbf{ext}}(2\colon \mathrm{N})]$$

5. According to (2-8) and (2-31):

$$\boldsymbol{\mathcal{F}}_{\mathbf{p}} \approx \mathrm{A_P^{atm}}\rho^{\mathrm{atm}}\left[\mathrm{ones(N-1,1)} + \beta_P^{total}\left(\mathbf{p} - \mathrm{p^{atm}} \times \mathrm{ones(N-1,1)}\right)\right]$$

$$\boldsymbol{\mathcal{F}}_{\dot{\mathbf{m}}} \approx 2\backslash\left[\boldsymbol{\mathcal{F}}_{\mathbf{p}}(1\mathrm{:N}-2) + \boldsymbol{\mathcal{F}}_{\mathbf{p}}(2\mathrm{:N}-1)\right] \quad \text{(Averaging as mentioned in Section 2.1.4)}$$

$$\boldsymbol{\mathcal{F}}_{\dot{\mathbf{m}}\_\mathbf{ext}} = \left[\mathrm{A_P^{atm}} \times \rho^{\mathrm{atm}} \quad \boldsymbol{\mathcal{F}}_{\dot{\mathbf{m}}}^{\mathbf{T}} \quad \mathrm{A_P^{atm}} \times \rho^{\mathrm{atm}}\right]^{\mathrm{T}}$$

6. Definition in (2-39):

$$\mathbf{v}_{\dot{\mathbf{m}}\_\mathbf{ext}} = \dot{\mathbf{m}}_{\mathbf{ext}} \,./\, \boldsymbol{\mathcal{F}}_{\dot{\mathbf{m}}\_\mathbf{ext}} \qquad (./ \triangleq \text{pointwise division})$$

7. From (2-29), (2-41) and averaging according to (Versteeg & Malalasekera, 1995): (In fact in that reference averaging is done on density at center of the control volumes for momentum)

$$\mathbf{p}_{\dot{\mathbf{m}}} = 2\backslash\left(\mathbf{p}(1\mathrm{:N}-2) + \mathbf{p}(2\mathrm{:N}-1)\right)$$

8. From (2-8), (2-32) and (2-33):

$$\boldsymbol{\rho}_{\dot{\mathbf{m}}} = \rho^{\mathrm{atm}} \times \left[\mathrm{ones(N-2,1)} + \beta \times \left(\mathbf{p}_{\dot{\mathbf{m}}} - \mathrm{p^{atm}} \times \mathrm{ones(N-2,1)}\right)\right]$$

$$\mathbf{A}_{\dot{\mathbf{m}}} = \boldsymbol{\mathcal{F}}_{\dot{\mathbf{m}}} \,./\, \boldsymbol{\rho}_{\dot{\mathbf{m}}}$$

$$\boldsymbol{\Pi}_{\dot{\mathbf{m}}} = \mathrm{sqrt}\,(4\pi\mathbf{A}_{\dot{\mathbf{m}}})$$

9. From (2-18) and (2-37): (.* denotes point wise multiplication)

$$\boldsymbol{\xi}_{\dot{\mathbf{m}}} = \left(-\frac{1}{2}\mathrm{f_P}\,\Delta\mathrm{x}\right)\left[\boldsymbol{\Pi}_{\dot{\mathbf{m}}} .*\ \boldsymbol{\rho}_{\dot{\mathbf{m}}} .*\ \mathrm{sign}\left(\mathbf{v}_{\dot{\mathbf{m}}_{\mathbf{ext}}}(2\mathrm{:}N-1)\right) .*\ \mathbf{v}_{\dot{\mathbf{m}}\_\mathbf{ext}}(2\mathrm{:}N-1)\right]$$

10. From (2-17), (2-29), (2-32) and (2-36):

$$\mathbf{F}_{\mathbf{p},\dot{\mathbf{m}}} = \mathbf{A}_{\dot{\mathbf{m}}} .*\ \left(\mathbf{p}(1\mathrm{:}N-2) - \ \mathbf{p}(2\mathrm{:}N-1)\right)$$

11. From (2-18) and (2-36):

$$\mathbf{F}_{\mathbf{G},\dot{\mathbf{m}}} = \Delta\mathrm{x}\,\mathrm{g}\,\sin\theta_{\mathrm{P}} \times \boldsymbol{\mathcal{F}}_{\dot{\mathbf{m}}\_\mathbf{ext}}(2\mathrm{:N}-1)$$

12. The matrix $\boldsymbol{\mathcal{A}}_{\dot{\mathbf{m}}}$ defined by (2-38) and (2-28) shall be calculated with a loop for i=1:N-2.

13. Finally momentum equations from (2-27):

$$\Delta x \frac{d\dot{\mathbf{m}}}{dt} = \boldsymbol{\mathcal{A}}_{\dot{\mathbf{m}}}(:,1) \times \mathbf{v}_{\dot{\mathbf{m}}_{\mathbf{ext}}}(2:N-1) + \boldsymbol{\mathcal{A}}_{\dot{\mathbf{m}}}(:,2) \times \mathbf{v}_{\dot{\mathbf{m}}_{\mathbf{ext}}}(1:N-2) + \boldsymbol{\mathcal{A}}_{\dot{\mathbf{m}}}(:,3) \times \mathbf{v}_{\dot{\mathbf{m}}\_\mathbf{ext}}(3:N) + \mathbf{F}_{\mathbf{G},\dot{\mathbf{m}}} + \mathbf{F}_{\mathbf{p},\dot{\mathbf{m}}}$$

2.1.6 Special Case: Neglecting Compressibility and Elasticity Effects

If compressibility of water and elasticity of the walls in a Penstock are neglected, a first order model can be derived. Conservation of mass in this case ensures that mass flow rate from the pipe cross section is constant with axial position everywhere along the pipe length. Furthermore if the pipe cross-section area is constant along the pipe length, axial velocity of the water will be constant with axial position. Momentum conservation can be applied to the whole mass of the water inside the pipe with considering the whole pipe as the control volume. Then the differential equation for the mass flow rate can be directly concluded from (2-17) to (2-19):

$$\begin{aligned} v_P &= \frac{\dot{m}_p}{A_P\, \rho_{atm}} \\ L_P\, \frac{d\dot{m}_p}{dt} &= -A_P\, (p_{PX} - p_{PI}) + L_P\, A_P\, \rho_{atm}\, g \sin\theta_P - \frac{1}{2} f_P\, L_P\, \Pi_P\, \rho_{atm}\, \mathrm{sign}(v_P)\, v_P^2 \end{aligned} \tag{2-39}$$

2.2 Francis Turbine

2.2.1 Introduction

Hydraulic power available to be converted into mechanical power by the turbine is given by the following equation (Kjølle, 2001):

$$P_t^h = \frac{1}{\rho^{atm}}\, \dot{m}_t\, \Delta p_t$$

Where

P_t^h: Hydraulic power available for conversion by turbine [W]

$\dot{m}_t$: Mass flow rate of water through turbine [Kg/sec]

Δp_t: Pressure drop across turbine inlet and outlet [Pa]

The above equation can be investigated using the Bernoulli equation with following assumptions:

- Incompressible water with inelastic turbine case walls are assumed so that the mass flow rate is the same at the inlet and outlet of the turbine. This is also the reason why in this case the water density is considered to be constant and equal to ρ^{atm}.
- Power used for accelerating the water inside the turbine case is neglected so that the steady-state turbine equations can be used to describe turbine operation in general case and hence the Bernoulli equation can be applied (considering the huge amount of water in the waterway other than the turbine case, this assumption is acceptable.)
- Difference between the turbine inlet and outlet diameters is neglected. Since the axial velocity of water at both the inlet and the outlet is about a few meters per second, this will cause a small error in estimation of the pressure drop across the turbine which is acceptable for high-head plants. In fact a rotational component is also present at the water leaving the turbine runner which is vanished across the draft tube and so its effect is partly recovered. The remaining effect of the rotational speed is considered in the efficiency of turbine by the manufacturer.

The mechanical output power of the turbine is then given by the following equation:

$$P_t^m = \frac{\eta_t}{\rho_{atm}} \dot{m}_t \, \Delta p_t \qquad (2\text{-}40)$$

Where

$P_t^m =$ Mechanical output power of the turbine [W]

$\eta_t =$ Overall efficiency of the turbine [-]

2.2.2 Turbine Efficiency and Similarity Laws[3]

Turbine efficiency is a function of pressure head across the turbine $H_n = \frac{\Delta p_t}{g\,\rho^{atm}}$ [m] , volumetric flow rate $Q_t = \frac{\dot{m}_t}{\rho^{atm}}$ $[m^3/sec]$, turbine rotational speed ω_m $[rad/sec]$, turbine guide-vane opening $Y_{GV}[\%\text{ or degrees}]$ and turbine mechanical output power $P_t^m[W]$. These five variables are interrelated and if any three of these variables are known, then the other two variables and also efficiency of the turbine can be found using detailed datasheets if provided by the turbine manufacturer. The key datasheet information for this purpose are the so called "hill curves". For using the hill curves one often should be familiar with some terminology, definitions and rules which will follow hereinafter.

Output Power Equation of the Turbine

Figure (2-4) shows trajectory of a water particle that leaves the guide vanes at the point a_0, enters in one of the water passages of the runner at the point a_1 and leaves the runner at the point a_2.

[3] This chapter is based on materials from (Farell, 1987), (Kjølle, 2001), (Selecting Hydraulic Reaction Turbines, 1976) and (Thoresen, 2010)

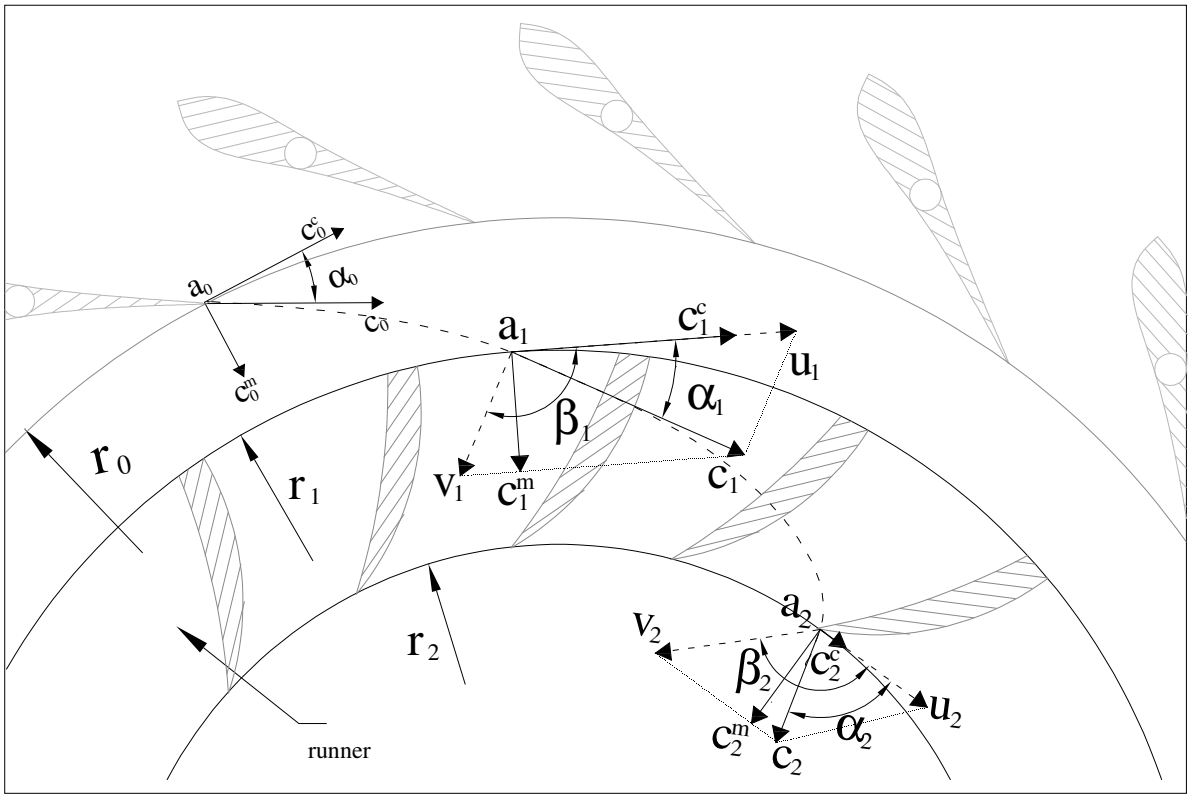

Figure (2-4) Trajectory of a water particle in the turbine (based on (Kjølle, 2001))

Descriptions of the various variables shown in the figure are as follows:

u: Peripheral velocity of the runner

c: Absolute velocity of the water particle measured in a reference frame fixed to the turbine case

$\mathbf{v} = \mathbf{c} - \mathbf{u}$: Relative velocity of the water particle measured in a reference frame fixed to the runner

$\mathbf{c}^c$: Circumferential component of the velocity **c**

$\mathbf{c}^m$: Meridional component of the velocity **c**

The torque induced on the turbine by the water flow is given by:

$$T_t = \dot{m}_t(r_1 c_1^c - r_2 c_2^c) \tag{2-41}$$

In the above equation it's assumed that all the water flowing through the turbine runs through the runner passages (in fact ideal sealing is impossible). The turbine mechanical output power will then be equal to:

$$\begin{aligned} P_t^m &= T_t \omega_m \\ &= \dot{m}_t (r_1 \omega_m c_1^c - r_2 \omega_m c_2^c) \\ &= \dot{m}_t (u_1 c_1^c - u_2 c_2^c) \end{aligned} \tag{2-42}$$

Mechanical losses due to friction are neglected in (2-42). The efficiency equation can be found from (2-40) and (2-42):

$$\eta_t = \rho^{atm} \frac{(u_1 c_1^c - u_2 c_2^c)}{\Delta p_t} \tag{2-43}$$

The efficiency found by (2-43) is in fact the "hydraulic efficiency" of the turbine because mechanical losses like friction losses are not considered in (2-42). If these losses be shifted to the generator side (which has a common shaft with turbine), then η_t in (2-43) can be considered as the overall efficiency of the turbine.

Similar Operating Conditions

Similar operating conditions for the same turbine means conditions under which water particle trajectories inside the turbine casing, runner passages and the draft tube will be the same. For this purpose all the velocities shall be proportional and all the directions (angles) shall be the same when the two operating conditions are being compared. The angle α_0 in Figure (2-4) is considered to be constant for all operating conditions under the same guide vane opening and is determined by the angle that guide vanes make with the circumferential direction at radius r_0. The angle β_2 is also considered to be constant and determined by the angle that the runner blades make with the circumferential direction at radius r_2. It's expected that meridional component of water absolute velocity in between the guide vanes and the runner is proportional to reciprocal of the radius. If travel of water particles in this area be assumed frictionless then water maintains its rotational momentum and hence circumferential component of velocity will also be proportional to reciprocal of the radius. Hence $\alpha_1 \approx \alpha_0$ and therefore $\alpha_1$is also nearly constant for all

operating conditions with fixed guide vane opening. Figure (2-5) shows the same turbine operating in a different condition in which the turbine speed and water flow is reduced.

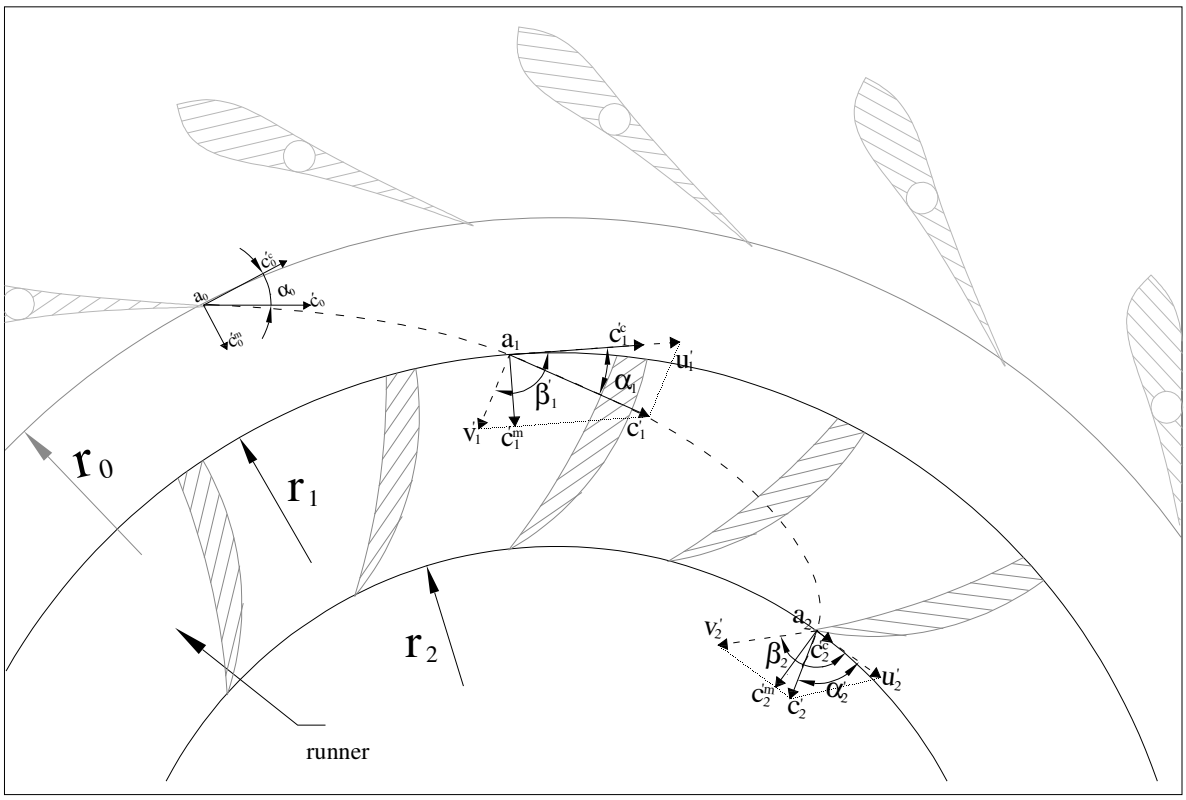

Figure (2-5) Turbine Operating in Different Operation Conditions (Continued from Figure (2-4))

For the two operating conditions shown in the Figure (2-4) and the Figure (2-5) to be similar, the following conditions shall be met:

$$\beta_1' = \beta_1 \, , \alpha_2' = \alpha_2 \, , \frac{u_1'}{u_1} = \frac{c_1'}{c_1} = \frac{v_1'}{v_1} = \frac{u_2'}{u_2} = \frac{c_2'}{c_2} = \frac{v_2'}{v_2} \tag{2-44}$$

It can be shown that only satisfaction of the following relation is enough for the two conditions to be similar:

$$\frac{u_1'}{u_1} = \frac{c_1'}{c_1} \tag{2-45}$$

Proof: The equality $\frac{u_1'}{u_1} = \frac{u_2'}{u_2}$ is obvious. Since $\alpha_1$is constant for all operating conditions, the equalities $\beta_1' = \beta_1$ and $\frac{u_1'}{u_1} = \frac{v_1'}{v_1}$ can be concluded from (2-45). It only remains to prove that equality $\frac{c_1'}{c_1} = \frac{v_2'}{v_2}$ holds by which satisfaction of $\alpha_2' = \alpha_2$ and $\frac{c_1'}{c_1} = \frac{c_2'}{c_2}$ will be proved already (since β_2 is constant). The water volumetric flow rate inside the runner passage in Figure (2-4) is given by $A_1 c_1^m = A_2 v_2$ where A_1 is the circumferential area of the runner passage inlet and $A_2$is the cross section area of the passage outlet perpendicular to v_2. The same holds for the Figure (2-5): $A_1 c_1'^m = A_2 v_2'$ (β_2 is constant so cross section area normal to v_2' is also A_2). Then it follows:

$$(\alpha_1 is\ constant) \Rightarrow \frac{c_1'}{c_1} = \frac{c_1'^m}{c_1^m} = \frac{v_2'}{v_2} \tag{2-46}$$

And this completes the proof.

From the above discussion a sufficient condition for similarity can be stated as below (Farell, 1987):

$$\frac{Q_t}{\omega_m} = constant \tag{2-47}$$

Then for similar operating conditions all the velocities are proportional to ω_m. It is expected that similar operating conditions result in equal efficiencies. So from (2-43) it follows that for similar operating conditions the following holds:

$$\frac{H_n}{\omega_m^2} = \text{constant},\ \frac{P_t^m}{\omega_m^3} = \text{constant}\ , \eta_t = \text{constant} \quad \text{where} \quad H_n = \frac{\Delta p_t}{g\,\rho^{atm}} \tag{2-48}$$

Since it's expected that under the conditions of fixed speed and fixed guide vane opening, each head value corresponds to one and only one discharge value, then the relation $\frac{H_n}{\omega_m^2} = \text{constant}$ can be used as an equivalent sufficient condition for similarity.

Turbine Efficiency Charts

Turbine efficiency charts or the so called "hill charts" or "hill curves" indicate the constant efficiency loci on (Q_t , H_n) or (P_t^m, H_n) plane for design operating speed. Figure (2-6) shows an example for the "hill chart". This chart gives efficiency as a function of the turbine volumetric flow and head at design speed for a specific series of turbines. If the values for design head and design power for a particular turbine in this series are known, then the design speed for that turbine can be found by the parameter N_s. The parameter N_s is the so called "Specific Speed" and defined in the metric system as:

$$N_s = \frac{N_{td}\ (P_{td})^{\frac{1}{2}}}{(H_{td})^{\frac{5}{4}}}$$

Where

N_{td}: Turbine design speed [rpm]

P_{td}: Turbine design power [kW]

H_{td}: Turbine design head [m]

The series of turbines with the hill chart shown in the Figure (2-6) have a specific speed equal to 111 in metric system. So if a particular turbine of this series is designed for operating in 100MW output power and 333m design head, then its design speed will be 500 rpm.

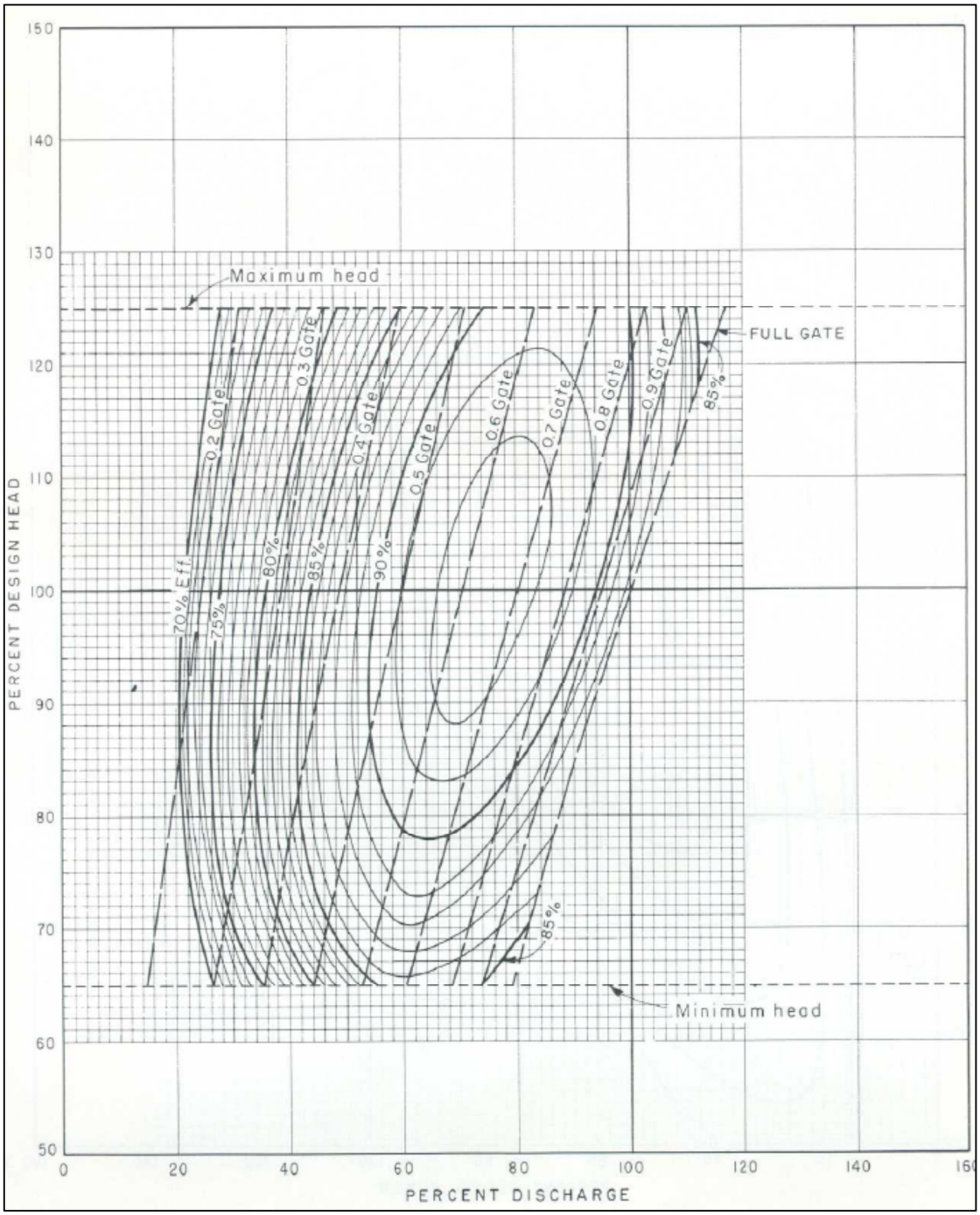

Figure (2-6) An Example of Hill Chat for a Turbine with $N_s = 111$ with Percent Discharge as the Horizontal Axis (Selecting Hydraulic Reaction Turbines, 1976)

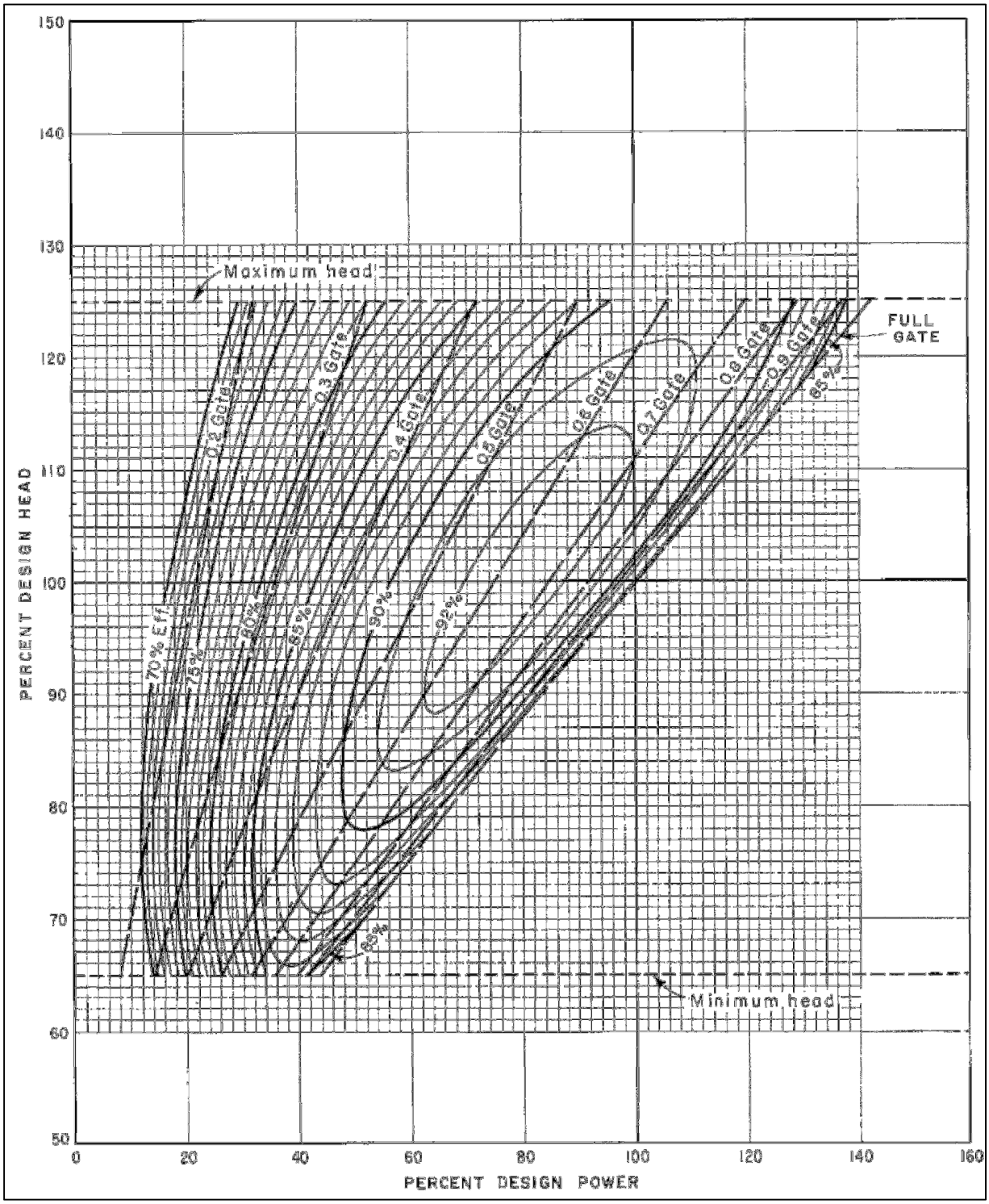

Figure (2-7) An Example of Hill Chat for a Turbine with $N_s = 111$ with Percent Power as the Horizontal Axis (Selecting Hydraulic Reaction Turbines, 1976)

The Figure (2-7) shows the hill chart for the same series of turbines in terms of head versus power. The 100 percent turbine discharge point shown in the Figure (2-6) coincides with the 100 percent design power point in Figure (2-7). If a particular turbine of this series is designed for operating in 100MW output power and 333m design head, then its 100% discharge can be found as follows:

$$P_{td} = \eta_{td}\rho g H_{td} Q_{td}$$

$$100 \times 10^6[\text{Watt}] = 0.85 \times 1000[\text{Kg/m}^3] \times 9.8[\text{m/sec}^2] \times 333[\text{m}] \times Q_{td}[\text{m}^3/\text{sec}]$$

$$Q_{td} = 36\ [\text{m}^3/\text{sec}]$$

Normally design power is chosen so that best efficiency power is equal to 80% of the design power.

The dashed sloped lines in Figure (2-6) show head variations with discharge for different guide vane openings at the design speed. Knowing two out of the three variables (discharge, head and guide vane opening) for the turbine running with the design speed, the third variable and the efficiency of the turbine can be found using the chart shown in the Figure (2-6). Also the turbine power can be determined using (2-40) or from the Figure (2-7).

The question of interest is that if the turbine operated in a speed other than the design speed, how the chart shown in the Figure (2-6) could be used for finding efficiency in the new operating condition. Let's consider that turbine discharge and head at a speed N [rpm] which is different from N_{td} (design speed) are equal to Q $[\text{m}^3/\text{sec}]$ and H [m] respectively. Let's denote this operating condition by (H, Q, N). A similar operating point (H^{eq}, Q^{eq}, N_{td}) can be found using (2-47) and (2-48):

$$\frac{H^{eq}}{N_{td}^2} = \frac{H}{N^2}, \quad \frac{Q^{eq}}{N_{td}} = \frac{Q}{N} \tag{2-49}$$

Since operating points (H, Q, N) and (H^{eq}, Q^{eq}, N_{td}) are similar, they should have equal efficiencies. So efficiency for the off-design operating point can be found by using the equivalent head and discharge values H^{eq} and Q^{eq} in Figure (2-6).

In Figure (2-6) by knowing the values of head and discharge at the design speed one can find the corresponding guide vane opening which resulted in that operating condition. What can be said about the guide vane opening at the operating condition $(\mathrm{H}, \mathrm{Q}, \mathrm{N})$ where N is off-design speed? Since similarity conditions are obtained under assumption of geometric similarity of the flows in scroll case, guide vanes, turbine and draft tube, so it's expected that guide vane opening will be the same for similar conditions. So the corresponding guide vane opening for the operating point $(\mathrm{H}, \mathrm{Q}, \mathrm{N})$ can be found by using the equivalent head and discharge H^{eq} and Q^{eq} in Figure (2-6). That means that: $\mathrm{Y}_{GV}^{\mathrm{eq}} = \mathrm{Y}_{GV}$.

2.2.3 Simulation of Turbine in Matlab

For being able to simulate a turbine in Matlab, data of the "hill chart" for that particular turbine (or series of similar turbines) shall be input into Matlab. For this purpose, an area (will be referred to as "interpolation area" throughout this report) in the hill chart shall be defined which has the following properties:

- Hill chart data shall be defined in allover the interpolation area (for example, this area shouldn't extend beyond the "full gate opening" locus where obviously no head-discharge relationship or efficiency is defined for that area.)
- The interpolation area shall cover as many operating points as possible (including the operating points with higher turbine efficiencies which are the most usual areas of the turbine operation)
- It shall be able to define a uniform grid for the interpolation area (for example if the interpolation area is a rectangle with sides parallel to H and Q axes, grid points can be defined by the following instruction in Matlab: $meshgrid(Q_1 : \Delta Q : Q_2, H_1 : \Delta H : H_2)$)

After deciding on the shape and size of the interpolation area, data (efficiency and/or guide vane opening) at some sample points inside that area can be entered into Matlab. Obviously these sample data points will be scattered and off-grid (no data available at every point). As many sample points as possible shall be chosen. Then data at uniform grid points can be found by 1D interpolation as described in the next paragraph. After data was estimated at the uniform grid points, uniform interpolation functions in Matlab (such as interp2) can be used for further interpolations. The function "interp2" in Matlab requires uniform grid points like the ones

created by the "meshgrid" command and also requires that data be available at all the grid points which these requirements are reflected in the required properties for the interpolation area listed above.

- **Efficiency as a function of Head and Guide-Vane opening**: Examining Figure (2-6) shows that the area defined by inequalities $0.3 \leq \mathrm{Y_{GV}} \leq 1$ and $65\% \leq \mathrm{H} \leq 125\%$ if mapped into a rectangular area in the $\mathrm{Y_{GV}} - \mathrm{H}$ Cartesian coordinates can be a suitable interpolation area. A uniform grid can be defined for that mapped area. The available data in the form of $(\mathrm{Y_{GV}}, \mathrm{H}, \eta)$ extracted from Figure (2-6) are listed in Appendix II. The data are scattered, i.e. there are not the same number of data points for different guide-vane openings and head values (H) are not the same for each data set corresponding to one guide vane opening value. Using a 1D spline interpolation for each set of data corresponding to a fixed guide vane opening, efficiency at fixed head values can be estimated for each guide vane opening. So an interpolated sample data at uniform grid points (like $meshgrid(0.3\!:0.1\!:1, 65\!:5\!:125)$) will be obtained. Then using a 2D interpolation function (like "interp2") a set of data at finer grid points (like $meshgrid(0.3\!:0.01\!:1, 65\!:1\!:125)$) can be generated. This way a look-up table with fine grid has been created. "Spline" or "cubic" interpolation methods are available as options with interp2 function. The look-up table further can be used to build the function $\eta = \mathrm{Eff\_Turb}(\mathrm{Y_{GV}}, \mathrm{H})$. This function interpolates (or extrapolates) the data of the look-up table to give efficiency at the new point $(\mathrm{Y_{GV}}, \mathrm{H})$. Matlab codes for simulation of turbine are given in the Appendix III. Figure (2-8) shows a sketch of the reproduced efficiency values based on the sample data for different guide vane and head values. Figure (2-9) gives a sketch of isocontours of the reproduced efficiency function in the $\mathrm{Y_{GV}} - \mathrm{H}$ plane.

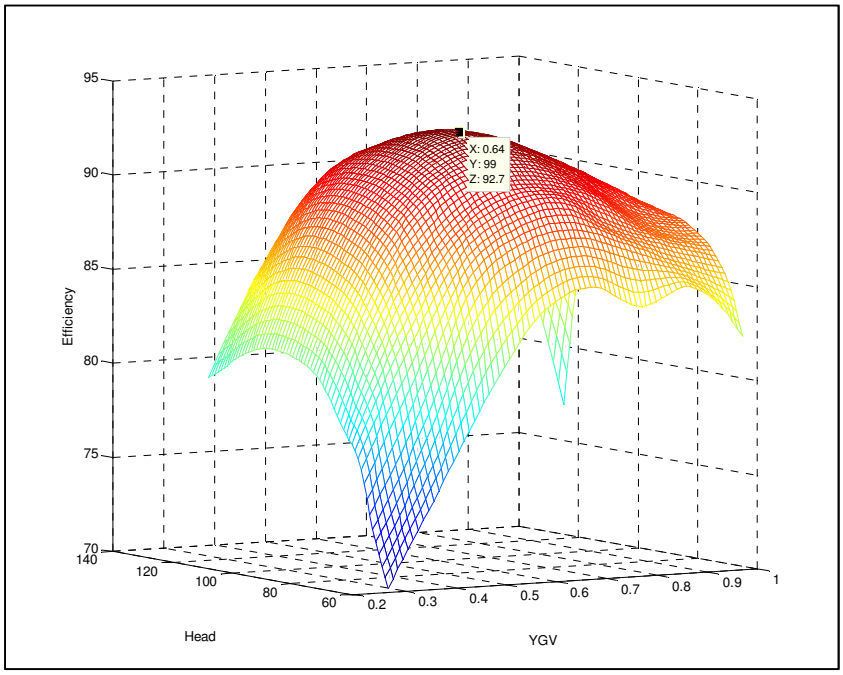

Figure (2-8) Turbine efficiency reproduced in MATLAB by Interpolation of Hill Chart Data

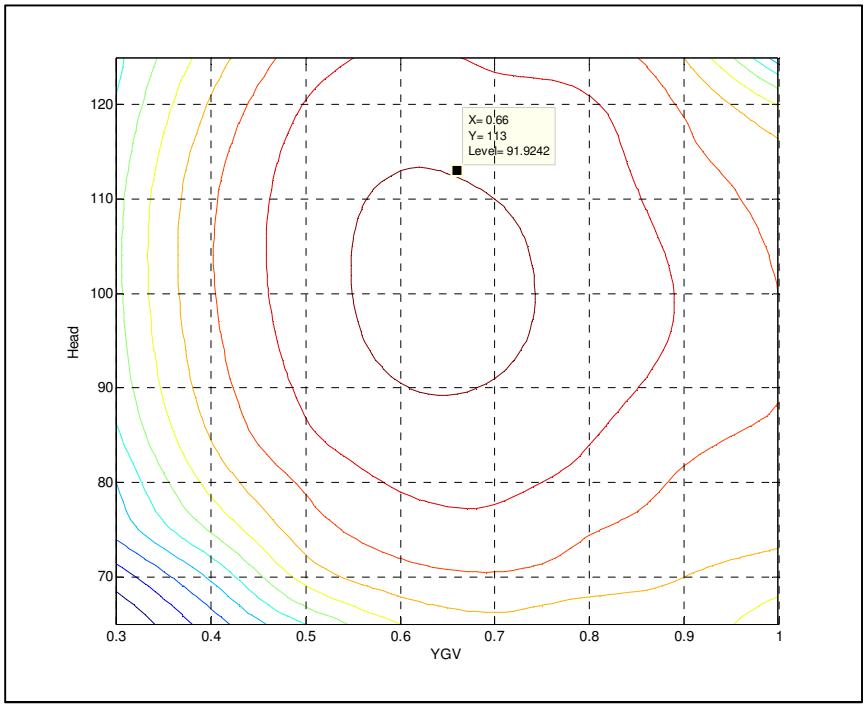

Figure (2-9) Isocontours of Turbine Efficiency Reproduced in MATLAB

- **Head as a function of Discharge and Guide-Vane opening:** From Figure (2-6) it's possible to find turbine discharge as a function of head and guide vane opening and use an interpolation function as described in the above paragraph to create a look-up table for discharge values. Since water flow is inertial and cannot change discontinuously, it's desirable to find head as a function of discharge and guide vane opening. One possible solution is to use a search function to find the head value corresponding to a given discharge and guide-vane opening from the above mentioned look-up table. This process might be slow in simulations. Alternatively another method is suggested in the following which is applicable to the chart in Figure (2-6).

Figure (2-11) shows that fixed guide-vane head-discharge loci in the chart of the Figure (2-6) are almost straight lines (in the range of variations of the head) which have a common intersection point. So a polar coordinate can be introduced for which fixed guide-vane head-discharge loci lie in the same direction as the "fixed-θ" lines. Figure (2-11) is created by importing and scaling the hill chart (image) in the AutoCAD environment. Relationship between position data ($R\,[\%], \theta\,[\text{degree}]$) of a particular point in the hill chart and corresponding (Q=percent discharge, H=percent head) values are as follows (θ is measured from the 100% give-vane opening loci in counterclockwise direction):

$$\begin{aligned} R\cos(72.04^{\circ} + \theta) &= 32.2 + Q \\ R\sin(72.04^{\circ} + \theta) &= 331.6 + (H - 60) \times \frac{134}{70} \end{aligned} \tag{2-50}$$

Figure (2-12) shows the angle θ for different guide vane openings as tabulated below:

θ [degrees]	0	0.64	1.50	2.56	3.30	5.30	6.76	8.16	10.09
Guide vane opening [p.u]	1	0.9	0.8	0.7	0.6	0.5	0.4	0.3	0.2

These data can be interpolated to give θ as a function of guide vane opening. Then from (2-50) with a known Q, the corresponding H value can be determined as the function $H\_Turb(Y_{GV}, Q)$. A sketch of the angle θ versus guide-vane opening found by interpolation is given in Figure (2-10).

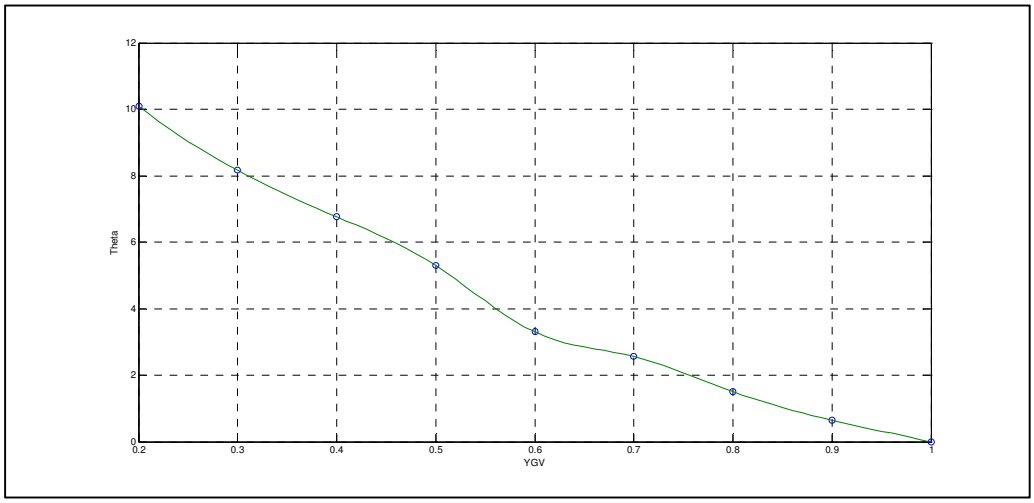

Figure (2-10) Interpolating θ values as a function of Y_{GV} (See text)

If the fixed guide-vane head-discharge loci have more curvature then using the straight line approximations would have less accuracy. In fact discharge of turbine for a given guide vane opening is proportional to the square root of difference between the head and the turbine motoring head. Turbine motoring head varies between 15% and 40% of the design head (Selecting Hydraulic Reaction Turbines, 1976). In the head ranges that turbine operates (between 65% and 125% of the design head) discharge variations with head might be considered almost linear. The accuracy of course might vary for different turbines. Extrapolations for head values outside the range between 65% and 125% of the design head might also have large errors and should be treated carefully.

In most of the literature like in (Machowski, 2008) it's been assumed for simplicity that for constant guide vane opening turbine discharge varies with square root of turbine head. This assumption simply neglects the turbine motoring head discussed in the above paragraph. This assumption implies that the discharge coefficient defined by the following formula for a given guide vane opening is independent of turbine head:

$$c_v = \frac{Q_t}{\sqrt{2gH_t}} \qquad \text{(discharge coefficient)}$$

The accuracy of this assumption can be investigated for the diagram of Figure (2-6). For the full guide vanes opening, discharge values for 65%, 100% and 125% of design head are 79%, 100%

and 117% respectively. Calculation of discharge coefficient at these conditions will result in discharge coefficient values equal to:

$$c_v\Big|_{H=H_{td}} = \frac{Q_{td}}{\sqrt{2gH_{td}}}$$

$$c_v\Big|_{H=0.65H_{td}} = \frac{0.79\ Q_{td}}{\sqrt{2g(0.65\ H_{td})}} = 0.98\ \frac{Q_{td}}{\sqrt{2gH_{td}}}$$

$$c_v\Big|_{H=1.25H_{td}} = \frac{1.17\ Q_{td}}{\sqrt{2g(1.25\ H_{td})}} = 1.05\ \frac{Q_{td}}{\sqrt{2gH_{td}}}$$

As evident, assuming c_v being constant with turbine head can cause up to 7% error in calculation of turbine discharge at full guide vane opening when turbine head varied between its minimum and maximum values.

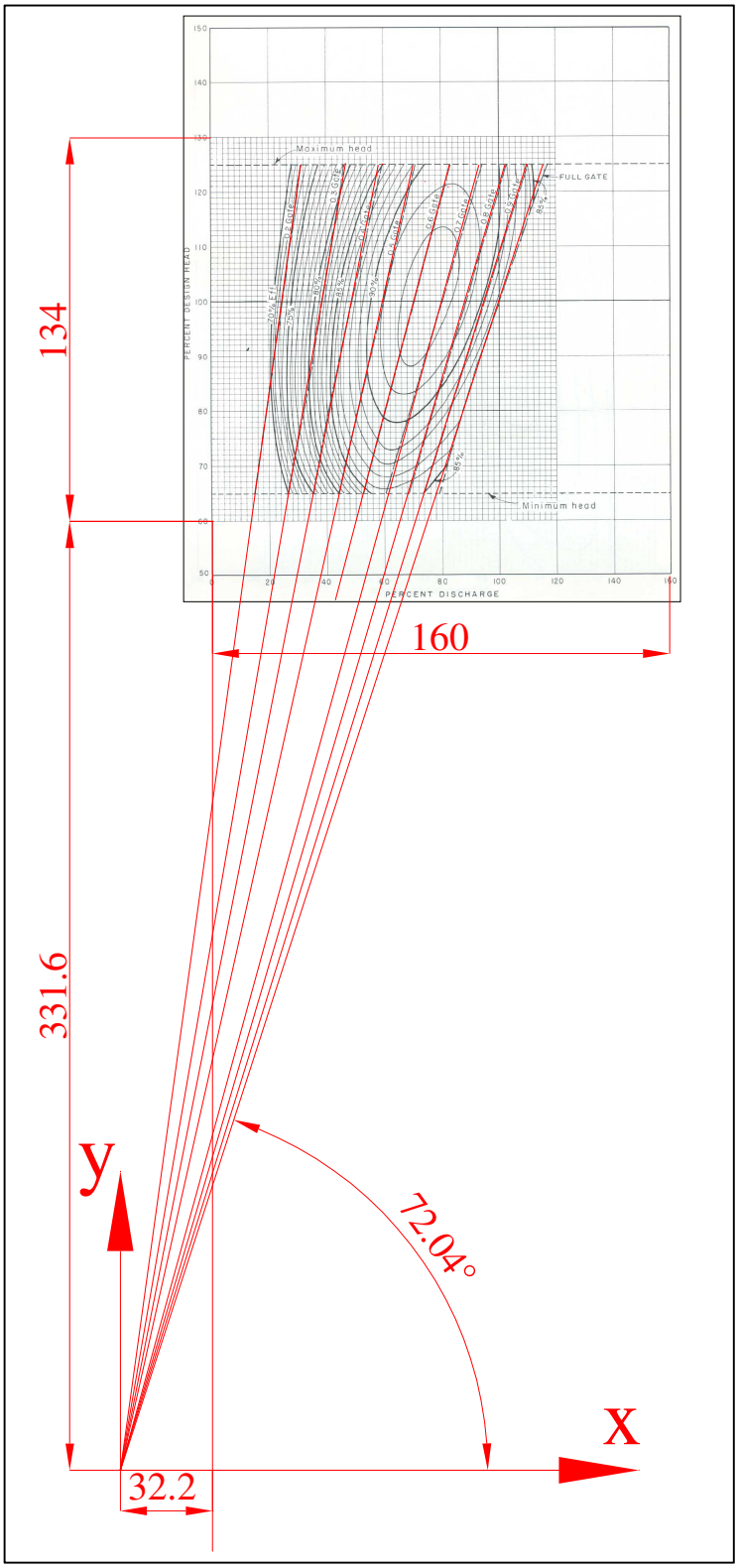

Figure (2-11) Relationship between Turbine Head and Discharge for Fixed Guide Vane Openings

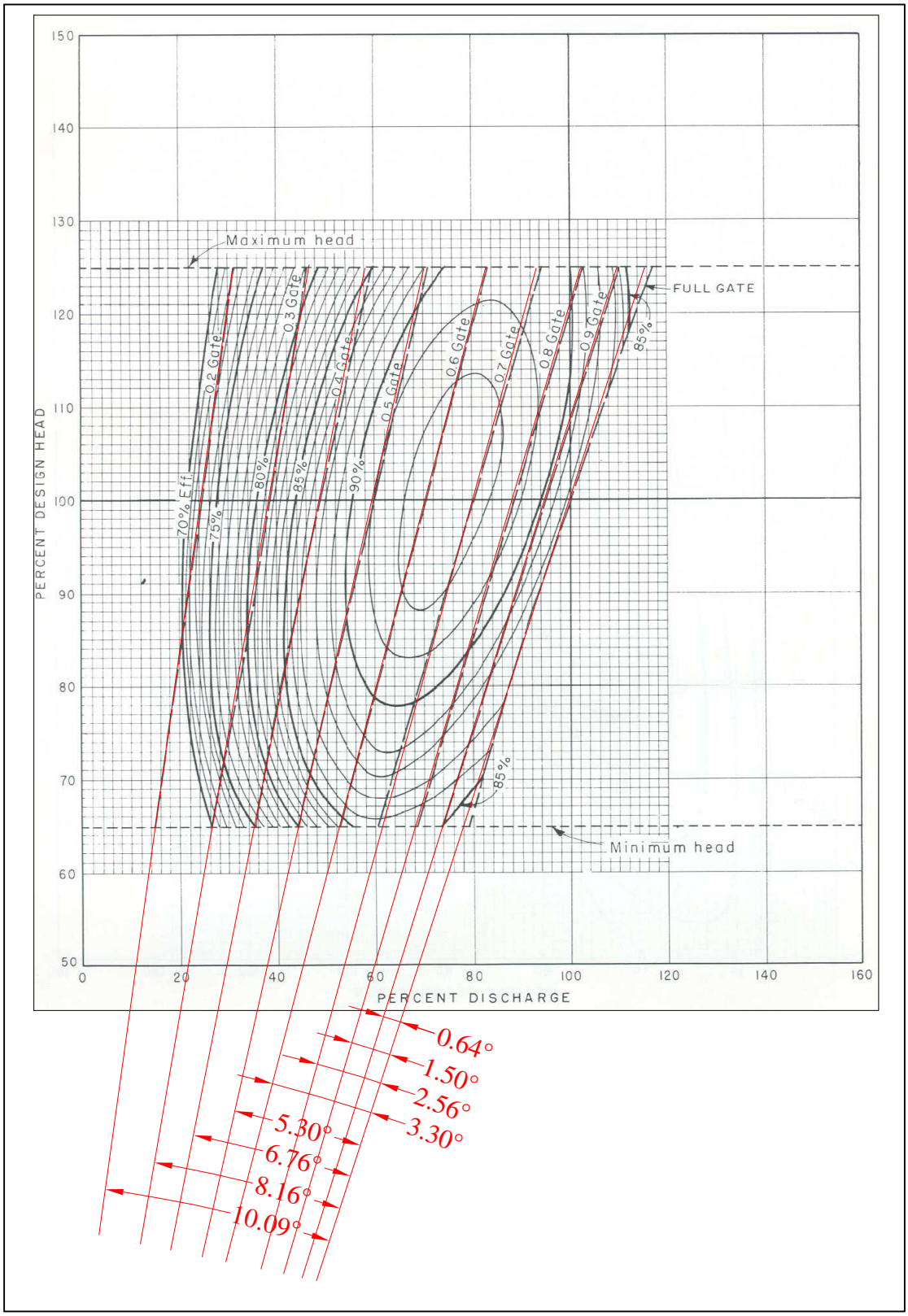

Figure (2-12) Same as Figure (2-11) with More Details

2.2.4 Summary Turbine Model in Matlab

The turbine model is summarized in Table (2-2) below:

Table (2-2) Summary Turbine Model

Q_t : volumetric discharge given [%]

$$Q'_t = \frac{Q_t}{\omega_m} \times \omega_m^{design}$$

$$H'_t = H\_Turb(Y_{GV}, Q'_t)$$

$$\eta_t = Eff\_Turb(Y_{GV}, H'_t)$$

$$H_t = \frac{H'_t}{\left(\omega_m^{design}\right)^2} \times \omega_m^2 \qquad \text{head [\%]}$$

$$P_t^m = \rho^{atm}\, g\, \eta_t\, H_t\, Q_t \quad (H_t \text{ in [m] and } Q_t \text{ in } [m^3/sec])$$

2.3 Models for Head-Water and Tail-Water

In this section models in the form of differential equations are introduced for head water and tail water systems. These models are available in the literature like in (Lie, 2011). **Here the models are further developed to interface elastic penstock.** Head water system consists of reservoir, intake, conduit, surge shaft and finally the penstock. Tail water system consists of turbine, draft tube, tail water tunnel and tail water reservoir. For simplicity it's assumed that level of water in both reservoirs doesn't change (for example because of make-up water flowing into the head water reservoir or water flowing out from the reservoir in tail water. Incompressible water and inelastic walls are assumed everywhere except for the penstock. First models for the case in which elastic penstock is considered will be given. Then the model for inelastic penstock case can be obtained as a special case.

2.3.1 Local Pressure Losses

Local pressure losses (hence energy losses) take place at the intake, bends, joints, orifices (surge shaft) and cross-section area widening or reduction in different places along the waterway. The total inertia of the water flowing in locations that these losses take place can be neglected compared to the inertia of the huge amount of water that flows in the whole waterway. So steady-state (instead of dynamic) models of these losses can be used in the dynamic model of the whole waterway with enough accuracy. The equations available as models for these losses are described in (Thoresen, 2010). Due to relatively low speed of water inside the waterway these losses are not very important in a high head plant. So they will be ignored in models that will be introduced in the next two subsections.

2.3.2 Head Water System

Figure (2-13) shows the components of the head water system that are considered in the model in this subsection.

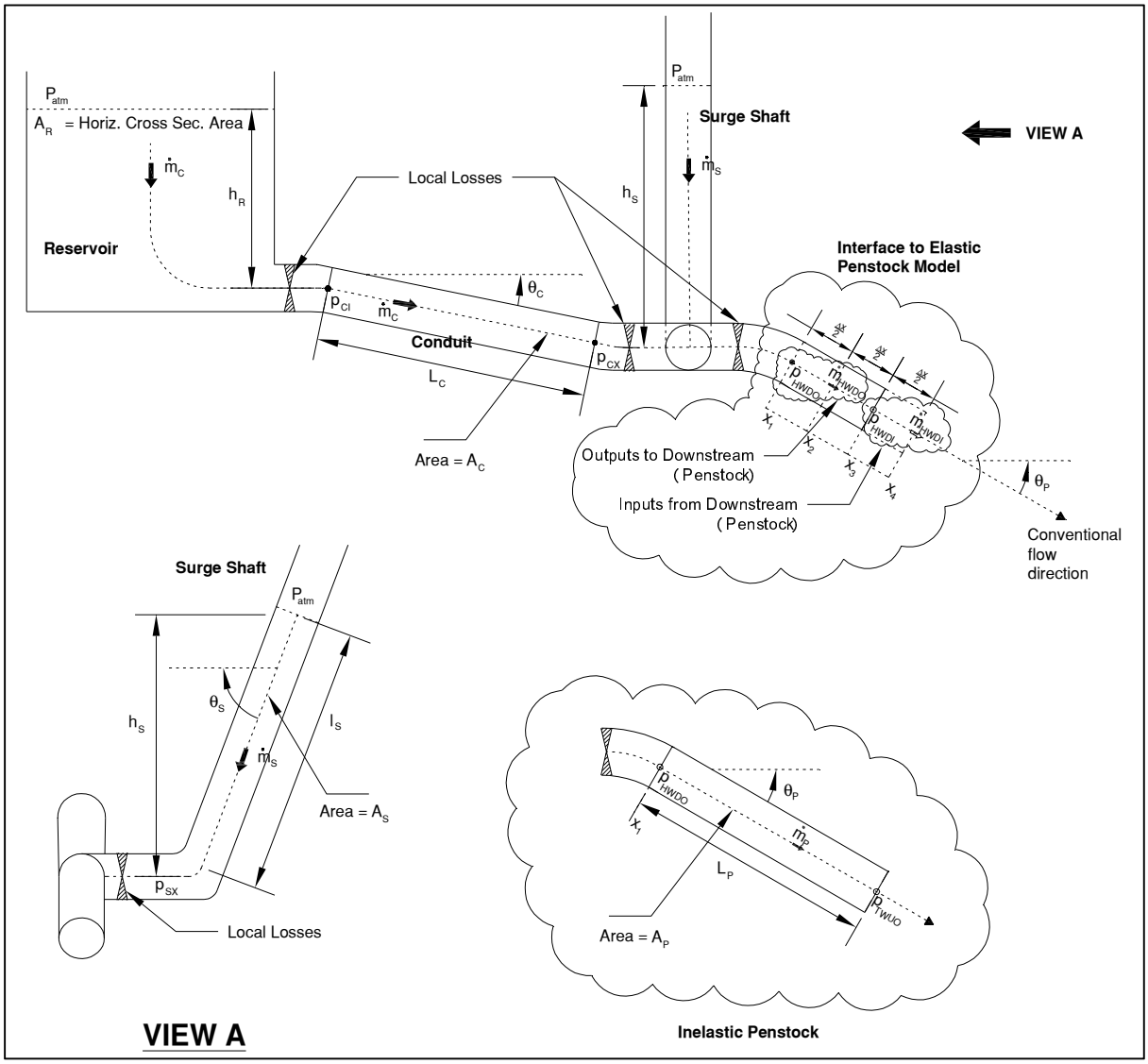

Figure (2-13) Head Water System with Interface to Elastic Penstock

Three subsystems can be recognized for modeling: Reservoir-conduit, surge shaft and finally penstock interface. These subsystems join together at a T-junction. Conservation of mass will result in the following relationship between mass flow rates in the conduit, surge shaft and penstock interface:

$$\dot{m}_{HWDO} = \dot{m}_C + \dot{m}_S \qquad (2\text{-}51)$$

If local losses and velocity heads are neglected at the conduit-surge shaft- penstock junction, the following approximation can be concluded:

$$p_{CX} \approx p_{SX} \approx p_{HWDO} \tag{2-52}$$

- **Reservoir-conduit Subsystem:** It's assumed that water is added to the reservoir surface to keep h_R constant. Horizontal components of the water velocity inside the reservoir are not modeled and it's assumed that vertical component of the water velocity is the same at all locations inside the reservoir. Axial mass flow rate $\dot{m}_C$ in the conduit is assumed to be equal to the mass flow rate across the horizontal cross-section area of the reservoir due to the assumption that make-up water is added just to the surface and there is just one intake where water flows out and also incompressible water assumption. Intake losses are neglected. Wall frictions inside the reservoir are neglected too. Writing the momentum equation (2-39) for the volume of water inside the reservoir and also for the conduit will result:

$$h_R \frac{d\dot{m}_C}{dt} = -A_R(p_{CI} - p^{atm}) + \rho^{atm} g h_R A_R \tag{2-53}$$

$$L_C \frac{d\dot{m}_C}{dt} = -A_C(p_{CX} - p_{CI}) + \rho^{atm} g\, L_C\, A_C \sin\theta_C - \mathcal{K}_C\, \dot{m}_C^2 \tag{2-54}$$

Where

$$\mathcal{K}_C = \frac{f_C\, L_C\, \Pi_C\, sign(\dot{m}_C)}{2\, A_C^2\, \rho^{atm}}$$

When $A_R \to \infty$, the reservoir can be considered as a fixed head source and the Equation (2-53) will change to the following approximate algebraic relation:

$$p_{CI} \approx p^{atm} + \rho^{atm}\, g\, h_R \tag{2-55}$$

- **Surge Shaft:** By applying the momentum conservation for the water volume inside the surge shaft using the equations (2-17) to (2-19) and (2-39) will result in the following equation:

$$l_S \frac{d\dot{m}_S}{dt} - \dot{m}_S \frac{dl_S}{dt} = -A_s(p_{SX} - p^{atm}) + \rho^{atm} g\, l_S\, A_S \sin\theta_S - \frac{f_S\, l_S\, \Pi_S\, sign(\dot{m}_S)}{2\, A_S^2\, \rho^{atm}}\, \dot{m}_S^2 \quad (2\text{-}56)$$

The term $\left(-\dot{m}_S \frac{dl_S}{dt}\right)$ in the above equation is because one of the boundaries for the control volume for momentum equation is moving with time by a speed equal to:

$$\frac{dl_S}{dt} = -\frac{\dot{m}_S}{A_S \rho^{atm}} \quad (2\text{-}57)$$

Substituting $\frac{dl_S}{dt}$ from (2-57) into (2-56) will result in the following equation:

$$l_S \frac{d\dot{m}_S}{dt} + \mathcal{K}_S \dot{m}_S^2 = -A_s(p_{SX} - p^{atm}) + \rho^{atm} g\, l_S\, A_S \sin\theta_S$$

Where

$$\mathcal{K}_S = \frac{f_S\, l_S\, \Pi_S\, sign(\dot{m}_S)}{2\, A_S^2\, \rho^{atm}} + \frac{1}{A_S\, \rho^{atm}} \quad (2\text{-}58)$$

- **Conduit Interface:** An equation of the form (2-39) can be developed for the volume enclosed between the axial positions X_1 and X_3 in Figure (2-13):

$$\Delta x \frac{d\dot{m}_{HWDO}}{dt} = -A_2(p_{HWDI} - p_{HWDO}) + \rho_{atm}\, g\, \Delta x\, A_2 \sin\theta_P - \mathcal{K}_{HW}\, \dot{m}_{HWDO}^2$$

Where

$$\mathcal{K}_{HW} = \frac{f_P\, \Delta x\, \Pi_2\, sign(\dot{m}_{HWDO})}{2\, A_2^2\, \rho^{atm}} \quad (2\text{-}59)$$

Equations (2-54), (2-58) and (2-59) are for variables which are linearly dependent according to (2-51). So the headwater subsystem's order actually is three. It's possible to omit the equation (2-58) to find p_{HWDO} in terms of other variables:

$$\left(\frac{A_C}{L_C}+\frac{A_2}{\Delta x}+\frac{A_s}{l_S}\right)p_{HWDO}=\left(\frac{A_C}{L_C}p_{CI}+\frac{A_2}{\Delta x}p_{HWDI}+\frac{A_s}{l_S}p^{atm}\right)+$$
$$\rho_{atm}\,g\,(A_C\sin\theta_C-A_2\sin\theta_P+A_S\sin\theta_S)-\frac{\mathcal{K}_C}{L_C}\dot{m}_C^2-\frac{\mathcal{K}_S}{l_S}(\dot{m}_{HWDO}-\dot{m}_C)^2+\frac{\mathcal{K}_{HW}}{\Delta x}\dot{m}_{HWDO}^2 \quad (2\text{-}60)$$

So the Equations (2-51), (2-52), (2-54), (2-55), (2-57), (2-59) and (2-60) define the model for the head water system. It's possible to replace for the variables $\dot{m}_S$, p_{CX} and p_{SX} from equations (2-51) and (2-52) to get the final set of equations for the head water system as summarized in Table (2-3).

Table (2-3) Summary Head Water System Model

$$\mathcal{K}_S=\frac{f_S\,l_S\,\Pi_S\,\mathrm{sign}(\dot{m}_{HWDO}-\dot{m}_C)}{2\,A_S^2\,\rho^{atm}}+\frac{1}{A_S\,\rho^{atm}}$$

$$\mathcal{K}_C=\frac{f_C\,L_C\,\Pi_C\,\mathrm{sign}(\dot{m}_C)}{2\,A_C^2\,\rho^{atm}}$$

$$\mathcal{K}_{HW}=\frac{f_P\,\Delta x\,\Pi_2\,\mathrm{sign}(\dot{m}_{HWDO})}{2\,A_2^2\,\rho^{atm}}$$

$$p_{CI}=p^{atm}+\rho^{atm}\,g\,h_R$$

$$p_{HWDO}=\left(\frac{A_C}{L_C}+\frac{A_2}{\Delta x}+\frac{A_s}{l_S}\right)^{-1}\left[\left(\frac{A_C}{L_C}p_{CI}+\frac{A_2}{\Delta x}p_{HWDI}+\frac{A_s}{l_S}p^{atm}\right)+\right.$$
$$\left.\rho_{atm}\,g\,(A_C\sin\theta_C-A_2\sin\theta_P+A_S\sin\theta_S)-\frac{\mathcal{K}_C}{L_C}\dot{m}_C^2-\frac{\mathcal{K}_S}{l_S}(\dot{m}_{HWDO}-\dot{m}_C)^2+\frac{\mathcal{K}_{HW}}{\Delta x}\dot{m}_{HWDO}^2\right]$$

$$\frac{dl_S}{dt}=\frac{\dot{m}_C-\dot{m}_{HWDO}}{A_S\rho^{atm}}$$

$$L_C \frac{d\dot{m}_C}{dt} = -A_C(p_{HWDO} - p_{CI}) + \rho^{atm} g\, L_C\, A_C \sin\theta_C - \mathcal{K}_C \dot{m}_C^2$$

$$\Delta x \frac{d\dot{m}_{HWDO}}{dt} = -A_2(p_{HWDI} - p_{HWDO}) + \rho^{atm} g\, \Delta x\, A_2 \sin\theta_P - \mathcal{K}_{HW} \dot{m}_{HWDO}^2$$

2.3.3 Turbine, Draft Tube and Tail Water System

The model discussed in this subsection consists of an interface to penstock, turbine, draft tube, tail water tunnel and tail water reservoir. Tail water tunnel always has a positive slope in the direction of water flow to insure submergence of the turbine in water and prevent cavitation problems. Like the head water, here also three subsystems can be verified:

- **Interface to Penstock:** The equation is similar to (2-59):

$$\Delta x \frac{d\dot{m}_{TWDO}}{dt} = -A_{2N}(p_{TWUO} - p_{TWUI}) + \rho^{atm} g\, \Delta x\, A_{2N} \sin\theta_P - \mathcal{K}_{TW} \dot{m}_{TWDO}^2$$

Where

$$\mathcal{K}_{TW} = \frac{f_P\, \Delta x\, \Pi_{2N}\, \mathrm{sign}(\dot{m}_{TWDO})}{2\, A_{2N}^2\, \rho^{atm}} \qquad (2\text{-}61)$$

- **Turbine and draft tube:** Turbine equations are given in Table (2-2). Dynamics of the draft tube is neglected in here to avoid complexity, but static pressure of the water column inside the draft tube may be accounted for in the model. So the following relationship will be held for the pressures from the turbine inlet to the draft tube outlet:

$$P_{TWUO} = \rho^{atm} g\, H_t - \rho^{atm} g\, h_{DT} + P_{TWTI} \qquad (2\text{-}62)$$

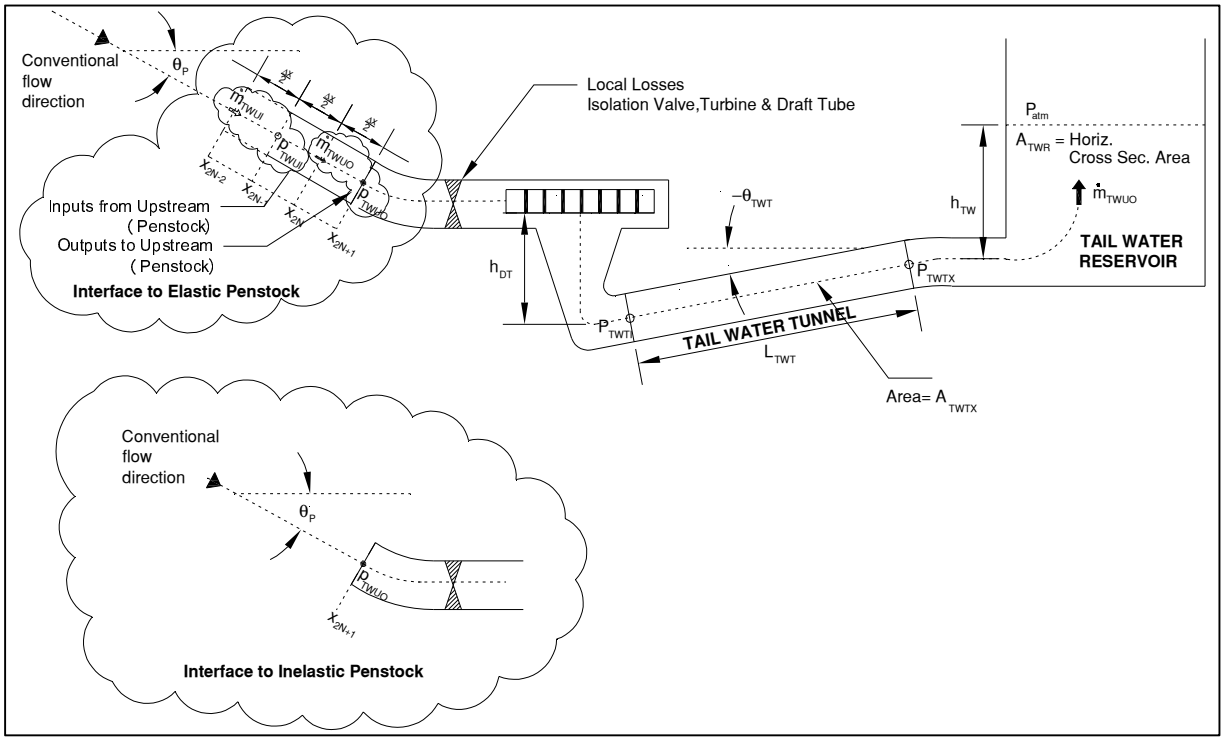

Figure (2-14) Tail Water System with Interface to Elastic Penstock

- **Tail Water Tunnel and Reservoir:** Like the reservoir at the head water if the horizontal cross section area of the tail water reservoir be quite large, then pressure at outlet of the tail water tunnel can be considered to be fixed:

$$p_{TWTX} = p^{atm} + \rho^{atm}\, g\, h_{TW} \tag{2-63}$$

The water flow rate in the tail water tunnel is equal to the water flow rate at the penstock interface (Penstock interface is inelastic and so is the whole of the downstream of the interface). So the pressure drop at the both ends of the head water tunnel can be determined from the following differential equation:

$$L_{TWT}\frac{d\dot{m}_{TWDO}}{dt} = -A_{TWT}(p_{TWTX} - p_{TWTI}) - \rho^{atm} g\, L_{TWT}\, A_{TWT} \sin\theta_{TWT} - \mathcal{K}_{TWT}\dot{m}^2_{TWDO} \tag{2-64}$$

Where

$$\mathcal{K}_{TWT} = \frac{f_{TWT}\, L_{TWT}\, \Pi_{TWT}\, \mathrm{sign}(\dot{m}_{TWDO})}{2\, A_{TWT}^2\, \rho^{atm}} \tag{2-65}$$

Solving (2-61), (2-62) and (2-64) for p_{TWUO} will give:

$$P_{TWUO} = \left(1 + \frac{L_{TWT}}{\Delta x}\frac{A_{2N}}{A_{TWT}}\right)^{-1} \left(\rho^{atm} g\, (H_t - h_{DT}) + p_{TWTX} + \frac{L_{TWT}}{\Delta x}\frac{A_{2N}}{A_{TWT}}\, p_{TWUI} + \right.$$
$$\left. \rho_{atm}\, g\, L_{TWT} \left(\sin\theta_{TWT} + \frac{A_{2N}}{A_{TWT}}\sin\theta_P\right) + \left(\mathcal{K}_{TWT} - \frac{L_{TWT}}{\Delta x}\mathcal{K}_{TW}\right)\frac{\dot{m}_{TWDO}^2}{A_{TWT}}\right) \tag{2-66}$$

Relations given in Table (2-2) together with Equations (2-61), (2-63) and (2-66) define the tail water system model which is summarized in Table (2-4) for convenience:

Table (2-4) Summary Tail Water Model

$Q_t = \frac{\dot{m}_{TWUO}}{\rho_{atm}} \times \frac{100}{Q_t^{design}}$	Turbine volumetric discharge [%]
$Q_t^{eq} = \frac{Q_t}{\omega_m} \times \omega_m^{design}$	
$H_t^{eq} = \mathrm{H\_Turb}(Y_{GV}, Q_t^{eq})$	
$\eta_t = \mathrm{Eff\_Turb}(Y_{GV}, H_t^{eq})$	
$H_t = \left[\frac{H_t^{eq}}{\left(\omega_m^{design}\right)^2} \times \omega_m^2\right] \times \frac{H_t^{design}}{100}$	Turbine head [m]
$P_t = \rho_{atm}\, g\, \eta_t\, H_t\, Q_t$	Turbine power [Watt]
$p_{TWTX} = p^{atm} + \rho^{atm}\, g\, h_{TW}$	

$$\mathcal{K}_{TWT} = \frac{f_{TWT}\, L_{TWT}\, \Pi_{TWT}\, \text{sign}(\dot{m}_{TWUO})}{2\, A_{TWT}^2\, \rho^{atm}}$$

$$\mathcal{K}_{TW} = \frac{f_P\, \Delta x\, \Pi_{2N}\, \text{sign}(\dot{m}_{TWUO})}{2\, A_{2N}^2\, \rho^{atm}}$$

$$P_{TWUO} = \left(1 + \frac{L_{TWT}}{\Delta x}\frac{A_{2N}}{A_{TWT}}\right)^{-1}\left(\rho^{atm} g\,(H_t - h_{DT}) + p_{TWTX} + \frac{L_{TWT}}{\Delta x}\frac{A_{2N}}{A_{TWT}}\, p_{TWUI} + \right.$$

$$\left. \rho_{atm}\, g\, L_{TWT}\left(\sin\theta_{TWT} + \frac{A_{2N}}{A_{TWT}}\sin\theta_P\right) + \left(\mathcal{K}_{TWT} - \frac{L_{TWT}}{\Delta x}\mathcal{K}_{TW}\right)\frac{\dot{m}_{TWUO}^2}{A_{TWT}}\right)$$

$$\Delta x \frac{d\dot{m}_{TWUO}}{dt} = -A_{2N}(p_{TWUO} - p_{TWUI}) + \rho^{atm} g\, \Delta x\, A_{2N} \sin\theta_P - \mathcal{K}_{TW}\dot{m}_{TWUO}^2$$

2.3.4 Waterway Model with Inelastic Penstock

The waterway Model with inelastic penstock walls and incompressible water inside the penstock consists of the equations in Table (2-3) and Table (2-4) except for the last equation in each table. Instead a differential equation based on the Equation (2-39) can be developed for mass flow rate in the penstock:

$$L_P \frac{d\dot{m}_P}{dt} = -A_P(p_{TWUO} - p_{HWDO}) + \rho_{atm}\, g\, L_P\, A_P \sin\theta_P - \mathcal{K}_P \dot{m}_P^2$$

$$\mathcal{K}_P = \frac{f_P\, L_P\, \Pi_P\, \text{sign}(\dot{m}_P)}{2\, A_P^2\, \rho^{atm}} \qquad (2\text{-}67)$$

Also in other equations of Table (2-3) and Table (2-4):

$\dot{m}_{TWDO}$ and $\dot{m}_{HWDO}$ will be replaced with $\dot{m}_P$

Δx will be replaced with L_P

A_2 and A_{2N} will be replaced with A_P

Π_2 and Π_{2N} will be replaced with Π_P

$\mathcal{K}_{HW}$ and $\mathcal{K}_{TW}$ will be replaced with $\mathcal{K}_P$

p_{HWDI} will be replaced with p_{TWUO}

p_{TWUI} will be replaced with p_{HWDO}

p_{HWDI} in Table (2-3) will changed to p_{TWUO}

Moreover, p_{HWDO} and p_{TWUO} can be found by solving the following set of equations:

$$(\mathcal{C}_1 + \mathcal{C}_2)p_{HWDO} - \mathcal{C}_2 p_{TWUO} = \mathcal{C}_3$$

$$-\mathcal{C}_4 p_{HWDO} + (1 + \mathcal{C}_4)p_{TWUO} = \mathcal{C}_5$$

Where

$$\mathcal{C}_1 = \frac{A_C}{L_C} + \frac{A_s}{l_S} \tag{2-68}$$

$$\mathcal{C}_2 = \frac{A_P}{L_P}$$

$$\mathcal{C}_3 = \frac{A_C}{L_C} p_{CI} + \frac{A_s}{l_S} p^{atm} + \rho^{atm} g\,(A_C \sin\theta_C - A_P \sin\theta_P + A_S \sin\theta_S) - \frac{\mathcal{K}_C}{L_C}\dot{m}_C^2 - \frac{\mathcal{K}_S}{l_S}(\dot{m}_P - \dot{m}_C)^2 + \frac{\mathcal{K}_P}{L_P}\dot{m}_P^2$$

$$\mathcal{C}_4 = \frac{L_{TWT}}{L_P}\frac{A_P}{A_{TWT}}$$

$$\mathcal{C}_5 = \rho^{atm} g\,(H_t - h_{DT}) + p_{TWTX} + \rho^{atm} g\, L_{TWT}\left(\sin\theta_{TWT} + \frac{A_P}{A_{TWT}}\sin\theta_P\right) + \left(\mathcal{K}_{TWT} - \frac{L_{TWT}}{L_P}\mathcal{K}_P\right)\frac{\dot{m}_P^2}{A_{TWT}}$$

2.4 Turbine Controller

A transient droop governor which has been used extensively in the hydropower installations will be considered for simulations in this chapter. First concepts of "swing equation" and "speed droop" shall be introduced.

Swing Equation: The mechanical energy stored in the rotating parts of the hydropower generation unit (turbine and generator rotor) is given by the following equation where J is the moment of inertia of the rotating body:

$$E = \frac{1}{2} J\omega^2$$

Rate of change of this stored energy is equal to the net power entering the system of rotating body. That means:

$$J\omega \frac{d\omega}{dt} = P_{in} - P_{loss} - P_{out} \quad (2\text{-}69)$$

Where

P_{in}: Hydraulic power transferred to turbine

P_{out}: Active electric power output at terminals of the generator

$P_{loss} =$: Power losses through turbine and generator

The equation (2-69) is known as the swing equation of the generator. The term P_{loss} may be considered equal to $(1 - \eta_g) \times P_{in}$ if all the mechanical losses of the turbine-generator body and resistive losses at the generator armature are accounted for in the generator efficiency (η_g) in which case the equation (2-69) will become:

$$J\omega \frac{d\omega}{dt} = \eta_g P_{in} - P_{out} = \eta_g \eta_t \rho g H_t Q_t - P_{out} \quad (2\text{-}70)$$

Speed Droop: According to the above paragraph electrical frequency in an interconnected network of generators and loads is a function of the stored energy in the rotating bodies of generators in that network. So changes in the electrical frequency depend on the balance between the total generated and consumed power in that network. If frequency drops below a reference value, each generator in that network will try to correct the frequency by increasing their active output power. This correction action is one of the turbine governor's duties. The frequency-power characteristic of a generator is a straight line with negative slope as shown in the Figure (2-15).

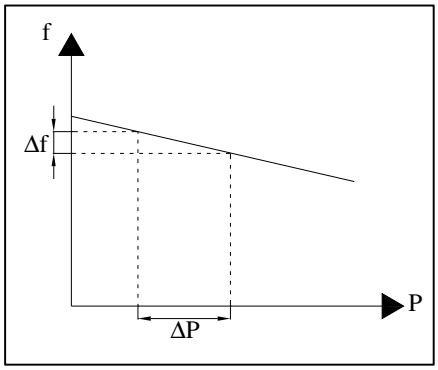

Figure (2-15) Turbine Governor Freq.-Speed Characteristics (Schavemaker, 2009)

Absolute value (in percent) of the negative slope of the frequency-speed characteristics of a generation unit when the power and the frequency are given in per unit system is known as the droop or regulation and can be expressed as (Schavemaker, 2009):

$$S = -100 \times \frac{\Delta f / f_{Ref}}{\Delta P / S_B} \quad (2\text{-}71)$$

Where

S: droop [%]

f_{Ref}: desired frequency of the network [Hz]

S_B: rated power of the generator [MVA]

If generation units in an interconnected network have zero droop (it means that each generation unit would increase its output power until frequency corrected exactly) then faster generation units would increase their output power after a decrease in the frequency more than generation units with slower response and this will cause the network load be distributed between the generation units randomly (Schavemaker, 2009) . Another unwanted scenario is also likely to occur (Warnick, 1984): It's impossible for the generation units to have exactly the same frequency set point (or better to say it's impossible for these units to have the same error pattern in measuring the frequency, some might have negative errors whilst others might have positive errors). Units with higher set point will try to increase the network frequency to their set point until they achieve this goal or reach their maximum power. If they be able to increase the

network frequency, the units with lower set point will decrease their load to lower the frequency. This will continue until the units with higher set point will take the entire network load to themselves (if they have enough capacity) and the other units will go to the standby mode.

Unwanted situations discussed above are resolved by assigning negative speed droops to the generation units. If a unique value is assigned as droop to all the generation units, then each unit will take part in the frequency correction with an amount of power which is proportional to its rating output power.

Transient Droop Governor: Governing system for hydropower turbines usually has two servomotors: Pilot servomotor and main servomotor. The pilot servomotor operates a relay valve which in turn operates the high power main servomotor. The main servomotor changes the guide vanes opening position. These servomotors usually are hydraulic devices and operate with hydraulic oil pressure. (Machowski, 2008)

A typical block diagram of the so called "transient droop controller" is shown in the Figure (2-16). The pilot servomotor is models as a first order system. The main servomotor is modeled as an integrator with limit on the output and also on the rate of change of the output in both directions (increasing or decreasing). Limits on the rate of change of the guide vanes position are necessary for preventing high pressure surges due to the water hammer effect. These limits can be different when the guide vane closing and opening. Guide vanes should be able to close fast so that over speed of the turbine is prevented in case of a large load rejection. (Thoresen, 2010)

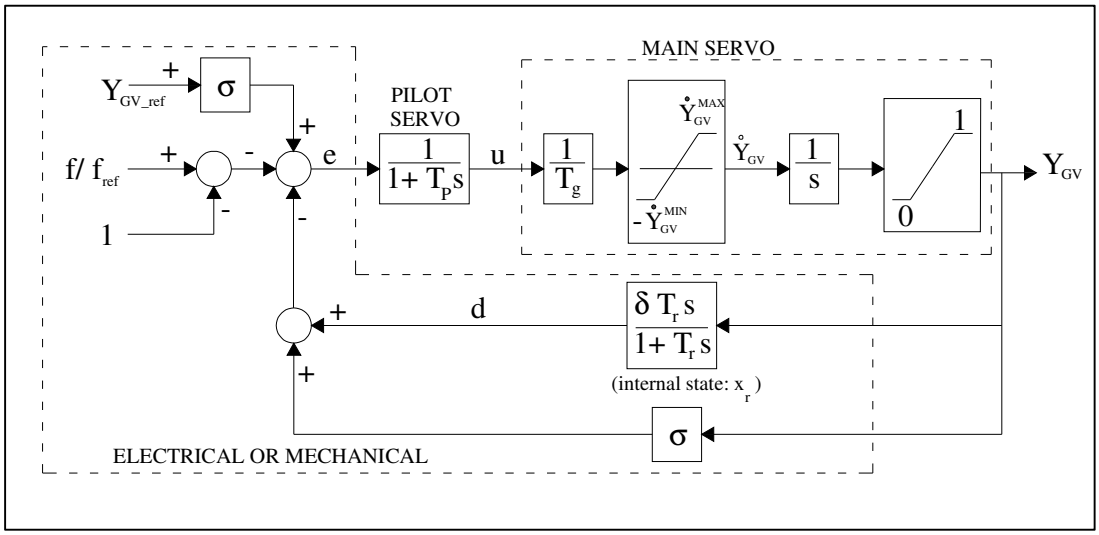

Figure (2-16) Block Diagram of Transient Droop Controller (Machowski, 2008)

Y_{GV} and Y_{GV_ref} vary between 0 and 1 (per unit values). Integral action of the main servomotor is used in the control. This action in the steady state will cause the error $\sigma(Y_{GV\_ref} - Y_{GV}) + (1 - f/f_{ref})$ vanish. So if the output power of turbine be proportional to Y_{GV}, then σ could actually be considered as the per unit value of the droop. The differentiating block $\frac{\delta T_r s}{1+T_r s}$ causes lower rate of change in Y_{GV} right after a disturbance and then rate of change increases gradually. This allows the water column velocity in the penstock to catch up the guide vanes movements. (Machowski, 2008)

The signal conditioning part of the block diagram in Figure (2-16) might be implemented mechanically or electrically. One disadvantage of the transient droop governor as is evident from the Figure (2-16) is that the feedback for implementing the static (steady state) droop is taken from the guide vanes position instead of generator output active power. This can cause deviations in power delivered to the network (Thoresen, 2010) . In (Thoresen, 2010) and (Johansson, 2009) controller configurations for using the feedback from the generator output active power are given. In (Johansson, 2009) also more complicated models for the pilot and main servomotors considering backlash and friction are introduced.

Typical values for parameters of a transient droop controller are given in (Machowski, 2008):

$T_P = 0.04$ [sec] , $T_g = 0.2$ [sec] , $T_r = 5T'_w$, $\delta = 2.5T'_w/T_m$

Where $T'_w = \frac{L_P Q_t^{oper.point}}{A_P g H_t^{oper.point}}$ is called "water starting time" and $T_m = \frac{J\omega_{sm}^2}{S_B}$ is called "Mechanical time constant. Typical values for the static droop σ are given as 3 to 6 percent in (Machowski, 2008) and 10 percent for Norway in 2010 in (Thoresen, 2010).

Set of equations modeling the controller shown in Figure (2-16) is given in Table (2-5).

Table (2-5) Transient Droop Controller Model

$d = \delta Y_{GV} - x_r$

$$e = \sigma\left(Y_{GV\_ref} - Y_{GV}\right) - \left(\frac{f}{f_{ref}} - 1\right) - d$$

$$T_r \frac{dx_r}{dt} + x_r = \delta Y_{GV}$$

$$T_P \frac{du}{dt} + u = e$$

$$\frac{dY_{GV}}{dt} = \begin{cases} 0 & \text{if } Y_{GV} \leq 0 \text{ or } Y_{GV} \geq 1 \\ \dot{Y}_{GV}^{max} & \text{if } \left(u/T_g\right) \geq \dot{Y}_{GV}^{max} \\ -\dot{Y}_{GV}^{min} & \text{if } \left(u/T_g\right) \leq -\dot{Y}_{GV}^{min} \\ u/T_g & \text{else} \end{cases}$$

2.5 Simulation Results

2.5.1 Validation of the General Penstock Model

In this section the model of penstock with elastic walls and compressible water will be validated by application to the classic problem of reservoir-penstock-valve. Consider the system shown in the Figure (2-17). When the valve closes suddenly, pressure before the valve increases and a pressure wave travels back to the reservoir. When this wave reaches the water surface at the reservoir, becomes reflected as a negative wave and travels toward the valve. The time that takes for the pressure wave to travel from the valve to the reservoir and then back to the valve is equal to:

$$\frac{2 \times L_P}{\text{Speed of the pressure wave}}$$

The height h_{TW} of the reservoir is considered to be much less than the length L_P of the penstock in deriving the above relation. Speed of the pressure wave inside penstock is equal to the speed

of sound inside the water in penstock which a relation was given for it in (2-5). (Parmakian, 1963) This can be one of the criteria for validation of the penstock model. Time for traveling of the pressure waves (and hence speed of the waves) can be found from the results of simulations and then it can be compared to the value obtained from (2-5).

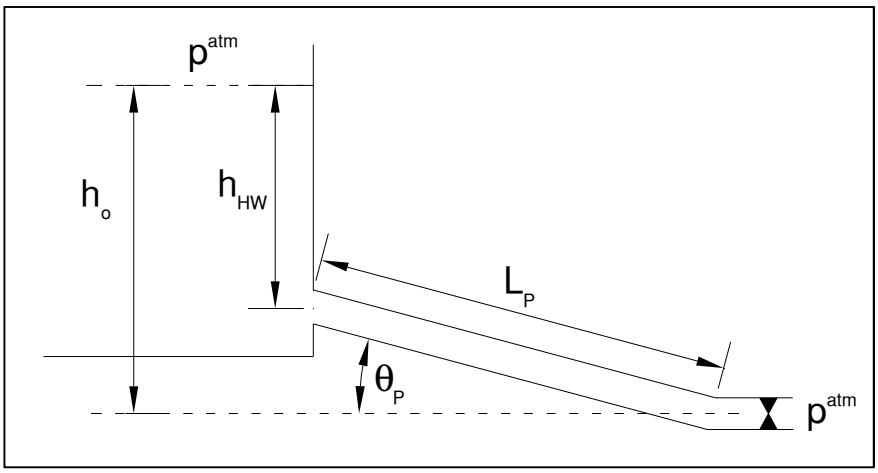

Figure (2-17) The Classic Penstock-Valve Problem

Maximum pressure rises before the valve when the valve starts closing from the steady-state condition with a uniform rate and reaches the complete closed position are tabulated by Allievi (Warnick, 1984). One of these charts is shown in Figure (2-18). This chart can be used as other criteria for validation of the penstock model. The maximum pressure rise found by simulation can be compared to the chart. Various parameters used for defining the axes of the chart in Figure (2-18) are as follows:

$$k = \frac{a\, v_o}{2gh_o} \quad , \quad n = \frac{a\, T}{2\, L_P} \quad , \quad z = \frac{\text{Max. head before the valve}}{\text{Operating head before the valve}} \qquad (2\text{-}72)$$

Where

$k =$	Time constant	[-]
$n =$	Pipe line constant	[-]
$a =$	Speed of the sound inside the penstock	[m/sec]

$v_o =$	Speed of water in steady-state condition before the valve closure	[m/sec]
$h_o =$	Gross head as shown in Figure (2-17)	[m]
$T =$	Valve closure time	[sec]

Details of the reservoir and valve with penstock interfacing parts are shown in Figure (2-19) and Figure (2-20) respectively. Following similar procedures of Sections 2.3.2 and 2.3.3 the equations governing these two systems can be obtained as follows:

The Reservoir:

$$\begin{gathered} p_{HWO} = p^{atm} + \rho^{atm}\, g\, h_{HW} \\ \Delta x \frac{d\dot{m}_{HWO}}{dt} = -A_P^{atm}(p_{HWI} - p_{HWO}) + \rho^{atm} g\, \Delta x\, A_P^{atm} \sin\theta_P \end{gathered} \tag{2-73}$$

Terms due to friction are neglected in the second equation of (2-73). Also the height h_{HW} is considered to be constant (for example due to make-up water flow to the reservoir.

The Valve:

$$\begin{gathered} \Delta p_{VALVE} = \frac{\dot{m}_{TWO}\,|\dot{m}_{TWO}|}{\rho^{atm^2} C_V{}^2} \\ p_{TWO} = p^{atm} + \Delta p_{VALVE} \\ \Delta x \frac{d\dot{m}_{TWO}}{dt} = -A_P^{atm}(p_{TWO} - p_{TWI}) + \rho^{atm}\, g\, \Delta x\, A_P^{atm} \sin\theta_P \end{gathered} \tag{2-74}$$

Again, Terms due to friction are neglected in the last equation.

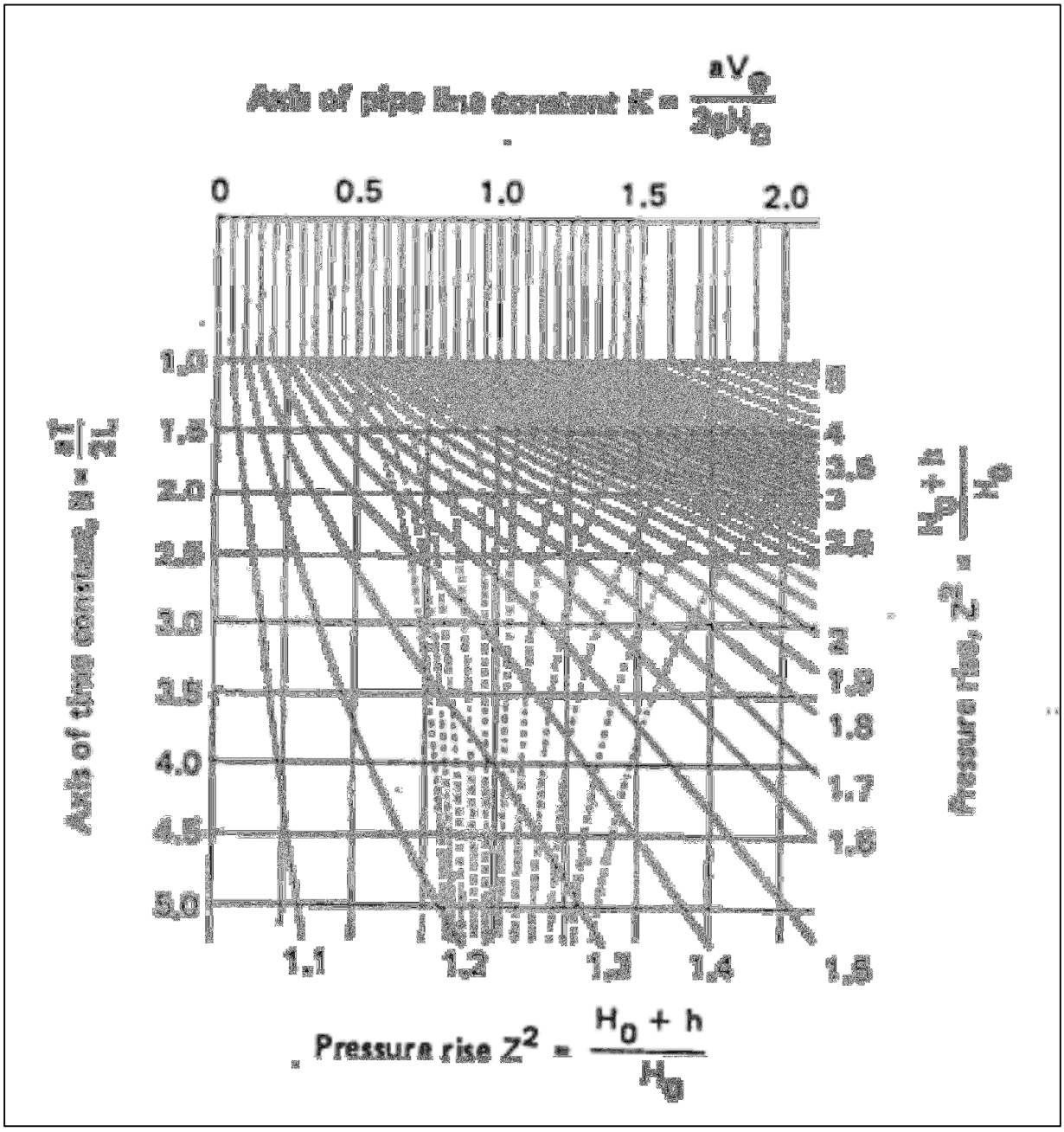

Figure (2-18) Allievi Chart Tabulating Maximum Pressure Rise before the Valve when Closing with Uniform Rate (Warnick, 1984)

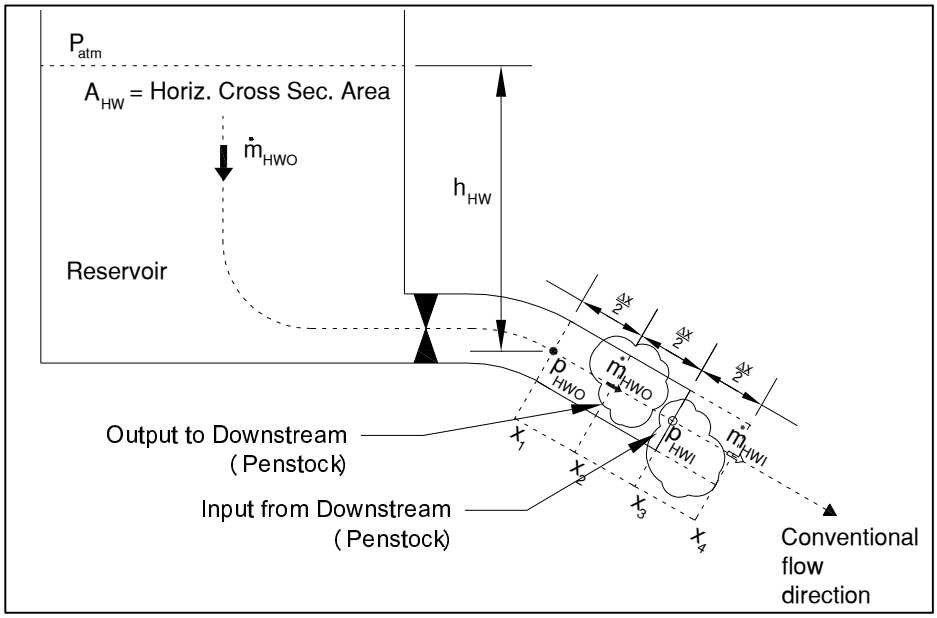

Figure (2-19) Details of the Reservoir with Penstock Interface

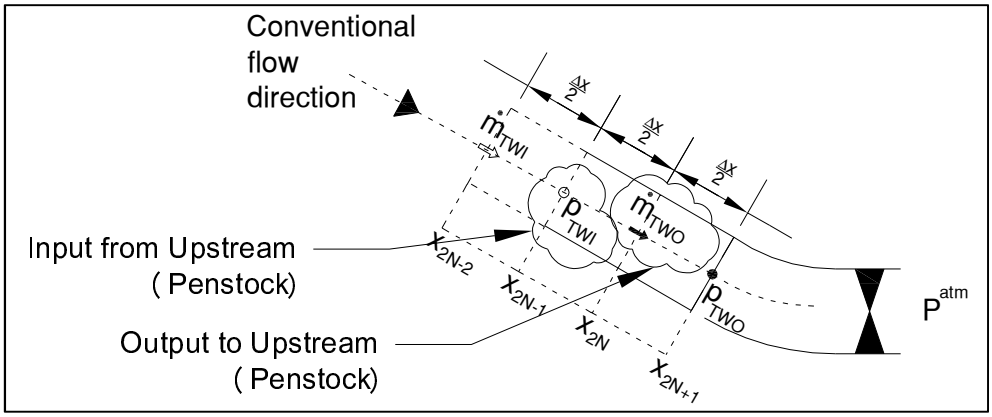

Figure (2-20) Details of the Valve with Penstock Interface

Simulation: Four different scenarios will be considered for simulation of the Penstock-Valve problem. The following parameters are the same for all the four scenarios:

$$L_P = 1000\ [m] \quad , \quad h_o = 100\ [m] \quad , \quad h_{HW} = 0\ [m] \quad , \quad a = 1000\ [m/sec] \qquad (2\text{-}75)$$

Valve closing times and steady-state initial velocity of water (hence the parameters k and n introduced in (2-72)) will be different for each scenario as follows:

Table (2-6) Scenarios for Simulation of the Penstock-Valve

	T [sec]	v_o [m/sec]	k	n	z (from Figure (2-18))
Scenario #1	1	1	0.5	0.5	2
Scenario #2	3	1	0.5	1.5	1.6
Scenario #3	5.2	1	0.5	2.6	1.3
Scenario #4	3	4	2	1.5	3.8

Valve starts closing at t=50 second in each scenario. Result of simulation for the above scenarios is included in Figure (2-21) to Figure (2-24) respectively. In Figure (2-21) to Figure (2-23) the values of head rise are in close agree with z values in the above table.

The result of simulation for the fourth scenario however is different. The value of head rise in this case is more than expected (3.47E+6/7.7E+5=4.5 whereas a value of 3.8 is expected from Allievi chart). The reason maybe because of the higher velocity which causes higher loses due to friction. The steady state value of the head before valve (before the time 50 sec when valve starts to close) is less than the other cases. For examining this guess, the case is simulated again with zero friction and the result is given in Figure (2-25). It appears that with zero friction the head rise is exactly in agree with Allievi chart. 4 m/sec here is an illustrative value and might not be a normal operating condition. In addition, the author of this report doesn't have any clue about the normal range of the friction factors for the penstock.

As mentioned earlier another criteria for validating the penstock model could be finding speed of the pressure waves from the simulation. MATLAB code for simulations in this part is included in the appendix III. In the code, value of β_{total} is calculated from the desired speed of sound. Then simulation is done with the calculated value of β_{total}. So the simulation results shall reflect this value of the pressure Waves. In the Figure (2-21) to the Figure (2-25) the time difference between two consecutive peaks is 2 seconds (except for the peaks that coincide with valve closure) and this agrees with the value $2L_P/a$.

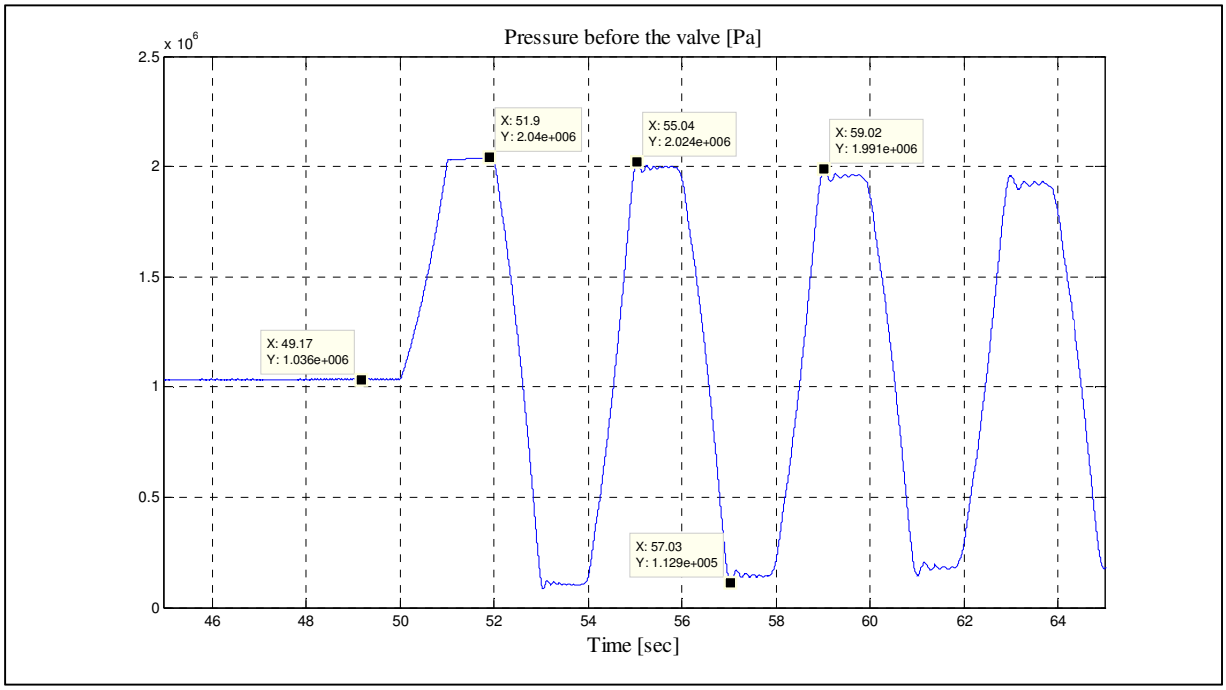

Figure (2-21) Result of Simulation of the Penstock-Valve for Scenario #1 (T=1 sec)

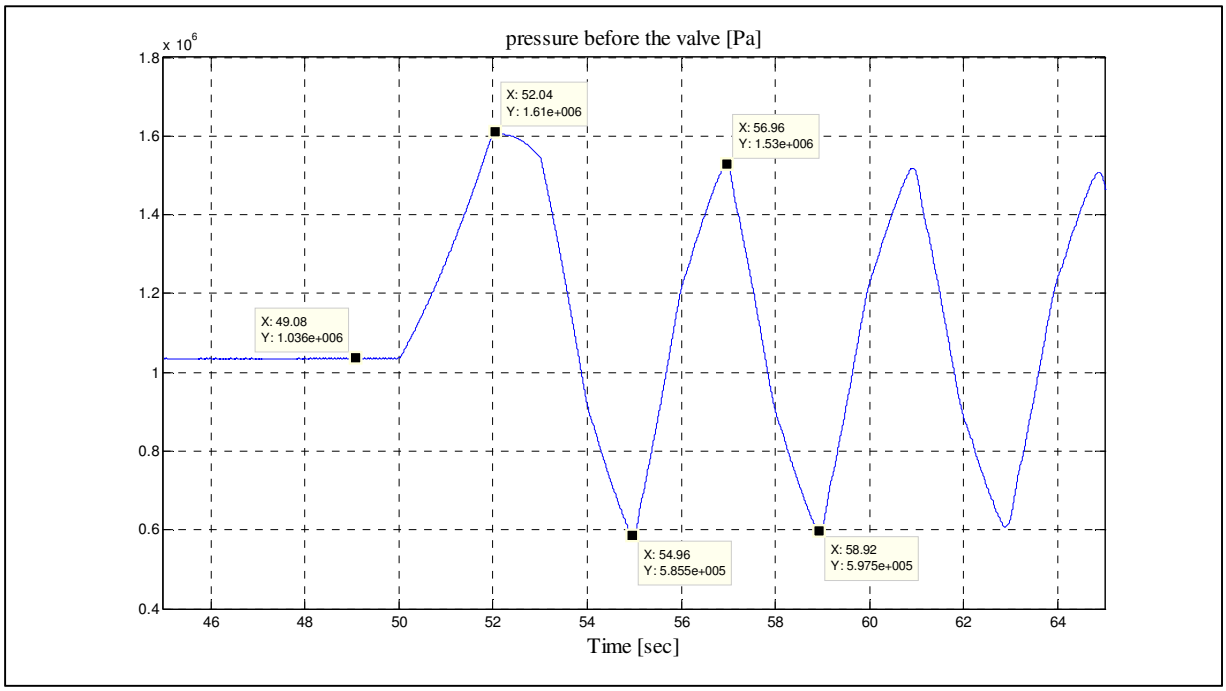

Figure (2-22) Result of Simulation of the Penstock-Valve for Scenario #2 (T=3 sec)

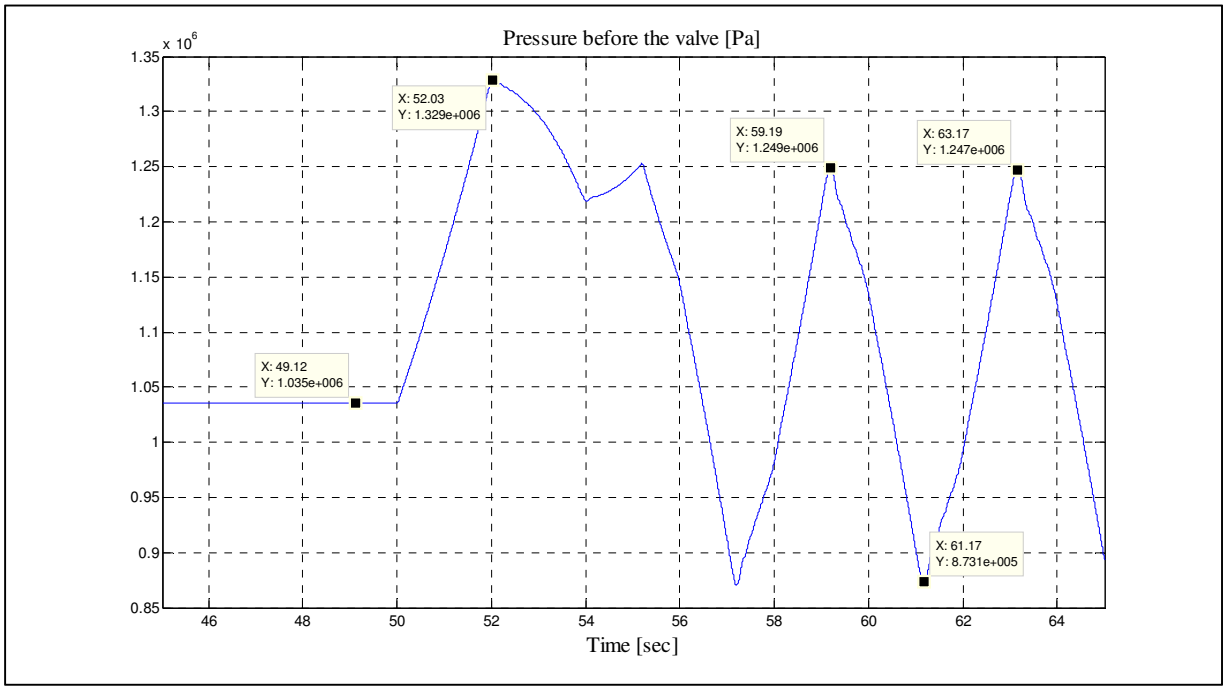

Figure (2-23) Result of Simulation of the Penstock-Valve for Scenario #3 (T=5.2 sec)

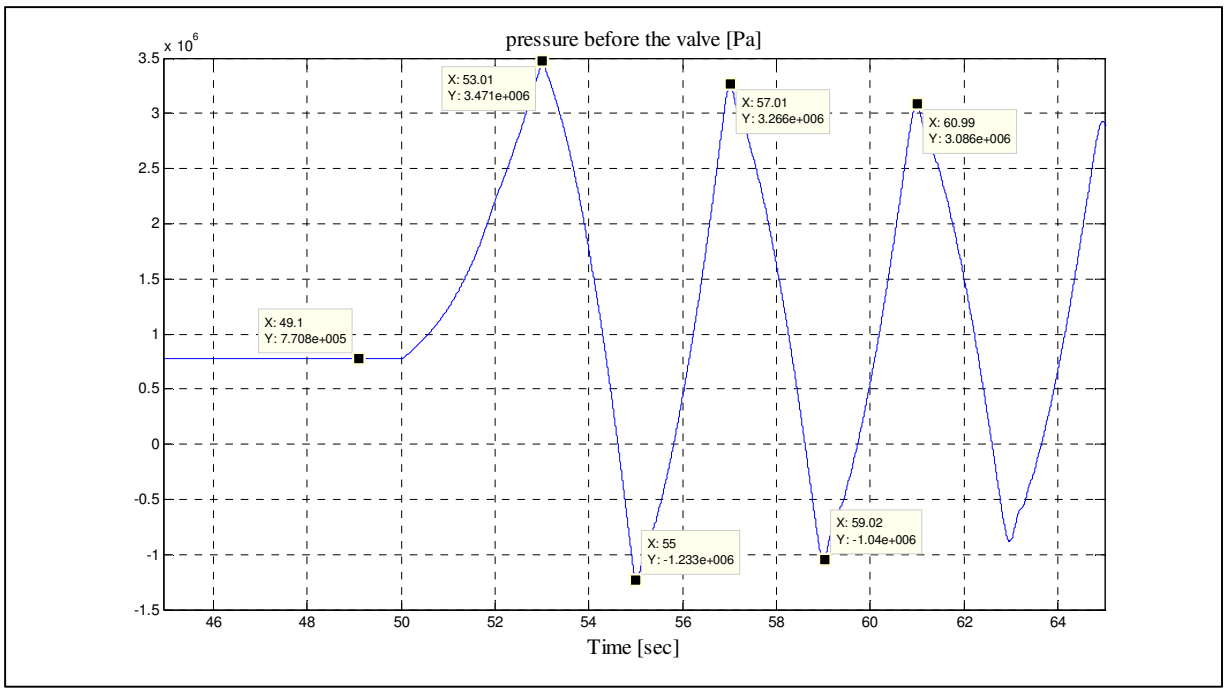

Figure (2-24) Result of Simulation of the Penstock-Valve for Scenario #4 (T=3 sec and v_o= 4 [m/sec] with $f_P = 0.04$)

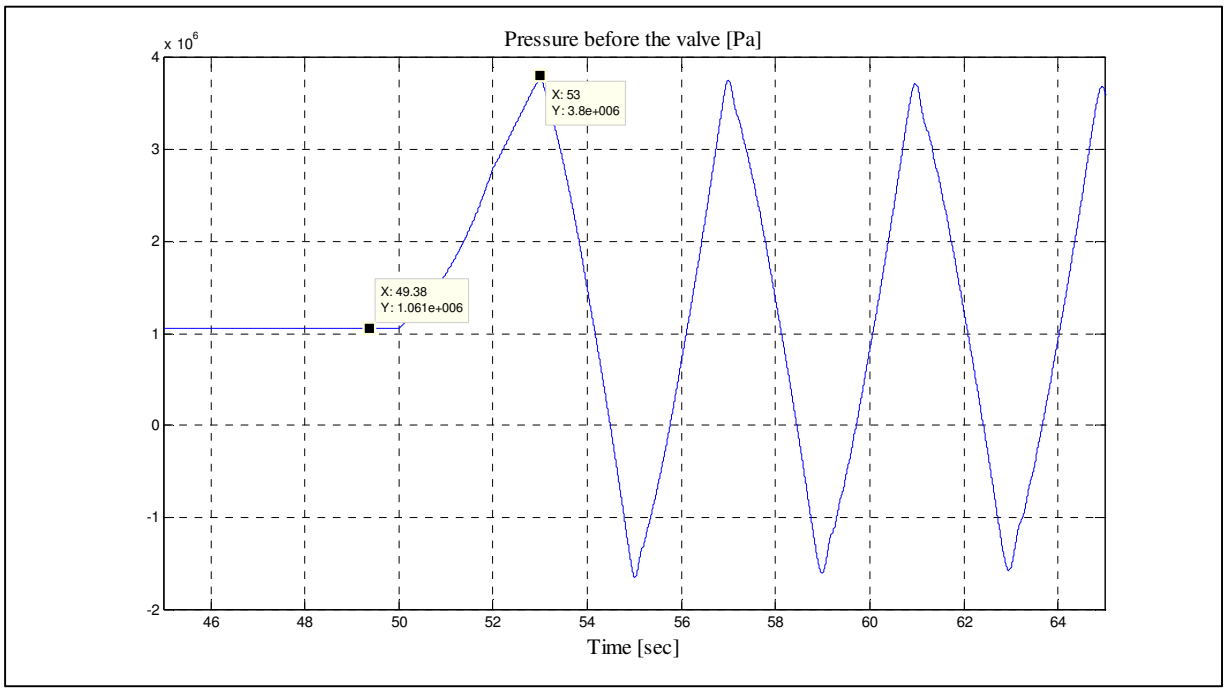

Figure (2-25) Result of Simulation of the Penstock-Valve for Scenario #4 (T=3 sec and v_o= 4 [m/sec] with $f_P = 0$)

Pressure and Mass Flow Rate at the middle and entrance (in Head Water Side) of the Penstock: Pressure and mass flow rate variations at different locations in the penstock is shown in the Figure (2-26). Range of variations of mass flow rate is almost constant through the penstock length but range of variations of the pressure reduces at closer locations to the head water as was expected. Mass flow rate at the valve is given in Figure (2-27). There is a small flow after t=50 sec at the valve because the valve just closes to 0.001(p.u). This is done on purpose to prevent divide by zero error (see the code in Appendix III).

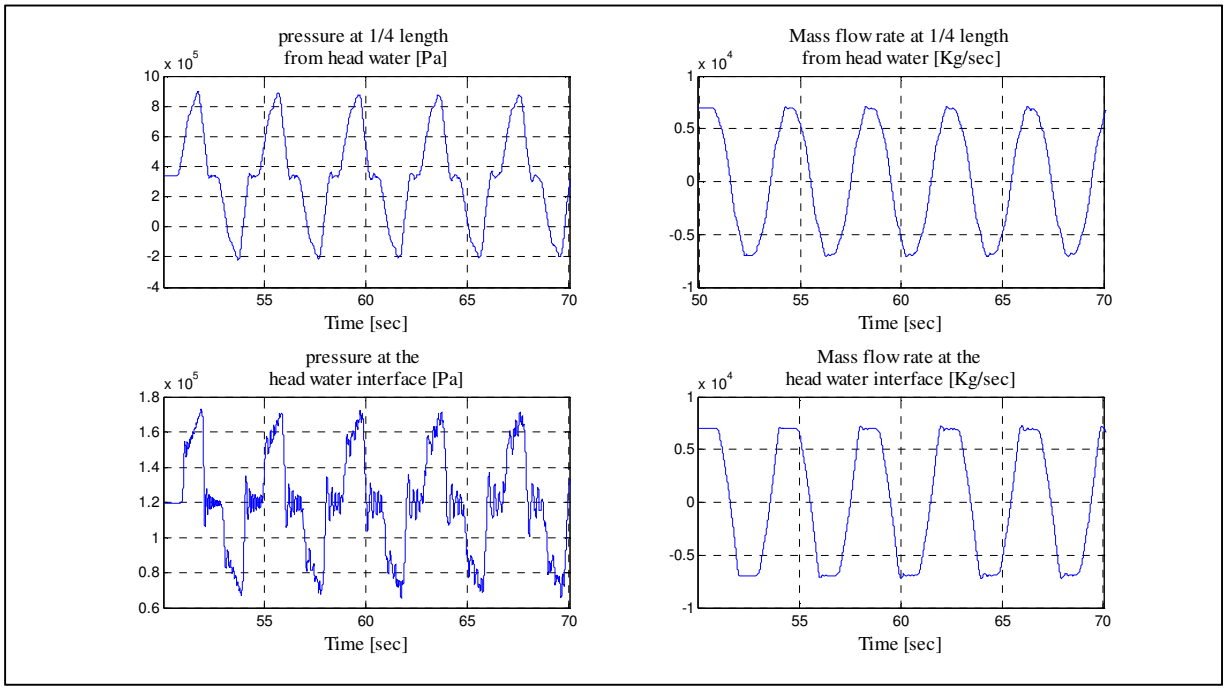

Figure (2-26) Variations of Pressure and Mass Flow Rate at different Locations of the Penstock for the Scenario #1 in Table (2-6)

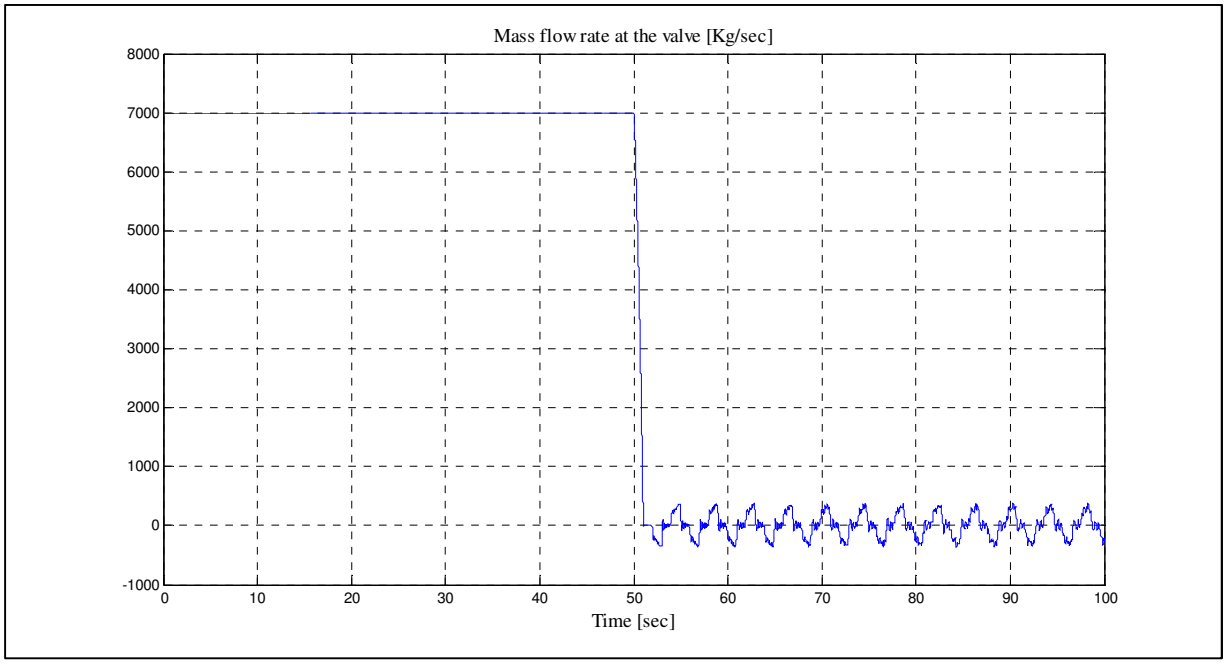

Figure (2-27) Mass Flow Rate at the Valve for the Scenario #1 in Table (2-6)

Partial Valve Closure: Partial valve closure for scenario #1 in Table (2-6) is simulated in Figure (2-28). The valve starts closing at time t=50 sec from full open position (with a rate of full closure per one second) and closes until 0.9 (p.u.) open position.

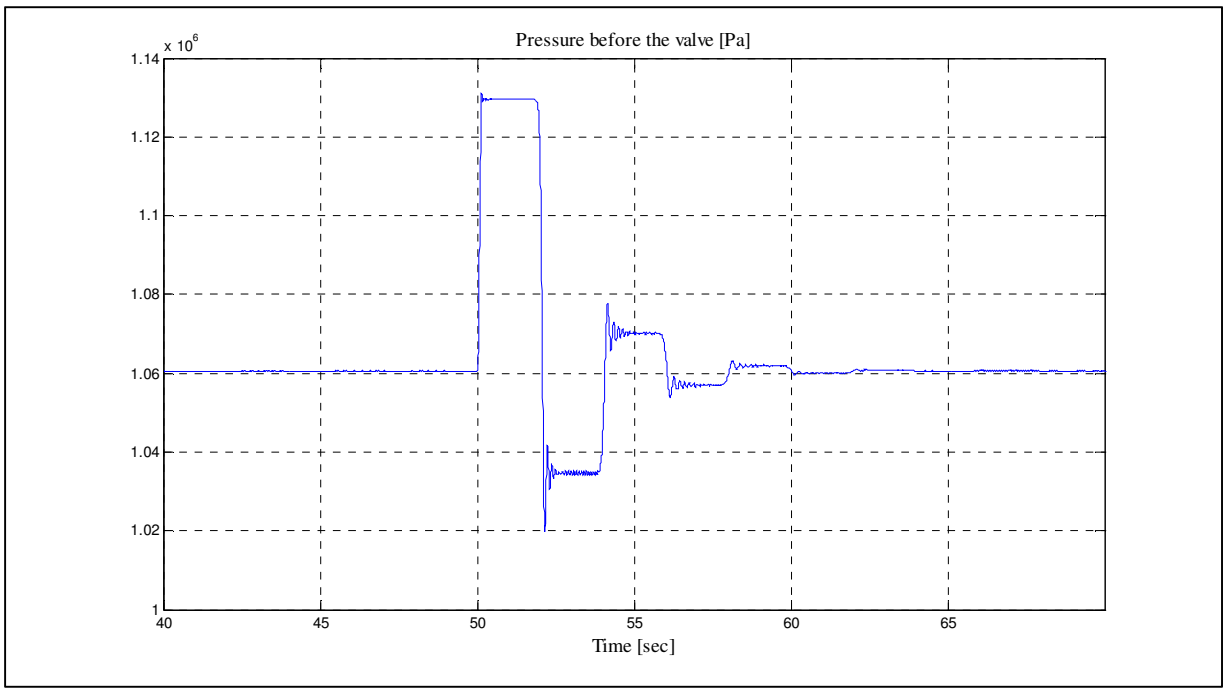

Figure (2-28) Simulation of Partial Valve Closure from 1 to 0.9 (p.u.) position

Options for ODE Solvers: All the simulations in Figure (2-21) to Figure (2-28) are done with the MATLAB "ODE15S" solver with the following options:

```
options=odeset('MaxOrder',5,'RelTol',1e-6,'AbsTol',1e-6);
```

What happens if default options are used for "ode15s"? The simulations of Figure (2-21) and Figure (2-28) are repeated with increased relative tolerance ('RelTol'=1e-3) and the result is given in Figure (2-29) and Figure (2-30) respectively. As can be seen, with increased relative tolerance the "ode15s" encounters numerical errors which completely distort the solution in case of small valve changes.

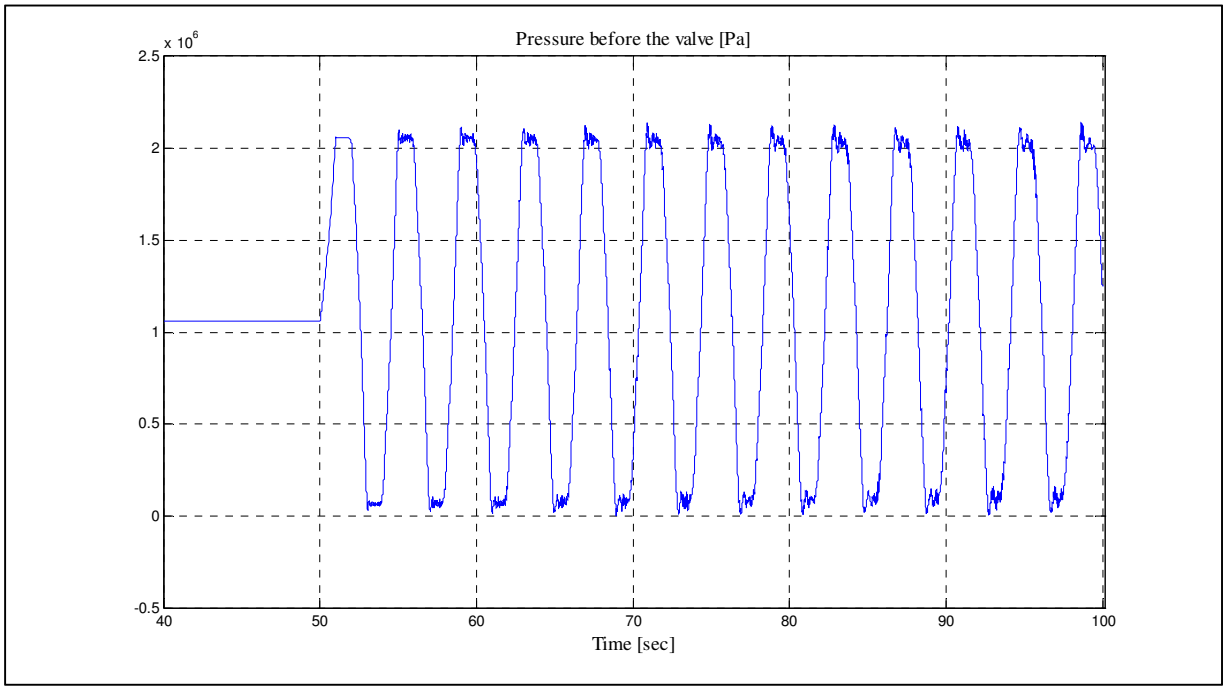

Figure (2-29) Simulation of Figure (2-21) with the option 'RelTol'=1e-3 for "ode15s"

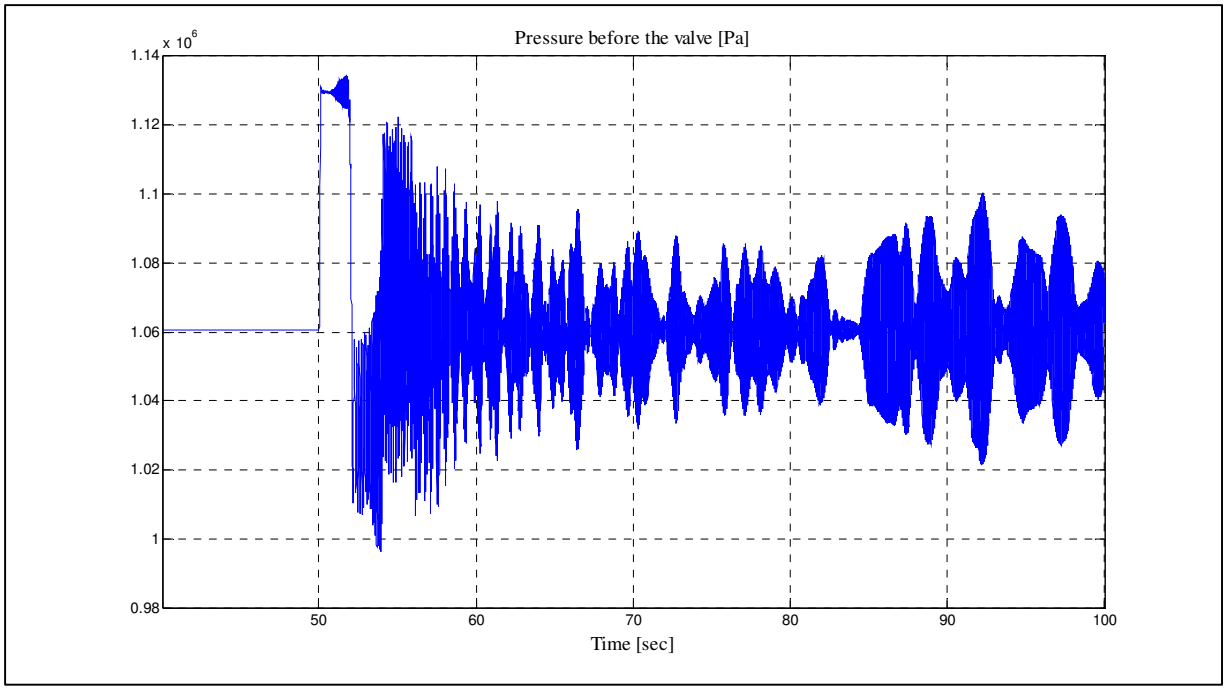

Figure (2-30) Simulation of Figure (2-28) with the option 'RelTol'=1e-3 for "ode15s"

Number of Penstock Segments: In all the above simulations, number of penstock segments is chosen to be 50. Figure (2-31) shows the result of the simulation for scenario #1 for two different N values (N=25 and N=50). As can be seen, number of segments has influence on the frequency of oscillations of the model.

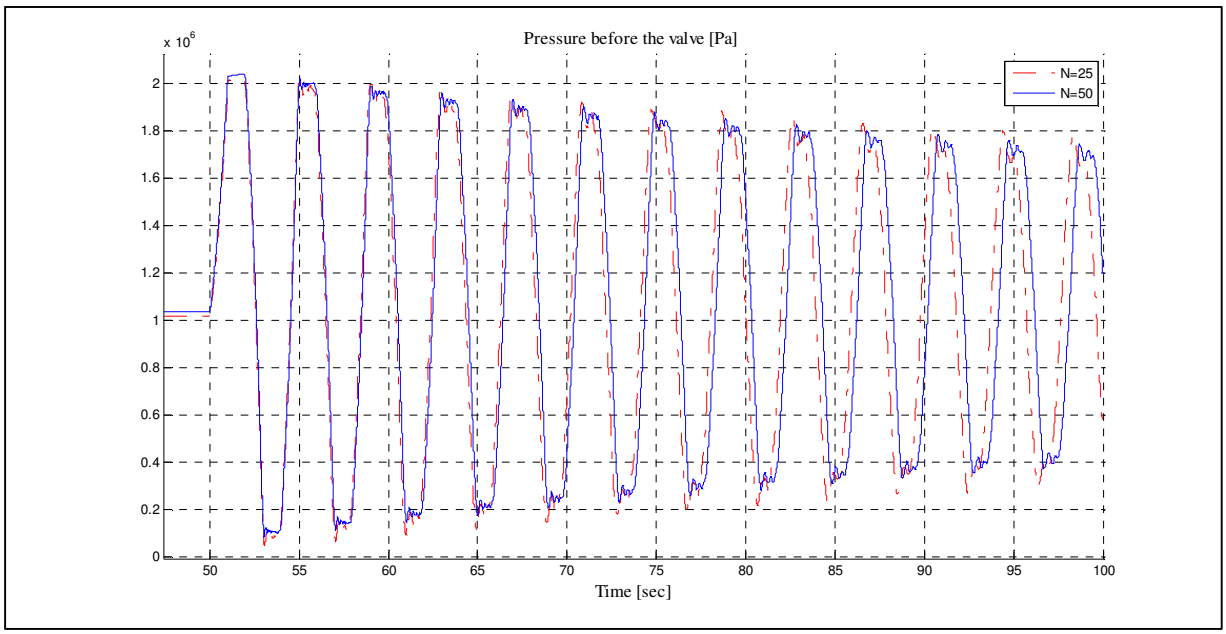

Figure (2-31) Simulation for Different Number of Penstock Segments

2.5.2 System with and without Compressibility and Elasticity Effects

In this section the models obtained for the waterway (both with elastic and non-elastic penstock) with transient droop controller are simulated simultaneously. The turbine load in these simulations is considered as a disturbance which consumes constant power. The system response when this disturbance changes to a new value or when the guide vanes opening reference value changes are simulated.

Figure (2-32) to Figure (2-42) show the results when guide vane reference is constant and power demand changes at t=400 sec and t=800 sec. Figure (2-32) shows that turbine power follows the

Demand to keep the frequency stable whereas Figure (2-34) shows that the steady state value of the frequency will not follow the frequency reference. This is due to the droop relation that its satisfaction requires the power be decreased with increasing frequency and vice versa.

Figure (2-43) to Figure (2-45) show the results of a simulation in which the power demand is constant during simulation but the reference value for guide vane changes at t=300 sec. Since power demand has not changed the actual guide vane position returns to its previous value. As it can be seen there are small differences between the responses of the elastic and inelastic models this time but due to the time constants of the guide vanes movement still the differences are not significant.

System parameters for these simulations can be found in Appendix III part C in the MATLAB code `Main_parameters.m`.

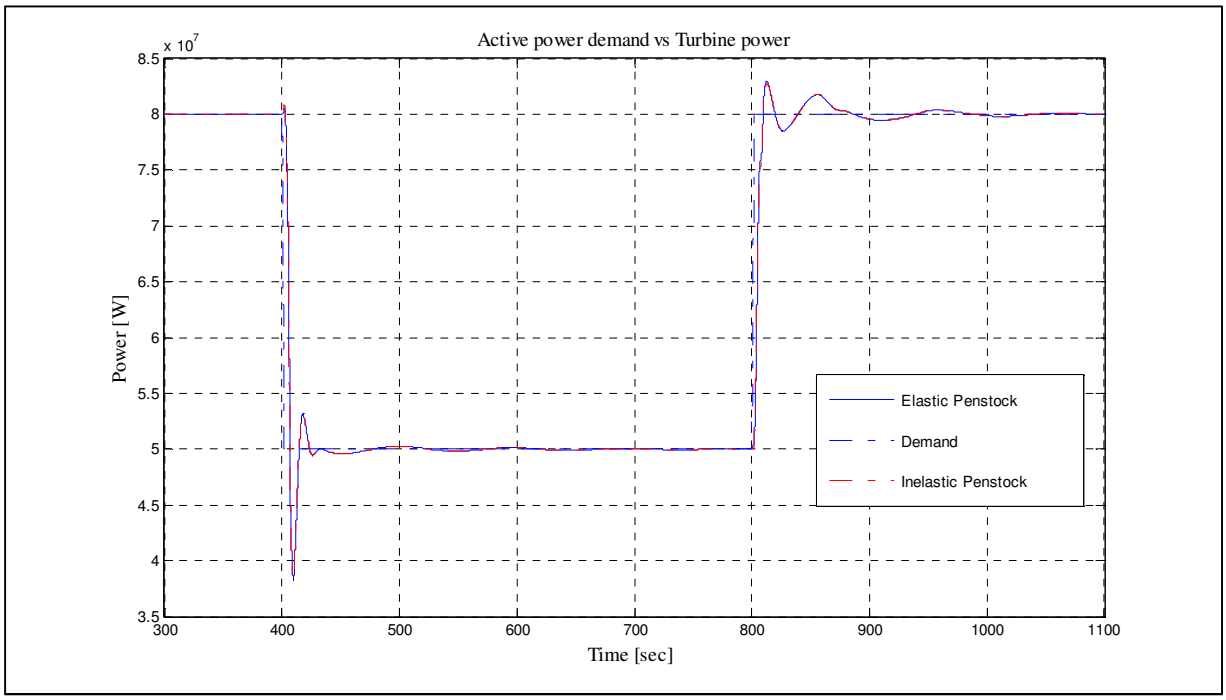

Figure (2-32) Simulation Results (ActivePower Demand changes to 50MW at t=400 sec and changes back to 80MW at t=800 sec)

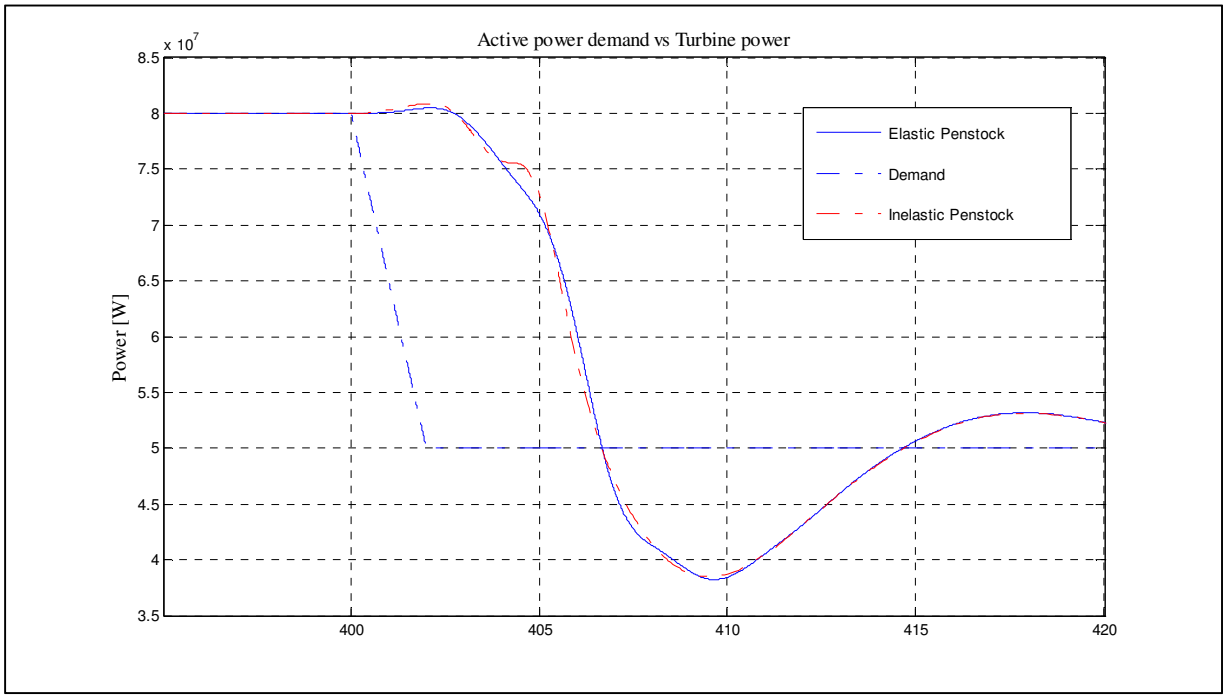

Figure (2-33) Same as the Figure (2-32) with Horizontal Zoom

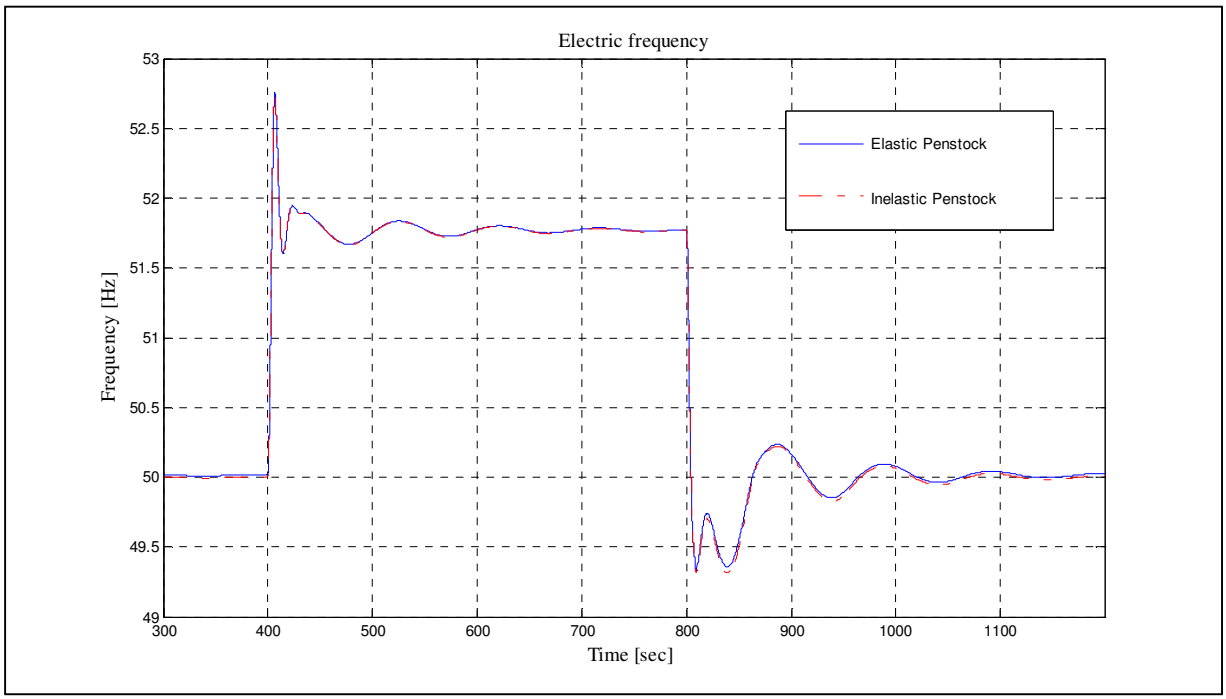

Figure (2-34) Simulation Results (Because of change in the active power demand and since the droop relationship shall be satisfied, frequency doesn't remain constant.)

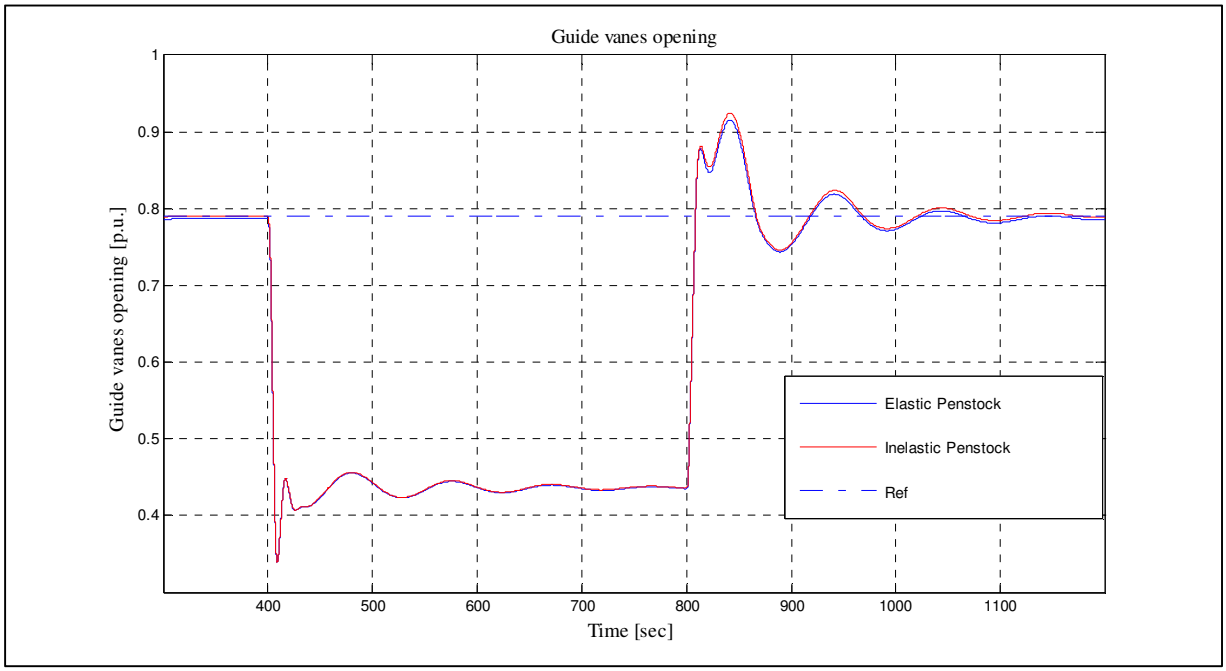

Figure (2-35) Simulation Results (Guide vanes reference and actual values)

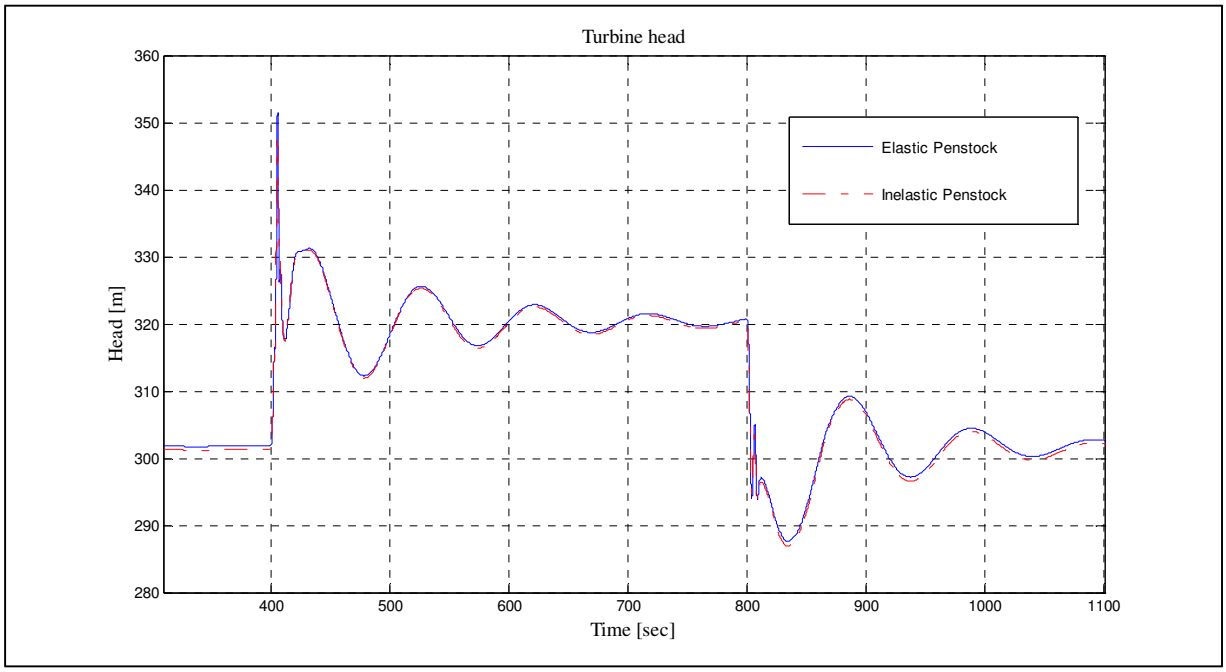

Figure (2-36) Simulation Results (Turbine head)

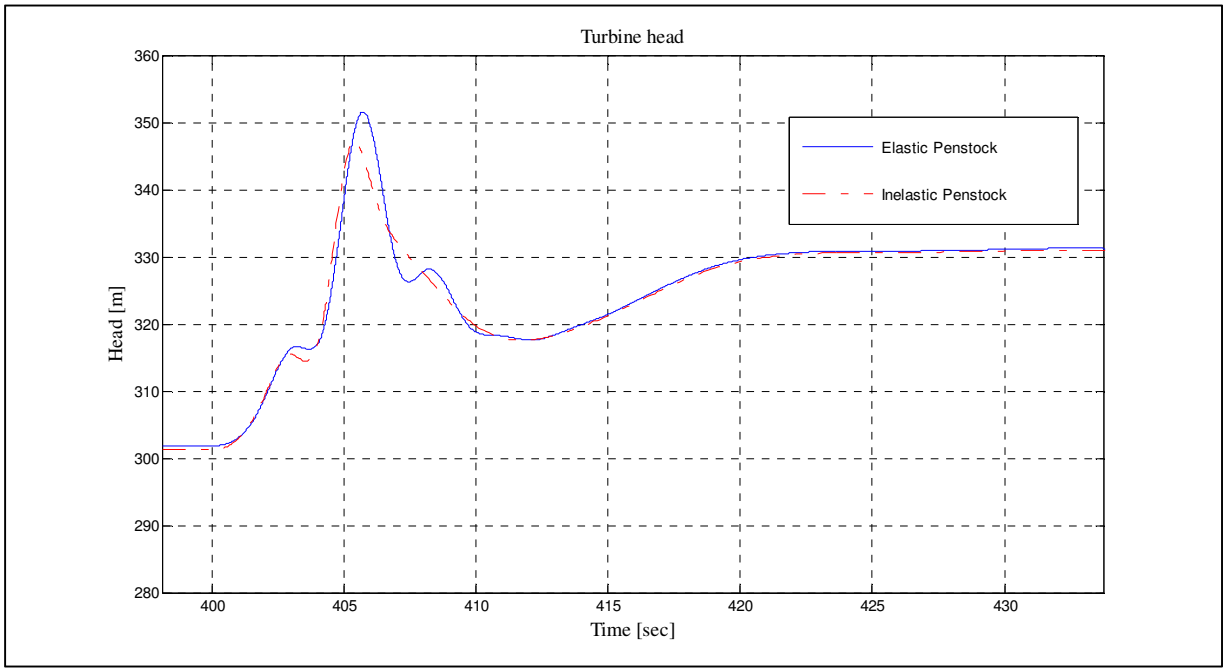

Figure (2-37) Same as the Figure (2-36) with Horizontal Zoom

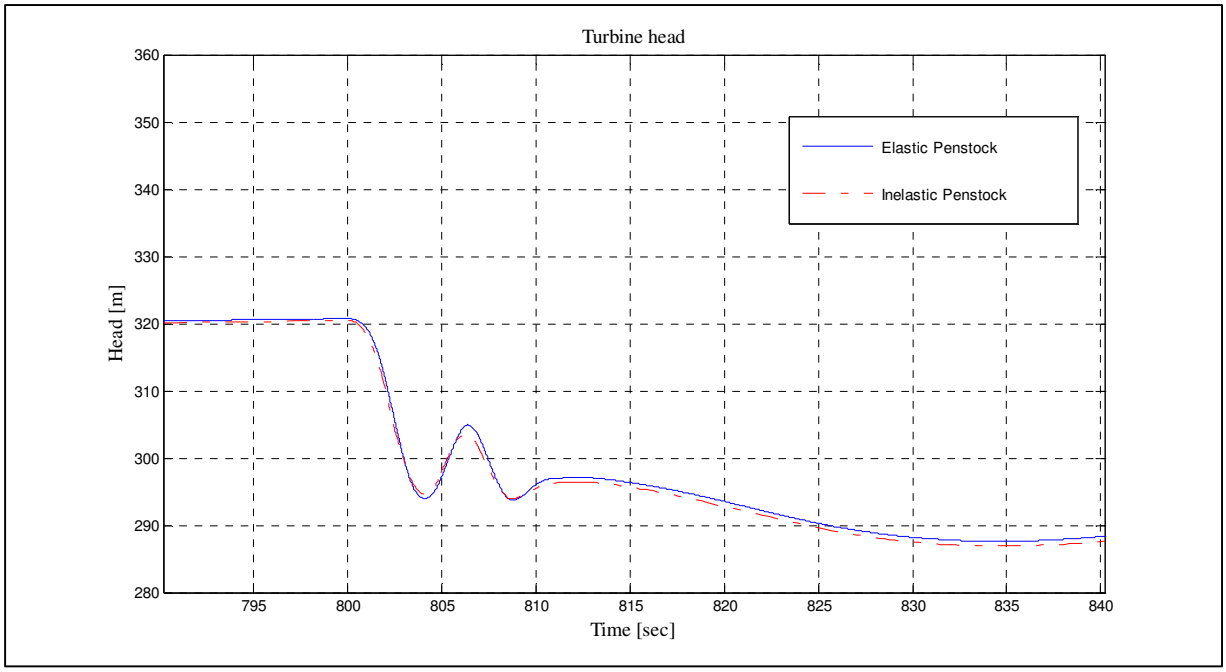

Figure (2-38) Same as the Figure (2-36) with Horizontal Zoom

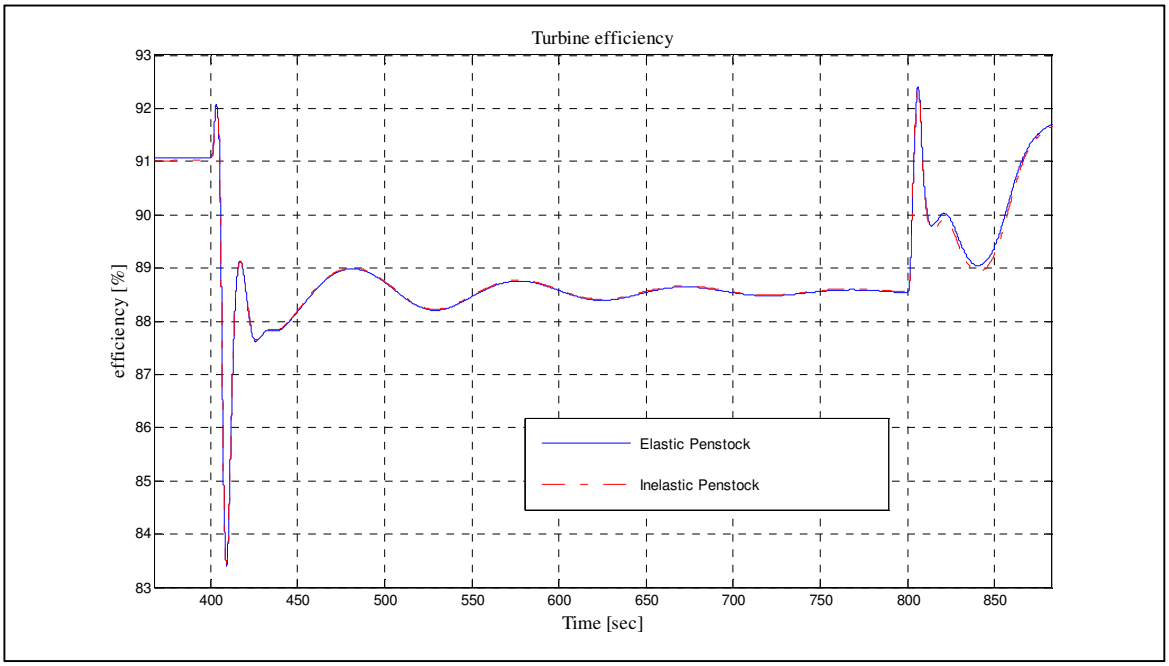

Figure (2-39) Simulation Results (Turbine head)

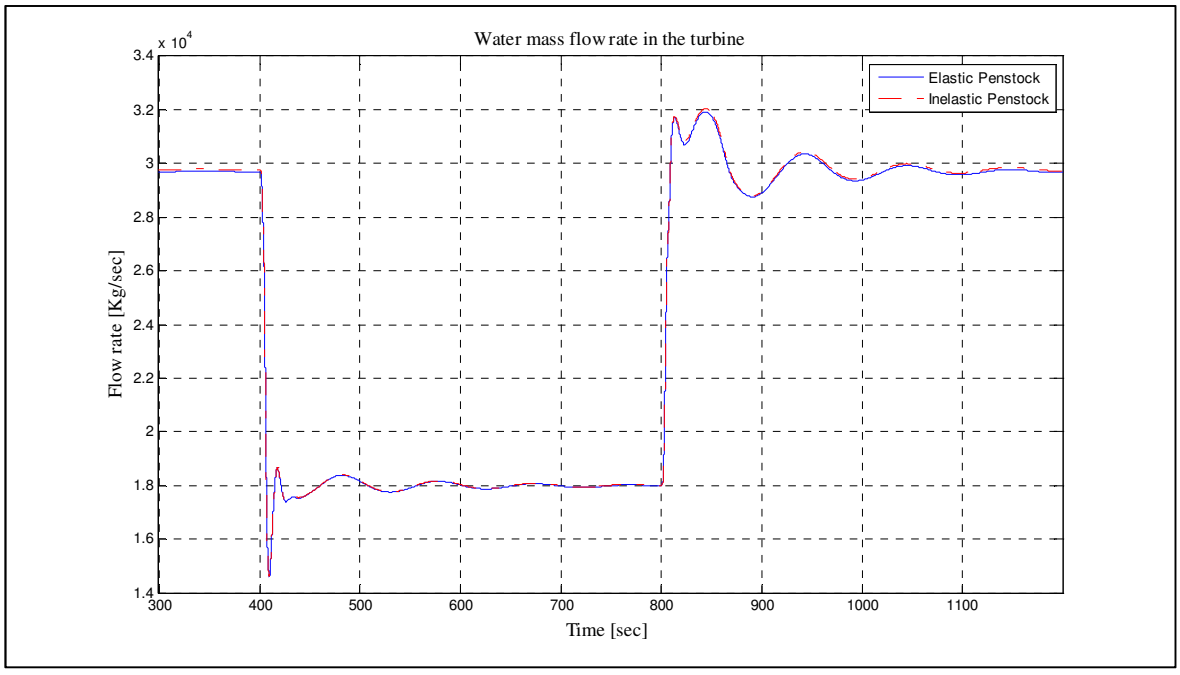

Figure (2-40) Simulation Results (Turbine Mass Flow Rate)

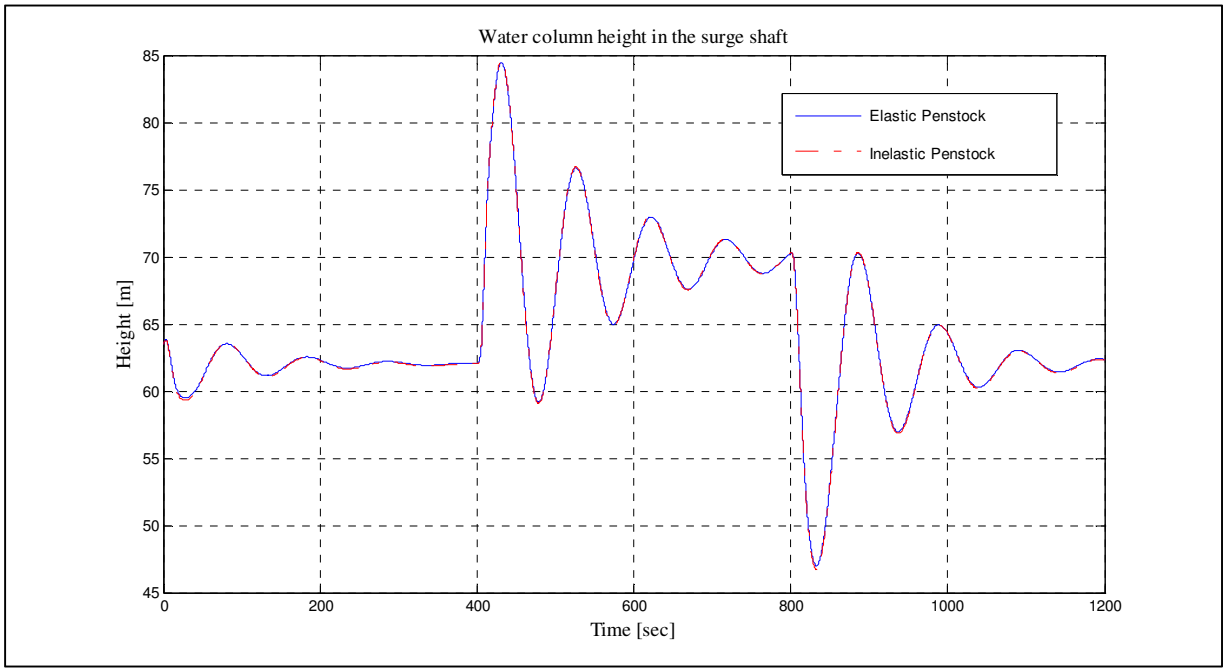

Figure (2-41) Simulation Results (Surge Shaft Level)

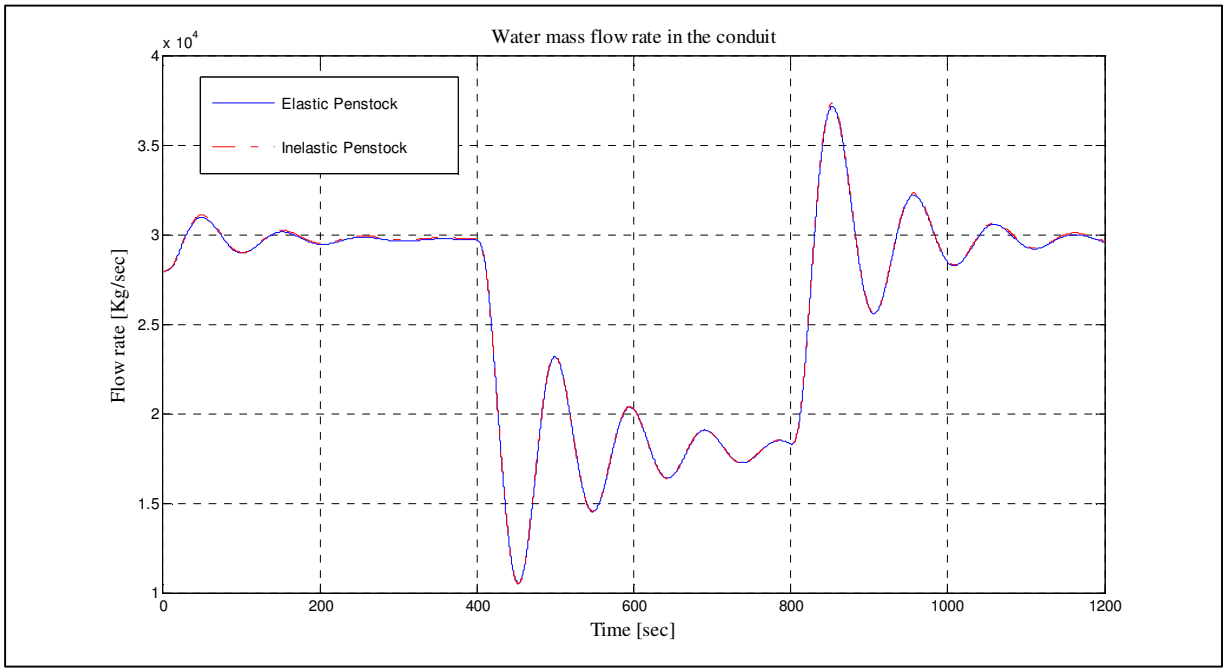

Figure (2-42) Simulation Results (Conduit Mass Flow Rate)

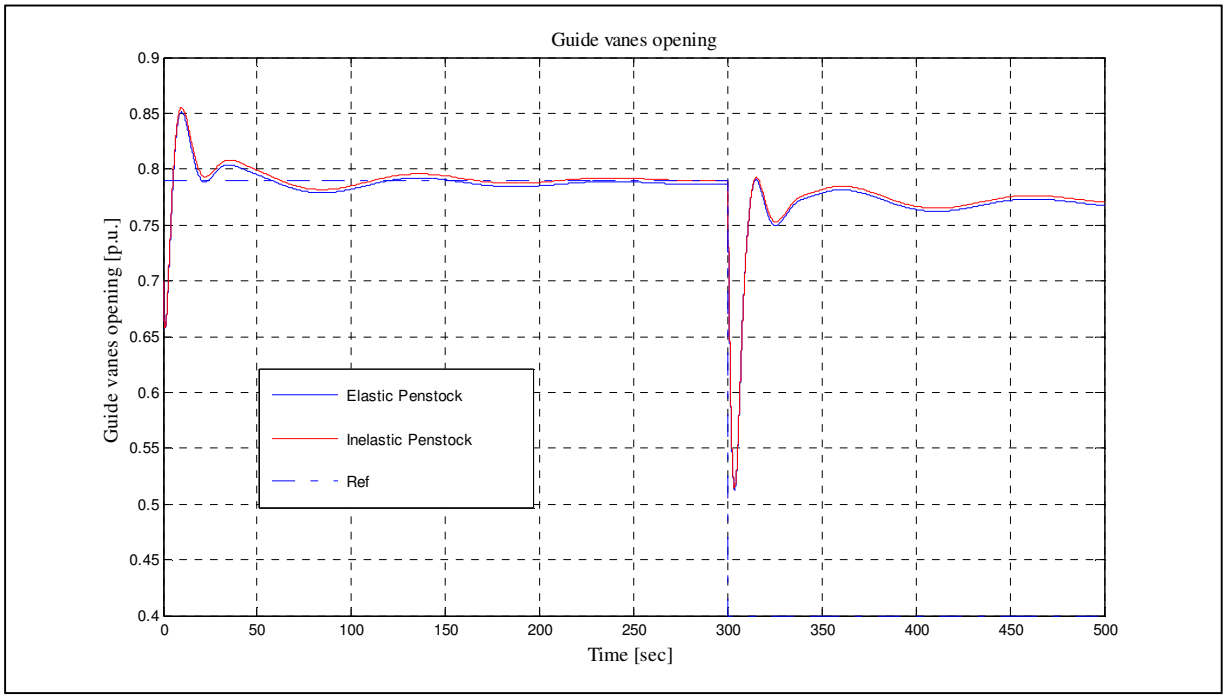

Figure (2-43) Simulation Results with fixed power demand and guide vanes reference change at t=300 sec

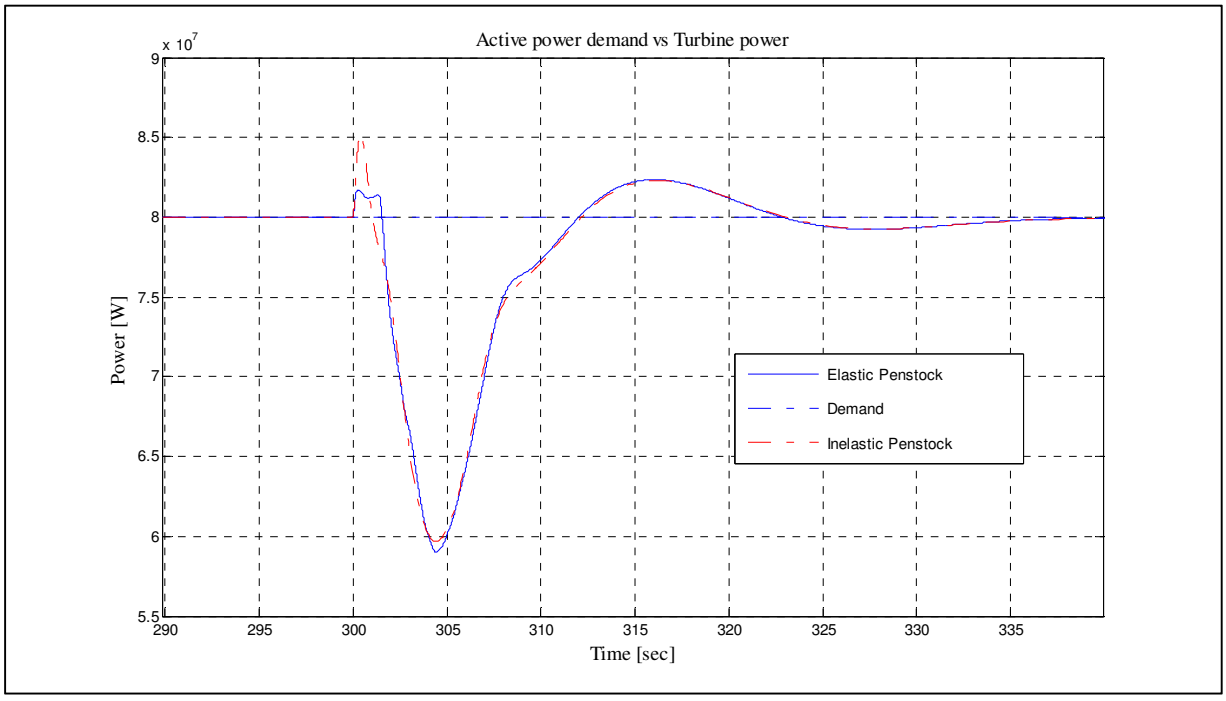

Figure (2-44) Simulation Results with fixed power demand and guide vanes reference change at t=300 sec.

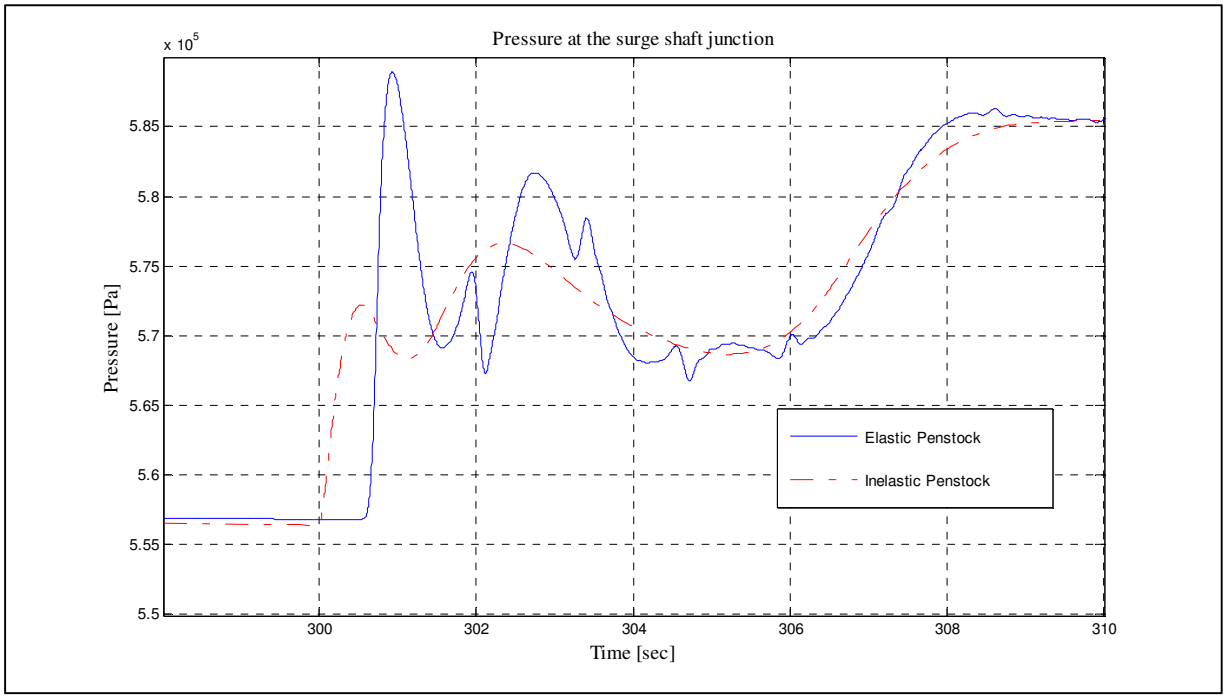

Figure (2-45) Simulation Results with fixed power demand and guide vanes reference change at t=300 sec.

Chapter 3 Electrical System

This chapter is devoted to study of the synchronous generator. In sections 3.1.1 to 3.1.3 structure of a multi-pole salient poles generator is discussed. In section 3.1.4 the self and mutual inductances of various windings in the machine are studied. Sections 3.1.5 to 3.1.7 the Park's transform and machine equations in the rotor reference frame are discussed. The power term in the swing equation which is relevant to the generator active power is discussed in Section 3.1.8. In Sections 3.1.9 to 3.1.11 available simplified models for the synchronous generator are introduced and it is shown how to relate the variables of these models to the network variables through the "phasors" concept. Finally a generator connected to an infinite bus is simulated with the waterway model (without elasticity).

3.1 Synchronous Generator

3.1.1 Typical Structure of a 12-Pole Machine

Figure (3-1) shows a radial cross-section sketch of a 12-poles synchronous generator. "Armature windings" carrying the generator output current and producing terminal voltages are fixed in the stator slots and are denoted by $a_1, a_2, \ldots, a_6$ for phase "a". Similar notation is used for denoting the phase "b" and phase "c" armature windings. Windings denoted by "F" are called "Field Windings" and are electrically connected in series with each other. The "field current" or the "rotor magnetizing current" flowing through these windings is a constant DC current in the steady-state operation of the generator and produces a radial magnetic field at the pole shoes. The field current is generated and controlled by circuits responsible for controlling the generator terminal voltage. "Damper Windings" D and Q are short circuited windings which stabilize the generator operation during rapid changes in the operating condition. A third damper winding model "g" is also introduced in (Machowski, 2008) which actually is not a winding but is a model of the currents induced in the rotor body. This "winding" is important in the high speed turbo generators and the parameters relevant to it are not normally given for salient pole generators.

3.1.2 Conventional Directions

Direction of magnetic fields: Conventional direction for magnetic field is shown in Figure (3-2) (a) and (b). Right-hand rule[4] can be used in the both cases to determine direction of the magnetic field.

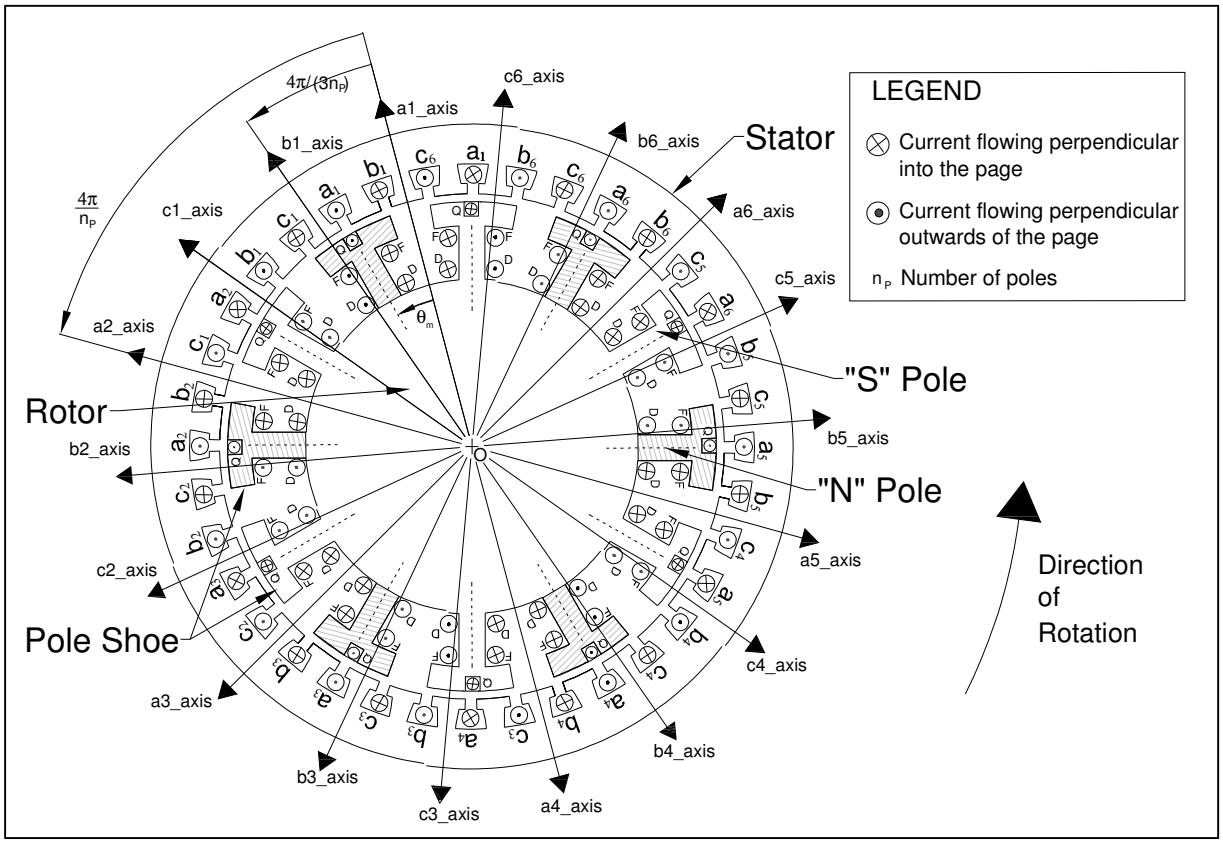

Figure (3-1) Cross-Section sketch of a 12-Poles Synchronous Generator based on 2-Poles Machine Structures given in (Andersson, 2010) and (Machowski, 2008)

[4] http://en.wikipedia.org/wiki/Right_hand_rule

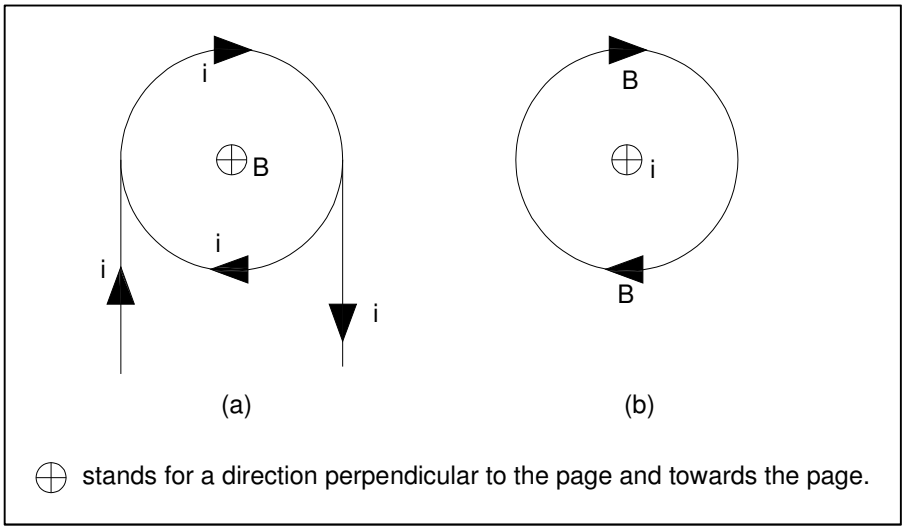

Figure (3-2) Direction of the Magnetic field in (a) center of a winding carrying current i (b) around a straight wire carrying current i

Direction of current, voltage and magnetic flux in two magnetically coupled windings: Direction of the current in two windings is chosen so that the magnetic flux produced by the windings will add to each other. In Figure (3-3) Ψ_{12} is the flux produced by the current in the second winding and passing through the first winding. Similarly, the flux Ψ_{21} is part of the flux produced by the current in the first winding which passes through the second winding. By choosing currents flowing in the indicated directions, Ψ_{12} and Ψ_{21}will be in the same direction in the magnetic circuit of the two windings. It can be written:

$$\Psi_1 = \Psi_{11} + \Psi_{12} = L_1 i_1 + L_{12} i_2$$
$$\Psi_2 = \Psi_{21} + \Psi_{22} = L_{21} i_1 + L_2 i_2 \qquad (3\text{-}1)$$

The so called "mutual inductances" L_{12} and L_{21}depend on the number of turns in both the first and second windings and also on properties of the magnetic circuit between the two windings. It is a known fact that the equality $L_{12} = L_{21} = M$ always holds. By the right choosing of the conventional current directions in the two windings, M will become positive. This usually is shown by two dots as indicated in Figure (3-3). If the conventional current direction is chosen into the winding at the doted end of the two windings, then the fluxes will add to each other and the M will be positive.

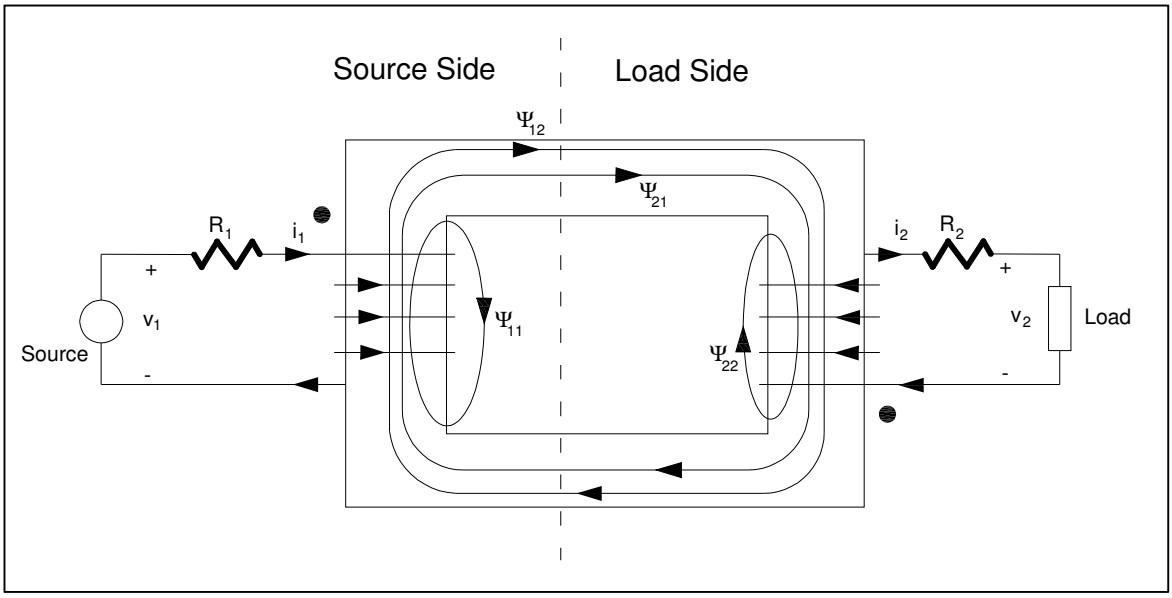

Figure (3-3) Two Magnetically Coupled Windings, Conventional Current and Voltage Directions

In Figure (3-3), one of the windings is connected to a source and the other is connected to a load. Note that conventional voltage directions in the load side and in the source side are different. It's because of the direction of energy flow. If the energy out of the source ($v_1 i_1$) is positive, then the energy given to the load ($v_2 i_2$) should also be positive. This has a consequence on the voltage equations:

$$v_1 = R_1 i_1 + \frac{d\Psi_1}{dt} = R_1 i_1 + L_1 \frac{di_1}{dt} + M \frac{di_2}{dt}$$
$$v_2 = -R_2 i_2 - \frac{d\Psi_2}{dt} = -R_2 i_2 - M \frac{di_1}{dt} - L_2 \frac{di_2}{dt} \qquad (3\text{-}2)$$

N and S poles of a magnet: Figure (3-4) shows a solenoid with a core made of magnetic material. If current in the solenoid flows in the indicated direction then order of the "N" and "S" poles of the magnet will be as shown in the figure.

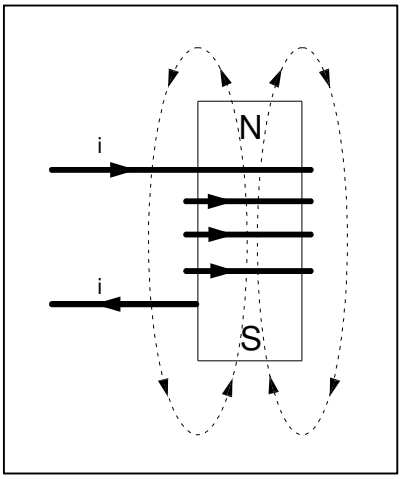

Figure (3-4) “N” and “S” Poles of a Magnet

N and S poles of the Rotor: If a dc current flows in the “F” windings of a synchronous generator in the directions indicated in the Figure (3-1), then the “hatched” poles will act as “N” poles of constant magnets and the other poles will be “S” poles.

Rotor Angle "θ_m": The rotor angle "θ_m" is measured from any of the “a” axes to the nearest “N” pole in counter-clockwise direction (direction of rotation). (See Figure (3-1))

3.1.3 Electrical Connections

In Figure (3-5) to Figure (3-7) a possible combination (illustrative based on (Chapman, 2005)) of electrical connections for different windings of the generator are indicated. Note the difference between defining conventional voltage polarities in the armature windings (Figure (3-5)) with those of the field windings (Figure (3-6)). The field windings are considered to be on the source side. (See section 3.1.2)

Conventional direction for current in the “F” and “D” windings are chosen such that when the rotor angle is equal to 0, mutual inductance between “F” (or “D”) and “a” windings will be maximum positive.

Conventional direction for current in the "Q" windings is chosen such that when the rotor angle is equal to (π/n_P), mutual inductance between "Q" windings with "a" windings will be maximum positive.

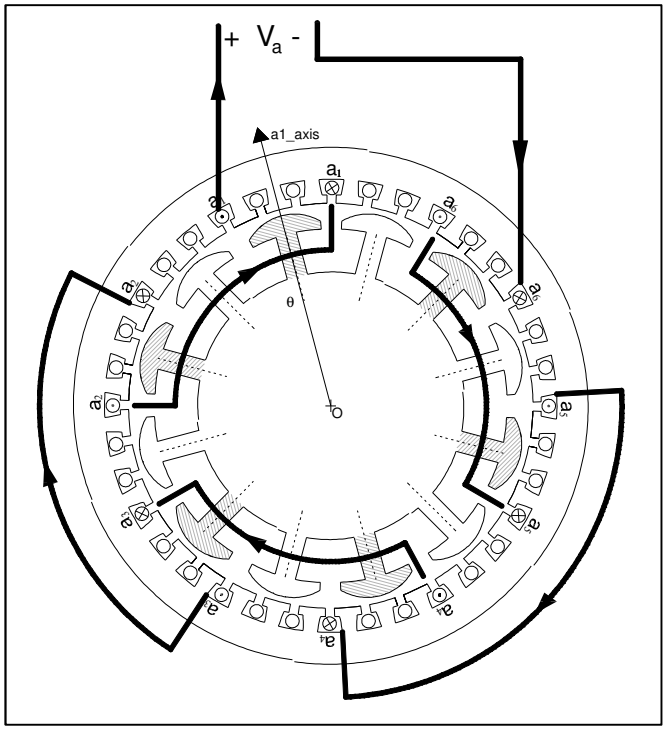

Figure (3-5) Illustrative Electrical Connections for "a" Windings (for other Armature Windings will be Similar)

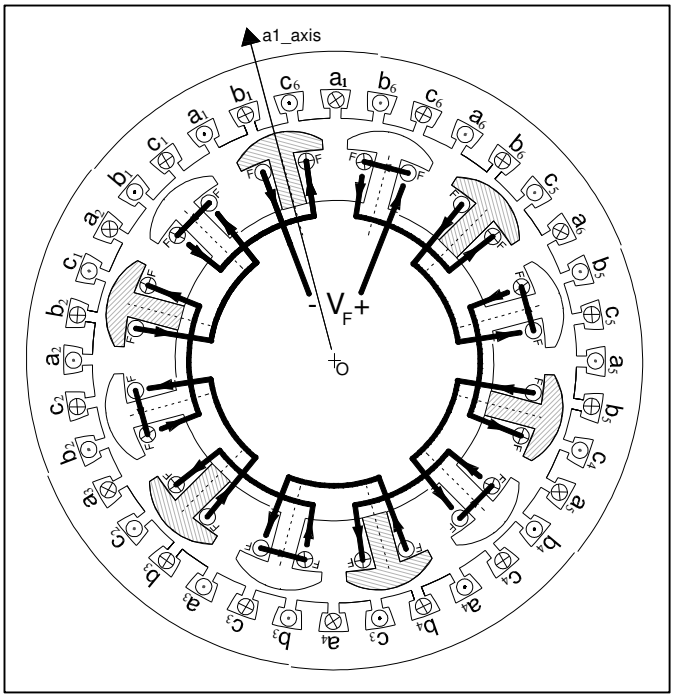

Figure (3-6) Connections of the "F" Windings

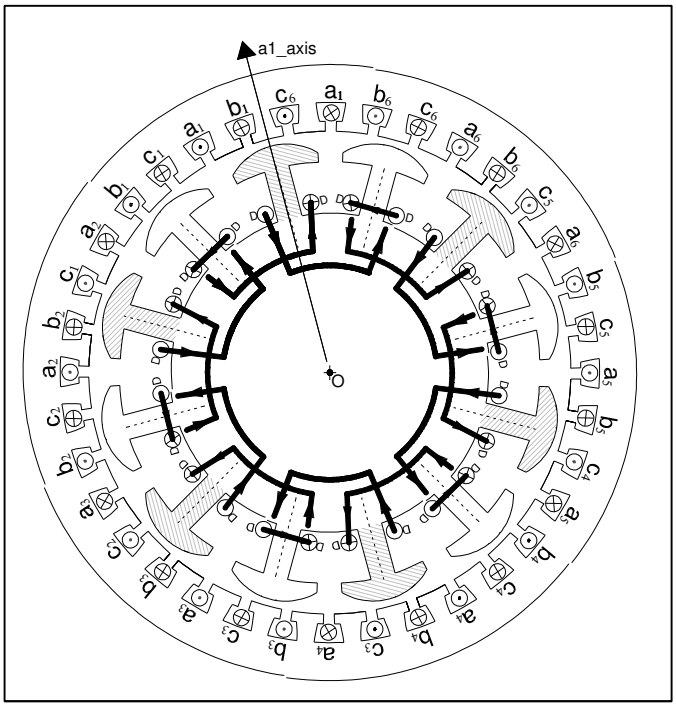

Figure (3-7) Connections of "D" Windings ("Q" Windings will be Short Circuited as well)

3.1.4 The Inductance Matrix

It is known from the theory of electromagnetism that the flux linkage in each of the machine windings can be considered as a linear function of the machine currents (if saturation and hysteresis effects can be neglected) (Machowski, 2008):

$$\underbrace{\begin{bmatrix}\Psi_a\\ \Psi_b\\ \Psi_c\\ \Psi_F\\ \Psi_D\\ \Psi_Q\end{bmatrix}}_{\boldsymbol{\Psi}} = \underbrace{\begin{bmatrix} L_{aa} & L_{ab} & L_{ac} & L_{aF} & L_{aD} & L_{aQ}\\ L_{ba} & L_{bb} & L_{bc} & L_{bF} & L_{bD} & L_{bQ}\\ L_{ca} & L_{cb} & L_{cc} & L_{cF} & L_{cD} & L_{cQ}\\ L_{Fa} & L_{Fb} & L_{Fc} & L_{FF} & L_{FD} & L_{FQ}\\ L_{Da} & L_{Db} & L_{Dc} & L_{DF} & L_{DD} & L_{DQ}\\ L_{Qa} & L_{Qb} & L_{Qc} & L_{QF} & L_{QD} & L_{QQ}\end{bmatrix}}_{\mathbf{L}} \underbrace{\begin{bmatrix}i_a\\ i_b\\ i_c\\ i_F\\ i_D\\ i_Q\end{bmatrix}}_{\mathbf{i}} \tag{3-3}$$

The values for each element in the matrix "**L**" is given in (Machowski, 2008) and (Andersson, 2010) for a two-pole machine. The relations for a general machine with n_p poles will be as follows (Lie, 2011):

$$\theta_e = (n_p/2)\theta_m \ , \ \theta'_e = \theta_e - 2\pi/3 \ , \theta''_e = \theta_e + 2\pi/3$$

$$L_{aa} = L_s + L_m \cos(2\theta_e)$$

$$L_{bb} = L_s + L_m \cos(2\theta'_e)$$

$$L_{cc} = L_s + L_m \cos(2\theta''_e)$$

$$L_{ab} = L_{ba} = -M_s - L_m \cos\left(2\theta_e + \frac{\pi}{3}\right)$$

$$L_{bc} = L_{cb} = -M_s - L_m \cos\left(2\theta'_e + \frac{\pi}{3}\right) \tag{3-4}$$

$$L_{ac} = L_{ca} = -M_s - L_m \cos\left(2\theta''_e + \frac{\pi}{3}\right)$$

$$L_{aF} = L_{Fa} = M_F \cos(\theta_e)$$

$$L_{bF} = L_{Fb} = M_F \cos(\theta'_e)$$

$$L_{cF} = L_{Fc} = M_F \cos(\theta''_e)$$

$$L_{aD} = L_{Da} = M_D \cos(\theta_e)$$

$$L_{bD} = L_{Db} = M_D \cos(\theta'_e)$$

$$L_{cD} = L_{Dc} = M_D \cos(\theta''_e)$$

$$L_{aQ} = L_{Qa} = M_Q \sin(\theta_e)$$

$$L_{bQ} = L_{Qb} = M_Q \sin(\theta'_e)$$

$$L_{cQ} = L_{Qc} = M_Q \sin(\theta''_e)$$

$$L_{FF} = L_F \ , \qquad L_{DD} = L_D \ , \qquad L_{QQ} = L_Q$$

$$L_{FD} = L_{DF} = M_R$$

$$L_{FQ} = L_{QF} = L_{DQ} = L_{QD} = 0$$

Where L_s , L_m , M_s , M_F , M_D , M_Q , L_F , L_D , L_Q and M_R are positive real values.

The relations for mutual inductances between the "Q" and the stator windings in (3-4) are in agree with (Machowski, 2008) but different from those given in (Andersson, 2010). The reason is the conventional direction of current in the "Q" winding is chosen differently.

In the following the relations (3-4) will be investigated intuitively for a multi-pole machine by examining the magnetomotive forces[5] and flux line paths in each case and for various rotor angles.

- L_{aa} : Self-inductance of "a" windings on the stator depends partly on the flux path through the stator itself and partly on the flux path between the stator and rotor. Reluctance of the rotor path is dependent on the rotor angle. Figure (3-8) shows the flux paths and magnetomotive forces generated by a constant dc current in the "a" windings for different rotor angles:

  (a) $\theta_m = \frac{2k\pi}{n_P}$ $(k = 0,1, \dots)$

[5] http://en.wikipedia.org/wiki/Magnetomotive_force (accessed 2011)

(b) $\theta_m = \frac{(2k+1)\pi}{n_P}$ $(k = 0,1, \dots)$

In the case (a), the poles are located in the same direction as the magnetomotive forces induced by "a" windings. So the rotor has the least reluctance seen by the "a" windings and hence L_{aa} has its maximum. In the case (b), due to symmetry no flux is generated in the rotor and the rotor magnetic circuit has the largest reluctance. Hence L_{aa} has its minimum.

- L_{ab} : Figure (3-9) shows the flux path induced by dc currents in the "a" and "b"windings for two different rotor angles and current directions:

  (a) $\theta_m = \left(2k\pi + \frac{2\pi}{3}\right)/n_P$ $(k = 0,1, \dots)$ and currents in the "a" and "b" windings are equal and positive

  (b) $\theta_m = \left(2k\pi - \frac{\pi}{3}\right)/n_P$ $(k = 1, \dots)$ and currents in the "a" and "b" windings are equal but positive in "a" and negative in "b"

  In case (a), the flux induced by the current in winding "a" has a maximum positive linkage with the winding "b". In case (b), the flux linkage is maximum and negative.

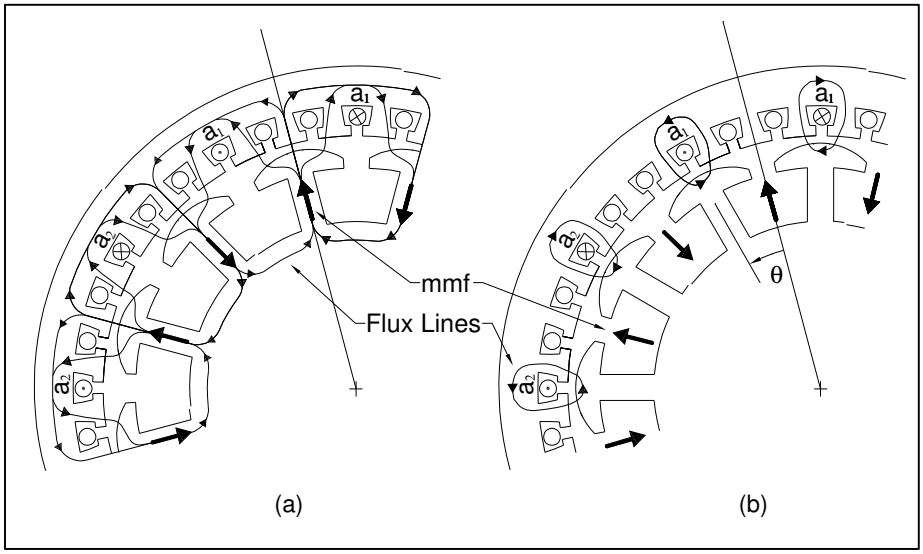

Figure (3-8) Flux Lines Generated Merely by the Current in "a" Windings for Different Rotor Positions

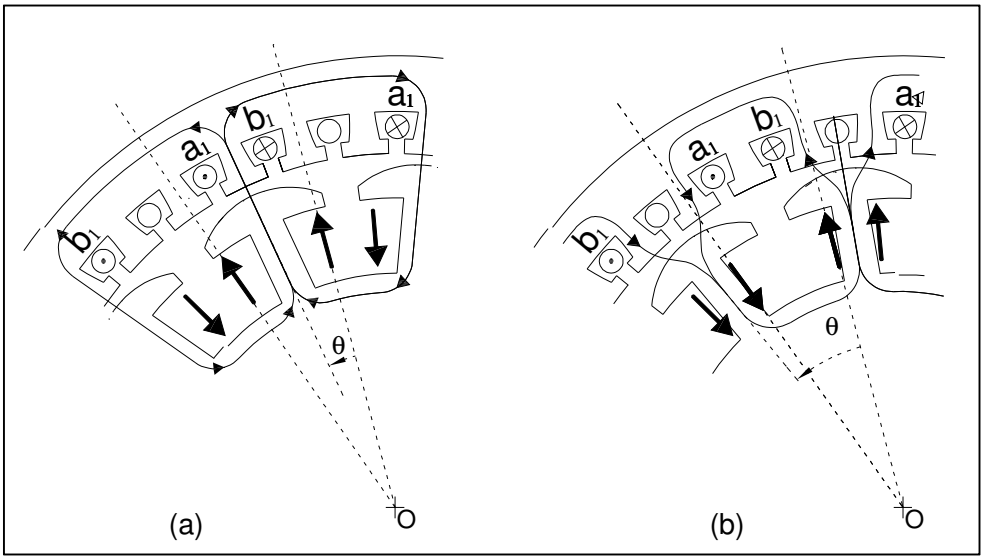

Figure (3-9) Flux Lines Generated by Currents in "a" and "b" Windings for Different Rotor Positions (Current in the "b" winding is negative in case (b).)

- L_{aF} and L_{aD} : Figure (3-10) shows the flux path induced by just the positive dc current in the "a" windings for different rotor angles:

  (a) $\theta_m = (4k\pi)/n_P \quad (k = 0,1, \dots)$

  (b) $\theta_m = (4k\pi + \pi)/n_P \quad (k = 0,1, \dots)$

  (c) $\theta_m = (4k\pi + 3\pi)/n_P \quad (k = 0,1, \dots)$

  (d) $\theta_m = (4k\pi + 2\pi)/n_P \quad (k = 0,1, \dots)$

  In cases (a) and (d) the flux linkages in the "F" windings are maximum in magnitude. In case (a) the flux passes the "F" windings in the same direction that flux induced by the "F" windings would have passed. So mutual inductance in this case is positive. However In case (d) the flux direction is opposite and the mutual inductance will be negative. In cases (b) and (c) due to symmetry there's no flux linkage in the "F" windings.

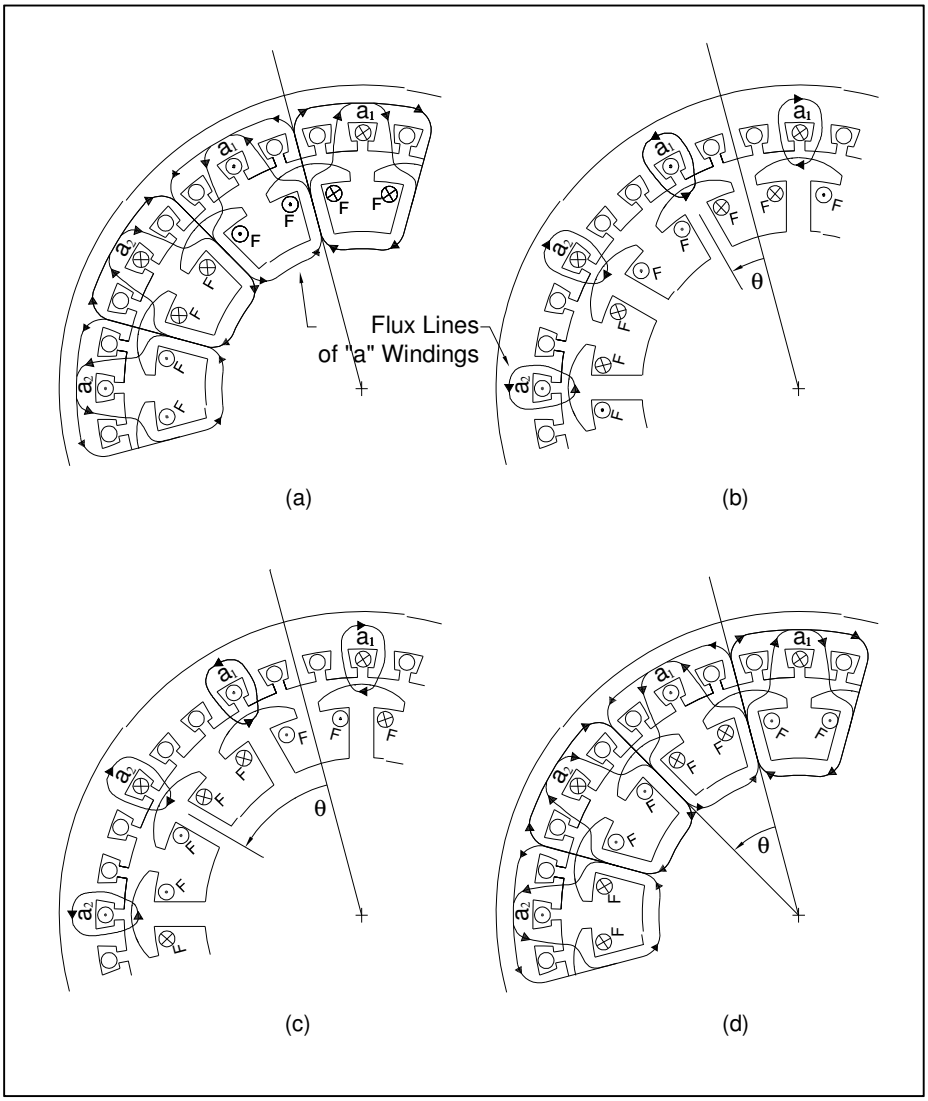

Figure (3-10) Flux Lines Generated Merely by the Current in "a" Windings and Linking the "F" Windings for Different Rotor Positions

- L_{aQ}, L_{FQ} and L_{DQ} : Figure (3-11) shows the flux paths induced by just the positive dc current in the "Q" windings for different rotor angles:

(a) $\theta_m = 2k\pi/n_P \quad (k = 0,1, \dots)$

(b) $\theta_m = (4k\pi + \pi)/n_P \quad (k = 0,1, \dots)$

(c) $\theta_m = (4k\pi + 3\pi)/n_P \quad (k = 0,1, \dots)$

At first site it is clear that in no case there is a flux linkage between the "Q" and "F" or between the "Q" and "D" windings. So values of L_{FQ} and L_{DQ} are always equal to zero. In

case (b) the flux induced by the current in "Q" windings are in the same direction as the flux induced by a current flowing into "a" windings would have been (see Figure (3-10) part (b)). So the mutual inductance L_{aQ} will be positive. A same conclusion results for a negative L_{aQ} in case (c). It is obvious due to symmetry that no flux linkage exists between "a" and "Q" windings in case (a).

3.1.5 The Park's Transformation

Equations for the synchronous generator are best described by using the so called Park's transformation. Consider Figure (3-12) where $n_P = 2$. This special case can be considered as when the area restricted to the a1_axis and a2_axis in Figure (3-1) be mapped into a complete circle by multiplying the angles with center at O by a factor of $(n_P/2)$. For this reason the rotor angle in Figure (3-12) is shown with $n_P\theta_m/2$.

The idea behind the Park's transform is to formulate the rotating magnetic field produced by a 3-phase sinusoidal current flowing in the armature windings in a coordinate system fixed to the rotor. This new coordinate system in Figure (3-12) is denoted by the "d" and the "q" axes. In the steady-state operation of the generator, the stator magnetic field will be stationary in the rotor reference frame. Thus the stator magnetic field can be modeled as the result of fictitious windings fixed to the rotor and carrying dc currents. An advantage of this transformation as will be shown later in this section is that self-inductances of these fictitious windings and their mutual inductance with rotor windings will no longer depend on the rotor angle.

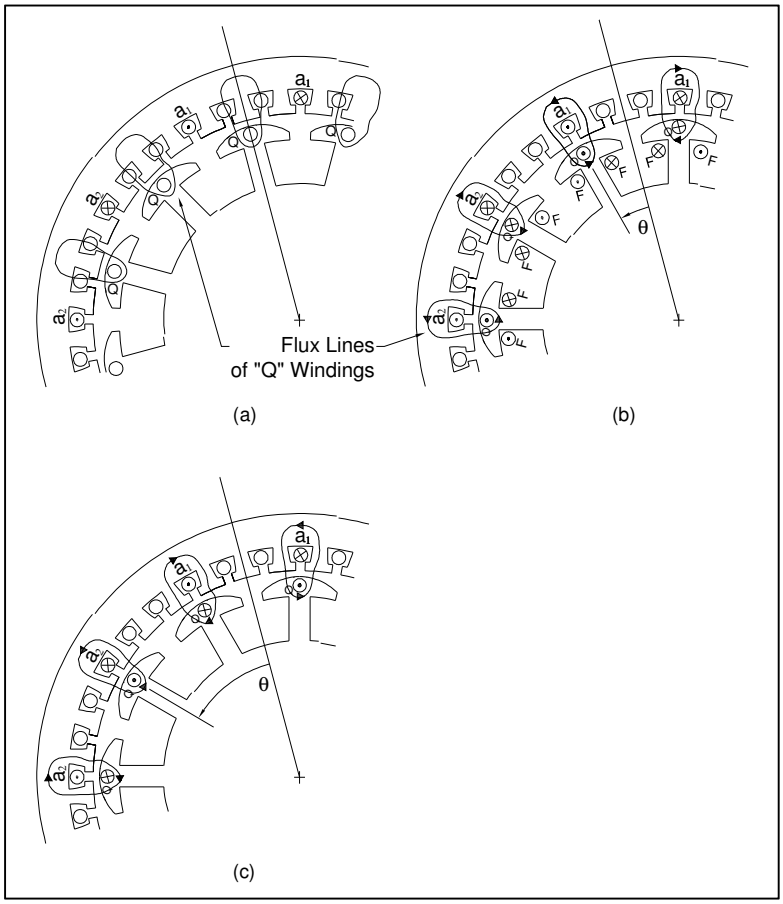

Figure (3-11) Flux Lines Generated Merely by the Current in "Q" Windings and Linking the "a" Windings for Different Rotor Positions

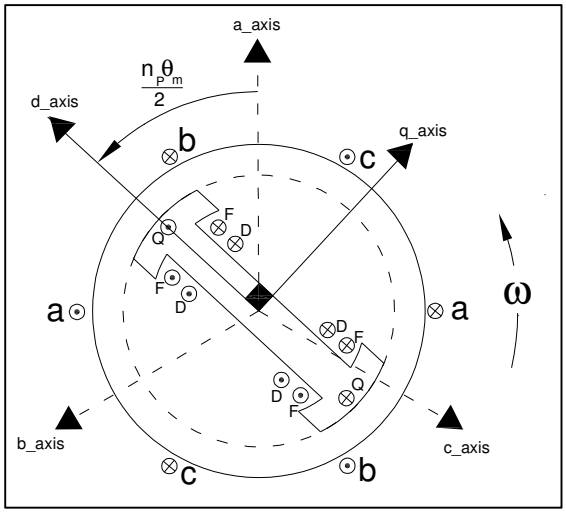

Figure (3-12) "d" and "q" Axes in a Two Poles Generator

In the following the projection of the stator magnetomotive force onto the rotor frame will be obtained. The resultant magnetomotive force in the stator frame at the rotor axis "O" is given by:

$$\mathbf{H} = \mathrm{H_a}\mathbf{u_a} + \mathrm{H_b}\mathbf{u_b} + \mathrm{H_c}\mathbf{u_c} \tag{3-5}$$

Where

$\mathbf{H} =$ Resultant magnetomotive force vector at the rotor axis measured in the stator reference frame [A. turns]

$\mathrm{H_a}(\mathrm{H_b}, \mathrm{H_c}) =$ Resultant magnetomotive force of the current flowing in the "a" ("b", "c") winding measured in the stator reference frame [A. turns]

$\mathbf{u_a}(\mathbf{u_b}, \mathbf{u_c}) =$ Unit vector along the "a" ("b", "c") axis

H can be presented in the rotor reference frame as:

$$\mathbf{H} = \widetilde{\mathrm{H}}_\mathrm{d}\mathbf{u_d} + \widetilde{\mathrm{H}}_\mathrm{q}\mathbf{u_q} \tag{3-6}$$

Where

$\widetilde{\mathrm{H}}_\mathrm{d}$ ($\widetilde{\mathrm{H}}_\mathrm{q}$) = Magnitude of projection of H onto the "d" ("q") axis [m^2]

$\mathbf{u_d}(\mathbf{u_q}) =$ Unit vector along the "d" ("q") axis

For calculation of $\widetilde{\mathrm{H}}_\mathrm{d}$ and $\widetilde{\mathrm{H}}_\mathrm{q}$, the unit vectors $\mathbf{u_a}, \mathbf{u_b}$ and $\mathbf{u_c}$ shall be written in terms of $\mathbf{u_d}$ and $\mathbf{u_q}$:

$$\begin{aligned}
\mathbf{u_a} &= \cos\left(\frac{\mathrm{n_P}\theta_\mathrm{m}}{2}\right)\mathbf{u_d} + \sin\left(\frac{\mathrm{n_P}\theta_\mathrm{m}}{2}\right)\mathbf{u_q} \\
\mathbf{u_b} &= \cos\left(\frac{\mathrm{n_P}\theta_\mathrm{m}}{2} - \frac{2\pi}{3}\right)\mathbf{u_d} + \sin\left(\frac{\mathrm{n_P}\theta_\mathrm{m}}{2} - \frac{2\pi}{3}\right)\mathbf{u_q} \\
\mathbf{u_c} &= \cos\left(\frac{\mathrm{n_P}\theta_\mathrm{m}}{2} + \frac{2\pi}{3}\right)\mathbf{u_d} + \sin\left(\frac{\mathrm{n_P}\theta_\mathrm{m}}{2} + \frac{2\pi}{3}\right)\mathbf{u_q}
\end{aligned} \tag{3-7}$$

From (3-5) and (3-7) it can be concluded:

$$\begin{aligned}\mathbf{H} &= \underbrace{\left[\mathrm{H_a}\cos\left(\frac{\mathrm{n_P}\theta_\mathrm{m}}{2}\right) + \mathrm{H_b}\cos\left(\frac{\mathrm{n_P}\theta_\mathrm{m}}{2}-\frac{2\pi}{3}\right) + \mathrm{H_c}\cos\left(\frac{\mathrm{n_P}\theta_\mathrm{m}}{2}+\frac{2\pi}{3}\right)\right]}_{\widetilde{\mathrm{H}}_\mathrm{d}}\mathbf{u}_\mathrm{d} \\ &+ \underbrace{\left[\mathrm{H_a}\sin\left(\frac{\mathrm{n_P}\theta_\mathrm{m}}{2}\right) + \mathrm{H_b}\sin\left(\frac{\mathrm{n_P}\theta_\mathrm{m}}{2}-\frac{2\pi}{3}\right) + \mathrm{H_c}\sin\left(\frac{\mathrm{n_P}\theta_\mathrm{m}}{2}+\frac{2\pi}{3}\right)\right]}_{\widetilde{\mathrm{H}}_\mathrm{q}}\mathbf{u}_\mathrm{q}\end{aligned} \tag{3-8}$$

Or:

$$\begin{bmatrix}\widetilde{\mathrm{H}}_\mathrm{d}\\ \widetilde{\mathrm{H}}_\mathrm{q}\end{bmatrix} = \begin{bmatrix}\cos\left(\frac{\mathrm{n_P}\theta_\mathrm{m}}{2}\right) & \cos\left(\frac{\mathrm{n_P}\theta_\mathrm{m}}{2}-\frac{2\pi}{3}\right) & \cos\left(\frac{\mathrm{n_P}\theta_\mathrm{m}}{2}+\frac{2\pi}{3}\right)\\ \sin\left(\frac{\mathrm{n_P}\theta_\mathrm{m}}{2}\right) & \sin\left(\frac{\mathrm{n_P}\theta_\mathrm{m}}{2}-\frac{2\pi}{3}\right) & \sin\left(\frac{\mathrm{n_P}\theta_\mathrm{m}}{2}+\frac{2\pi}{3}\right)\end{bmatrix}\begin{bmatrix}\mathrm{H_a}\\ \mathrm{H_b}\\ \mathrm{H_c}\end{bmatrix} = \tilde{P}\begin{bmatrix}\mathrm{H_a}\\ \mathrm{H_b}\\ \mathrm{H_c}\end{bmatrix} \tag{3-9}$$

It can be shown that:

$$\tilde{P}\tilde{P}^T = \begin{bmatrix}\frac{3}{2} & 0\\ 0 & \frac{3}{2}\end{bmatrix} \qquad and \qquad \tilde{P}\begin{bmatrix}1\\1\\1\end{bmatrix} = \begin{bmatrix}0\\0\end{bmatrix} \tag{3-10}$$

This suggests the following orthonormal transformation from $\mathcal{R}^3$ to $\mathcal{R}^3$:

$$\mathbf{P} = \sqrt{\frac{2}{3}}\begin{bmatrix}\frac{1}{\sqrt{2}} & \frac{1}{\sqrt{2}} & \frac{1}{\sqrt{2}}\\ \cos\left(\frac{\mathrm{n_P}\theta_\mathrm{m}}{2}\right) & \cos\left(\frac{\mathrm{n_P}\theta_\mathrm{m}}{2}-\frac{2\pi}{3}\right) & \cos\left(\frac{\mathrm{n_P}\theta_\mathrm{m}}{2}+\frac{2\pi}{3}\right)\\ \sin\left(\frac{\mathrm{n_P}\theta_\mathrm{m}}{2}\right) & \sin\left(\frac{\mathrm{n_P}\theta_\mathrm{m}}{2}-\frac{2\pi}{3}\right) & \sin\left(\frac{\mathrm{n_P}\theta_\mathrm{m}}{2}+\frac{2\pi}{3}\right)\end{bmatrix} \tag{3-11}$$

$$\mathrm{PP^T} = \mathrm{P^T P} = \begin{bmatrix}1 & 0 & 0\\ 0 & 1 & 0\\ 0 & 0 & 1\end{bmatrix}$$

By applying the transform **P** to the vector $\begin{bmatrix} H_a \\ H_b \\ H_c \end{bmatrix}$ one can get:

$$\begin{bmatrix} H_0 \\ H_d \\ H_q \end{bmatrix} = \begin{bmatrix} \sqrt{\frac{1}{3}}(H_a + H_b + H_c) \\ \sqrt{\frac{2}{3}}\widetilde{H}_d \\ \sqrt{\frac{2}{3}}\widetilde{H}_q \end{bmatrix} = \mathbf{P} \begin{bmatrix} H_a \\ H_b \\ H_c \end{bmatrix} \quad (3\text{-}12)$$

At the following operating condition the sum $H_a + H_b + H_c$ will be equal to zero:

- The armature windings are star connected without ground connection
- No saturation effect or no imbalance armature currents

So values of the set (H_a, H_b, H_c) at any time instant are uniquely determined if the values of the set $(\widetilde{H}_d, \widetilde{H}_q)$ are known and vice versa.

H_d and H_q in (3-12) will preserve the direction of the stator magnetic field measured in the rotor frame and preserve its strength if a correction factor of $\sqrt{\frac{3}{2}}$ is applied. $\begin{bmatrix} H_a \\ H_b \\ H_c \end{bmatrix}$ is ideally proportional to the armature currents vector $\begin{bmatrix} i_a \\ i_b \\ i_c \end{bmatrix}$. So the transform **P** can be used to study the effects of a three phase sinusoidal current flowing in the armature windings on the magnetic field seen by the rotor. Voltages across the armature windings can also be transformed by **P** into the rotor frame and the transformed currents, voltages and fluxes can be associated to fictitious windings "d" and "q" fixed to the rotor frame as shown in the Figure (3-13). In the next section relations for the self-inductances of these fictitious windings and the mutual inductance between them and the rotor windings will be derived. In section 0 relations for voltages across these fictitious windings will be found so that the inverse transform of these voltages will give the terminal voltages of the generator.

The relation for matrix **P** in (3-11) is in agrees with (Machowski, 2008) but differs from that of (Andersson, 2010). The reason is that in (Machowski, 2008) and here the "q" axis is chosen to lag "d" axis. According to (Machowski, 2008) this is the configuration recommended by IEEE. According to the same reference when studying equations transformed into "d-q" frame, one should always note which Park's transform has been used.

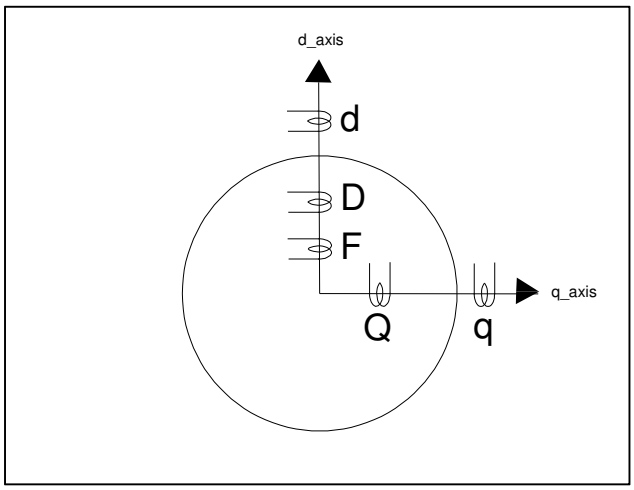

Figure (3-13) Reproduction of the Stator Magnetic Field by Fictitious Rotor Windings "d" and "q"

Using notations from (3-4) the Park's transform matrix can be written in the following form:

$$\mathbf{P} = \sqrt{\frac{2}{3}}\begin{bmatrix} \frac{1}{\sqrt{2}} & \frac{1}{\sqrt{2}} & \frac{1}{\sqrt{2}} \\ \cos(\theta_e) & \cos(\theta'_e) & \cos(\theta''_e) \\ \sin(\theta_e) & \sin(\theta'_e) & \sin(\theta''_e) \end{bmatrix} \tag{3-13}$$

3.1.6 Flux Linkage Equations in the 0dq Frame

An extended Park's transformation matrix is defined by:

$$\mathbf{P}_{\text{ext}} = \begin{bmatrix} \mathbf{P} & \mathbf{O}^{3\times3} \\ \mathbf{O}^{3\times3} & \mathbf{I}^{3\times3} \end{bmatrix} \qquad \mathbf{P}_{\text{ext}}^{\text{T}}\mathbf{P}_{\text{ext}} = \mathbf{P}_{\text{ext}}\mathbf{P}_{\text{ext}}^{\text{T}} = \mathbf{I} \tag{3-14}$$

Applying the extended transform to (3-3) will result:

$$\begin{bmatrix}\Psi_0\\ \Psi_d\\ \Psi_q\\ \Psi_F\\ \Psi_D\\ \Psi_Q\end{bmatrix} = \mathbf{P}_{ext}\begin{bmatrix}\Psi_a\\ \Psi_b\\ \Psi_c\\ \Psi_F\\ \Psi_D\\ \Psi_Q\end{bmatrix} = \mathbf{P}_{ext}\mathbf{L}\begin{bmatrix}i_a\\ i_b\\ i_c\\ i_F\\ i_D\\ i_Q\end{bmatrix} = \underbrace{\mathbf{P}_{ext}\mathbf{L}\,\mathbf{P}_{ext}^{T}}_{\mathbf{L_r}}\begin{bmatrix}i_0\\ i_d\\ i_q\\ i_F\\ i_D\\ i_Q\end{bmatrix} \tag{3-15}$$

$\mathbf{L_r}$ is the new inductance matrix in the rotor frame and can be shown to be independent from rotor angle. The flux linkage equations then will become:

$$\begin{bmatrix}\Psi_0\\ \Psi_d\\ \Psi_q\\ \Psi_F\\ \Psi_D\\ \Psi_Q\end{bmatrix} = \underbrace{\begin{bmatrix}L_0 & 0 & 0 & 0 & 0 & 0\\ 0 & L_d & 0 & kM_F & kM_D & 0\\ 0 & 0 & L_q & 0 & 0 & kM_Q\\ 0 & kM_F & 0 & L_F & M_R & 0\\ 0 & kM_D & 0 & M_R & L_D & 0\\ 0 & 0 & kM_Q & 0 & 0 & L_Q\end{bmatrix}}_{\mathbf{L_r}}\begin{bmatrix}i_0\\ i_d\\ i_q\\ i_F\\ i_D\\ i_Q\end{bmatrix} \tag{3-16}$$

Where

$$L_0 = L_s - 2M_s\ ,\ L_d = L_s + M_s + k^2L_m\ ,$$

$$L_q = L_s + M_s - k^2L_m\ ,\ k = \sqrt{\frac{3}{2}}$$

3.1.7 Voltage Equations

Consider electrical connections of Figure (3-5) to Figure (3-7). Especially the conventional direction for currents and voltages shall be noticed. Regarding the discussion in section 3.1.2 and the voltage directions, the equation (3-2) applies in here. Sign of the mutual inductances depends on the rotor angle:

$$\begin{bmatrix} v_a \\ v_b \\ v_c \\ -v_F \\ 0 \\ 0 \end{bmatrix} = -\underbrace{\begin{bmatrix} r & & & & & \\ & r & & & & \\ & & r & & & \\ & & & r_F & & \\ & & & & r_D & \\ & & & & & r_Q \end{bmatrix}}_{\mathbf{R}} \begin{bmatrix} i_a \\ i_b \\ i_c \\ i_F \\ i_D \\ i_Q \end{bmatrix} - \frac{d}{dt} \underbrace{\begin{bmatrix} \Psi_a \\ \Psi_b \\ \Psi_c \\ \Psi_F \\ \Psi_D \\ \Psi_Q \end{bmatrix}}_{\mathbf{\Psi}} \tag{3-17}$$

Applying the extended transform to (3-17) will result:

$$\begin{bmatrix} v_a \\ v_b \\ v_c \\ -v_F \\ 0 \\ 0 \end{bmatrix} = -(\mathbf{P}_{ext}\mathbf{R}\,\mathbf{P}_{ext}^{T}) \begin{bmatrix} i_a \\ i_b \\ i_c \\ i_F \\ i_D \\ i_Q \end{bmatrix} - \mathbf{P}_{ext}\,\frac{d}{dt}\left(\mathbf{P}_{ext}^{T} \begin{bmatrix} \Psi_a \\ \Psi_b \\ \Psi_c \\ \Psi_F \\ \Psi_D \\ \Psi_Q \end{bmatrix} \right)$$

$$= -(\mathbf{P}_{ext}\mathbf{R}\,\mathbf{P}_{ext}^{T}) \begin{bmatrix} i_0 \\ i_d \\ i_q \\ i_F \\ i_D \\ i_Q \end{bmatrix} - \mathbf{P}_{ext}\left(\mathbf{P}_{ext}^{T} \begin{bmatrix} \dot{\Psi}_0 \\ \dot{\Psi}_d \\ \dot{\Psi}_q \\ \dot{\Psi}_F \\ \dot{\Psi}_D \\ \dot{\Psi}_Q \end{bmatrix} + \dot{\mathbf{P}}_{ext}^{T} \begin{bmatrix} \Psi_0 \\ \Psi_d \\ \Psi_q \\ \Psi_F \\ \Psi_D \\ \Psi_Q \end{bmatrix} \right) = -\mathbf{R} \begin{bmatrix} i_0 \\ i_d \\ i_q \\ i_F \\ i_D \\ i_Q \end{bmatrix} - \begin{bmatrix} \dot{\Psi}_0 \\ \dot{\Psi}_d \\ \dot{\Psi}_q \\ \dot{\Psi}_F \\ \dot{\Psi}_D \\ \dot{\Psi}_Q \end{bmatrix} - \mathbf{P}_{ext}\dot{\mathbf{P}}_{ext}^{T} \begin{bmatrix} \Psi_0 \\ \Psi_d \\ \Psi_q \\ \Psi_F \\ \Psi_D \\ \Psi_Q \end{bmatrix}$$

It can be shown that:

$$\mathbf{P}_{ext}\dot{\mathbf{P}}_{ext}^{T} = \begin{bmatrix} \mathbf{P}\dot{\mathbf{P}}^{T} & \mathbf{0}^{3\times3} \\ \mathbf{0}^{3\times3} & \mathbf{0}^{3\times3} \end{bmatrix} = \begin{bmatrix} 0 & 0 & 0 & & \\ 0 & 0 & -1 & \mathbf{0}^{3\times3} & \\ 0 & 1 & 0 & & \\ & \mathbf{0}^{3\times3} & & \mathbf{0}^{3\times3} & \end{bmatrix} \times \underbrace{\left(\frac{d\theta_e}{dt}\right)}_{\omega_e}$$

So the voltage equations become:

$$\begin{bmatrix} v_0 \\ v_d \\ v_q \\ -v_F \\ 0 \\ 0 \end{bmatrix} = -\underbrace{\begin{bmatrix} r & 0 & 0 & 0 & 0 & 0 \\ 0 & r & 0 & 0 & 0 & 0 \\ 0 & 0 & r & 0 & 0 & 0 \\ 0 & 0 & 0 & r_F & 0 & 0 \\ 0 & 0 & 0 & 0 & r_D & 0 \\ 0 & 0 & 0 & 0 & 0 & r_Q \end{bmatrix}}_{\mathbf{R}} \begin{bmatrix} i_0 \\ i_d \\ i_q \\ i_F \\ i_D \\ i_Q \end{bmatrix} - \begin{bmatrix} \dot{\Psi}_0 \\ \dot{\Psi}_d \\ \dot{\Psi}_q \\ \dot{\Psi}_F \\ \dot{\Psi}_D \\ \dot{\Psi}_Q \end{bmatrix} - \underbrace{\begin{bmatrix} 0 \\ \omega_e\Psi_q \\ -\omega_e\Psi_d \\ 0 \\ 0 \\ 0 \end{bmatrix}}_{\mathbf{P}_{ext}\dot{\mathbf{P}}_{ext}^{T}\mathbf{\Psi}} \tag{3-18}$$

3.1.8 The Swing Equation

The swing equation first was introduced in Chapter 2. Here it is repeated for convenience:

$$J\omega_m \frac{d\omega_m}{dt} = P_{in} - P_{loss} - P_{out} = \eta_g \eta_t \rho g H_t Q_t - P_{out}$$
$$\omega_m = \frac{d\theta_m}{dt} \tag{3-19}$$

Where

$P_{in} =$ Hydraulic power transferred to turbine [W]

$P_{out} =$ Active electric power output at terminals of the generator [W]

$P_{loss} =$ Power losses through turbine and generator [W]

$H_t =$ Turbine head [m]

$Q_t =$ Turbine volumetric discharge [m^3/sec]

$\eta_t =$ Overall efficiency of turbine (hydraulic and mechanical)

$\eta_g =$ Overall efficiency of generator

The relation giving the P_{out} is as follows:

$$P_{out} = v_a i_a + v_b i_b + v_c i_c$$
$$= \begin{bmatrix} v_a \\ v_b \\ v_c \end{bmatrix}^T \begin{bmatrix} i_a \\ i_b \\ i_c \end{bmatrix} = \begin{bmatrix} v_a \\ v_b \\ v_c \end{bmatrix}^T \mathbf{P}^T \mathbf{P} \begin{bmatrix} i_a \\ i_b \\ i_c \end{bmatrix} = \begin{bmatrix} v_0 \\ v_d \\ v_q \end{bmatrix}^T \begin{bmatrix} i_0 \\ i_d \\ i_q \end{bmatrix} = v_0 i_0 + v_d i_d + v_q i_q \tag{3-20}$$

According to Figure (3-14) the amount of power losses within the generator can be categorized in four groups:

- Armature resistive losses with an instantaneous value equal to $r(i_a^2 + i_b^2 + i_c^2)$ or equivalently $r(i_0^2 + i_d^2 + i_q^2)$
- Core losses: These losses are due to Eddy currents and hysteresis and depend on the generator load and frequency
- Mechanical losses: These losses are due to friction and windage and are a function of the rotational speed ($P_{Loss-Mech} = K_D \omega_m^2$)
- Stray losses: Losses that cannot be categorized in other groups. "For most machines, stray losses are taken by convention to be one percent of full load." (Chapman, 2005)

The efficiency of generator may vary by the generator load. Sometimes the armature resistive losses and/or mechanical losses are treated separately in the relevant equations as appear in the literature in general.

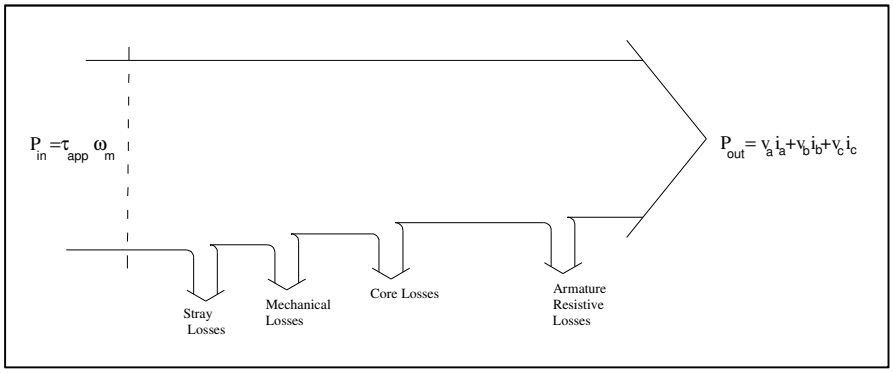

Figure (3-14) Power Flow Diagram of a Synchronous Machine (Chapman, 2005)

The flux linkage equations (3-16), the voltage equations (3-18), the Park's transform (3-13), the swing equation (3-19) and differential equations governing the waterway in a hydropower generation unit will make the complete model for the hydropower generation unit.

3.1.9 Simplified Generator Models[6]

Usually the following assumptions are made to reduce order of the model given by equations (3-13), (3-16), (3-18) and (3-19):

[6] Material of this section are mostly taken from (Machowski, 2008).

$$|\dot{\Psi}_d| \ll |\omega_e \Psi_q| \quad , \quad |\dot{\Psi}_q| \ll |\omega_e \Psi_d| \tag{3-21}$$

The new model will be obtained by ignoring the terms $\dot{\Psi}_d$ and $\dot{\Psi}_q$ in (3-18). Under the assumptions of balanced currents and voltages, v_0 and i_0 and hence Ψ_0 and $\dot{\Psi}_0$ will always be equal to zero. So actually the flux linkage and the voltage equation along the "0" axis can also be removed to reduce the model order further. It is also customary to ignore existence of one or both of the damper windings to obtain simpler models. And finally the dynamics for the changes in the field current can be ignored by ignoring the term $\dot{\Psi}_F$ in (3-18) to obtain the steady-state voltage-current relationship for the generator. (Machowski, 2008)

By application of the assumptions (3-21) and ignoring the terms $\dot{\Psi}_d$ and $\dot{\Psi}_q$ in (3-18), equations for v_d and v_q regarding (3-16) and (3-18) will become as the following:

$$\begin{bmatrix} v_d \\ v_q \end{bmatrix} = -\begin{bmatrix} r & 0 \\ 0 & r \end{bmatrix}\begin{bmatrix} i_d \\ i_q \end{bmatrix} + \begin{bmatrix} -\omega_e \psi_q \\ \omega_e \psi_d \end{bmatrix}$$
$$= -\begin{bmatrix} r & 0 \\ 0 & r \end{bmatrix}\begin{bmatrix} i_d \\ i_q \end{bmatrix} + \begin{bmatrix} -\omega_e (L_q i_q + kM_Q i_Q) \\ \omega_e (L_d i_d + kM_F i_F + kM_D i_D) \end{bmatrix} \tag{3-22}$$

Frequency of the generator (ω_e), when operating stably in a large network, is not normally fixed and has zero-mean small oscillations around the system center of inertia frequency $f_s(t)$. Normally $f_s(t)$ has very slow variations (and can be regarded constant if the time duration for studying the generator dynamics is not too long) (Andersson, 2010). The rotor electrical angle of the generator then can be written in the form:

$$\theta_e(t) = 2\pi f_s t + \delta_e(t)$$
$$\delta_e(t) = \delta_e(0) + \int_0^t [\omega_e(\tau) - 2\pi f_s] d\tau = \delta_e(0) + \int_0^t \Delta\omega_e(\tau) d\tau \tag{3-23}$$

For stable operation of the generator, $\delta_e(t)$ should be bounded and hence frequency fluctuations $\Delta\omega_e(t)$ should have zero mean. For simplification purposes in (3-22), it is assumed that:

$$|\Delta\omega_e(t)| \ll \omega_s = 2\pi f_s \quad , \quad f_s: \text{system frequency (almost constant)} \tag{3-24}$$

With the above assumption, (3-22) turns into:

$$\begin{bmatrix} v_d \\ v_q \end{bmatrix} = -\begin{bmatrix} r & x_q \\ -x_d & r \end{bmatrix}\begin{bmatrix} i_d \\ i_q \end{bmatrix} + \begin{bmatrix} -\omega_s k M_Q i_Q \\ \omega_s k M_F i_F + \omega_s k M_D i_D \end{bmatrix} \qquad (3\text{-}25)$$

$$x_d = \omega_s L_d \quad , \quad x_q = \omega_s L_q$$

Note that $\Delta\omega_e(t)$, when its effect accumulated in time as in (3-23), still affects the system model's voltage-current relationship through changes in the Park's transform. Consider generator be paralleled with an ideal three-phase voltage source so that its terminal voltages are given by:

$$v_a(t) = V\sin\omega_s t\,, \quad v_b(t) = V\sin\left(\omega_s t - \frac{2\pi}{3}\right), \quad v_c(t) = V\sin\left(\omega_s t + \frac{2\pi}{3}\right)$$

In this case the transformed voltages will become as $\begin{bmatrix} v_d \\ v_q \end{bmatrix} = \begin{bmatrix} V\sin\delta \\ V\cos\delta \end{bmatrix}$ and hence $\Delta\omega_e(t)$ affects $\begin{bmatrix} v_d \\ v_q \end{bmatrix}$ by changing the rotor angle.

Steady-state Operation of the Generator:

The steady state value of the field current i_F is equal to v_F/r_F . If the transient term in the field current is denoted by Δi_F, i.e. $i_F = v_F/r_F + \Delta i_F$, then (3-25) can be rewritten as:

$$\begin{bmatrix} v_d \\ v_q \end{bmatrix} = -\begin{bmatrix} r & x_q & 0 \\ -x_d & r & -\omega_s k M_F/r_F \end{bmatrix}\begin{bmatrix} i_d \\ i_q \\ v_F \end{bmatrix} + \begin{bmatrix} -\omega_s k M_Q i_Q \\ \omega_s k M_F \Delta i_F + \omega_s k M_D i_D \end{bmatrix} \qquad (3\text{-}26)$$

The equation (3-26) is the output equation for a linear system with three inputs, two outputs and three states (i_D, i_Q and Δi_F which tend to zero as the system reaches a steady-state condition). Any of the combinations (i_d, i_q, v_F), (v_d, i_q, v_F), (i_d, v_q, v_F) or (v_d, v_q, v_F) can be chosen as independent variables (inputs). The other two variables out of i_d, i_q, v_d, v_q, v_F will be the outputs in each case. It's possible that (i_d, i_q) will be correlated with (v_d, v_q) through the load dynamics. The field voltage v_F will also be correlated with (v_d, v_q) through the excitation system. So it's expected that after any disturbance in the system all the variables in (3-26) experience a change in their values. If the cause of disturbance is in the form of a step change (for example in the load), then system will reach a new steady-state condition as the induced currents i_D, i_Q and Δi_F decay and vanish. Then the steady-state values of i_d, i_q, v_d, v_q, v_F shall satisfy the following equation:

$$\begin{bmatrix} v_d \\ v_q \end{bmatrix} = -\begin{bmatrix} r & x_q & 0 \\ -x_d & r & -\omega_s k M_F / r_F \end{bmatrix} \begin{bmatrix} i_d \\ i_q \\ v_F \end{bmatrix}$$

Or in another notation:

$$\begin{bmatrix} v_d \\ v_q \end{bmatrix} = -\begin{bmatrix} r & x_q \\ -x_d & r \end{bmatrix} \begin{bmatrix} i_d \\ i_q \end{bmatrix} + \begin{bmatrix} 0 \\ e_q \end{bmatrix}$$
$$e_d = 0 \quad , \quad e_q = e_f = \omega_s k M_F v_F / r_F \tag{3-27}$$

Equation (3-27) along with the swing equation ((3-19) and (3-20)) and Park's transform (3-13) together define the simplest generator model in which the transient currents induced in the field and damper windings are neglected. Equation (3-27) can also be used for determining the steady state operating point of the generator.

Transient and Subtransient Operations:

The following assumptions are vital for the discussion that follows:

After any disturbance system will reach a new steady-state condition as the induced currents i_D, i_Q and Δi_F in (3-26) decay and vanish:

- Induced currents in the damper windings decay faster than any other phenomena in the generator (with a time constant of order 0.01 to 0.1 second). During this time duration variables other than i_D and i_Q in (3-26) can be considered almost constant. Generator dynamics within this time interval is referred to as "subtransient operation".
- Time constant for transients in the field windings (Δi_F) has an order of 1 to 10 seconds. Dynamics of generator after damper currents are vanished until generator reaches the new steady state is referred to as the "transient operation" of generator.

(3-28)

The time separation effect introduced by assumption (3-28) results in sort of simplification when studying each effect.

Generator dynamics with transient phenomenon: It's possible to get a model more detailed than (3-27) by considering the effect of transient field current Δi_F on the voltage-current characteristics of the generator. From (3-25) by neglecting the damper currents it's concluded:

$$\begin{bmatrix} v_d \\ v_q \end{bmatrix} = -\begin{bmatrix} r & x_q \\ -x_d & r \end{bmatrix}\begin{bmatrix} i_d \\ i_q \end{bmatrix} + \begin{bmatrix} 0 \\ \omega_s k M_F i_F \end{bmatrix} \tag{3-29}$$

The field current i_F can be calculated from (3-16) by neglecting the damper current i_D and from (3-18) as follows:

$$\begin{gathered} \Psi_F = k M_F i_d + L_F i_F \;\Rightarrow\; i_F = \frac{1}{L_F}\Psi_F - \frac{k M_F}{L_F} i_d \\ v_F = r_F i_F + \dot{\Psi}_F \;\Rightarrow\; i_F = \frac{v_F}{r_F} - \frac{1}{r_F}\,\dot{\Psi}_F \end{gathered} \tag{3-30}$$

Substituting i_F from the first equation in (3-30) into (3-29) will give the voltage equation as follows:

$$\begin{gathered} \begin{bmatrix} v_d \\ v_q \end{bmatrix} = -\begin{bmatrix} r & x'_q \\ -x'_d & r \end{bmatrix}\begin{bmatrix} i_d \\ i_q \end{bmatrix} + \begin{bmatrix} e'_d \\ e'_q \end{bmatrix} \\ x'_d = \omega_s L'_d \;\;,\qquad x'_q = x_q \\ L'_d = L_d - \frac{k^2 M_F^2}{L_F} \\ e'_d = 0 \;\;,\;\; e'_q = \omega_s \frac{k M_F}{L_F}\Psi_F \end{gathered} \tag{3-31}$$

A differential equation can be obtained for e'_q by eliminating i_F from the first and second equations in (3-30):

$$\frac{v_F}{r_F} - \frac{1}{r_F}\,\dot{\Psi}_F = \frac{1}{L_F}\Psi_F - \frac{k M_F}{L_F} i_d$$

Multiplying both sides by $\omega_s k M_F$ will result:

$$\frac{L_F}{r_F}\,\omega_s \frac{k M_F}{L_F}\dot{\Psi}_F + \omega_s \frac{k M_F}{L_F}\Psi_F - \omega_s \frac{k^2 M_F^2}{L_F} i_d - \omega_s k M_F \frac{v_F}{r_F}$$

In another notation regarding (3-27) and (3-31):

$$T'_{do}\ \frac{de'_q}{dt} = -e'_q + e_q + (x_d - x'_d)i_d$$

$$T'_{do} = \frac{L_F}{r_F} \tag{3-32}$$

Assumption: $\dot{\omega}_s \approx 0$

In deriving (3-32) it's assumed that the system frequency ω_s is almost constant so that the equality $\frac{de'_q}{dt} = \frac{d}{dt}\left(\omega_s \frac{kM_F}{L_F}\Psi_F\right) = \omega_s \frac{kM_F}{L_F}\dot{\Psi}_F$ will be held.

Equations (3-31) and (3-32) and definitions of x_d, x_q, e_d and e_q from (3-25) and (3-27) along with the swing equation ((3-19) and (3-20)) and Park's transform (3-13) together define the model of generator in which transient variations of the field current is taken into account.

Generator dynamics with both transient and subtransient phenomena: Now let's consider (3-26) complete without neglecting any terms. From (3-16) it's possible to compute i_F, i_D and i_Q in terms of i_d, i_q, Ψ_F, Ψ_D and Ψ_Q:

$$\Psi_Q = kM_Q i_q + L_Q i_Q \quad \Rightarrow \quad i_Q = \frac{1}{L_Q}\Psi_Q - \frac{kM_Q}{L_Q} i_q$$

$$\left.\begin{aligned}\Psi_F &= kM_F i_d + L_F i_F + M_R i_D \\ \Psi_D &= kM_D i_d + M_R i_F + L_D i_D\end{aligned}\right\} \quad \Rightarrow \quad \begin{cases} i_F = \dfrac{L_D(\Psi_F - kM_F i_d) - M_R(\Psi_D - kM_D i_d)}{L_F L_D - M_R^2} \\ i_D = \dfrac{-M_R(\Psi_F - kM_F i_d) + L_F(\Psi_D - kM_D i_d)}{L_F L_D - M_R^2} \end{cases} \tag{3-33}$$

Substituting i_F, i_D and i_Q from the above relations into (3-26) will result:

$$\begin{bmatrix} v_d \\ v_q \end{bmatrix} = -\begin{bmatrix} r & x''_q \\ -x''_d & r \end{bmatrix}\begin{bmatrix} i_d \\ i_q \end{bmatrix} + \begin{bmatrix} e''_d \\ e''_q \end{bmatrix}$$

$$x''_q = \omega_s L''_q \ , \ L''_q = L_q - \frac{kM_Q}{L_Q} \ , \quad e''_d = -\omega_s \frac{kM_Q}{L_Q}\Psi_Q$$

$$x''_d = \omega_s L''_d \ , \qquad L''_d = L_d - k^2\left(\frac{L_D M_F^2 + L_F M_D^2 - 2M_R M_D M_F}{L_F L_D - M_R^2}\right) \tag{3-34}$$

$$e''_q = \omega_s k\left(\frac{M_F L_D - M_D M_R}{L_F L_D - M_R^2}\right)\Psi_F + \omega_s k\left(\frac{M_D L_F - M_F M_R}{L_F L_D - M_R^2}\right)\Psi_D$$

Again e''_q and e''_d each are a solution of a differential equation. Substituting the relations for i_F, i_D and i_Q from (3-33) into the equations for $\dot{\Psi}_F, \dot{\Psi}_D$ and $\dot{\Psi}_Q$ in (3-16) and using the definitions in (3-31) and (3-34) will result in the following differential equations for e''_q and e''_d:

$$T''_{do}\frac{de''_q}{dt} = e'_q - e''_q + i_d(x'_d - x''_d)$$

$$T''_{qo}\frac{de''_d}{dt} = e'_d - e''_d - i_q(x'_q - x''_q)$$

$$T''_{do} = \left(L_D - \frac{M_R^2}{L_F}\right)\frac{1}{r_D} \tag{3-35}$$

$$T''_{qo} = \frac{L_Q}{r_Q}$$

Assumption: $\dot{\omega}_s \approx 0$

Equations (3-32), (3-34), (3-35), definitions of x'_d, x'_q, e'_d and e'_q from (3-31) and definitions of x_d, x_q, e_d and e_q from (3-25) and (3-27) along with the swing equation ((3-19) and (3-20)) and Park's transform (3-13) together define the most complete generator model.

3.1.10 System Reference Frame

Let f_s be an agreed reference frequency in the power system which is fixed or varies slowly (like the frequency of center of inertia of the system (Andersson, 2010)). Also consider a particular time instant as the reference for measuring of the time t for all the system (for example the instant that a particular voltage within the system reaches its maximum positive value compared to the ground voltage). Any current or voltage signal within the system which is of the form

$$\mathbf{s}(t) = \sqrt{2}S(t)\begin{bmatrix}\cos(2\pi f_s t + \alpha(t)) \\ \cos\left(2\pi f_s t - \frac{2\pi}{3} + \alpha(t)\right) \\ \cos\left(2\pi f_s t + \frac{2\pi}{3} + \alpha(t)\right)\end{bmatrix}$$

can be indicated uniquely by its phasor $\underline{S(t)} = S(t)e^{j\alpha(t)}$ in the complex plane (Chapman, 2005). It's assumed that variations of $S(t)$ and $\alpha(t)$ are slow enough so that the signal still maintains its sinusoidal shape. $S(t)$ is the "root mean square" (rms) value of each of the entries of the vector $\mathbf{s}(t)$.

In a single machine system in which a synchronous generator supplies an isolated load, it's possible to study the load and the generator together in the rotor reference frame of the generator. In a multi-machine system however another reference frame should be used for all the system components. The best reference frame in this case is the complex plane. So it's desirable to derive equations like (3-35) for phasors of the terminal voltages and currents of the generator.

As stated in the previous section, frequency of a generator when operating stably in a large network has zero-mean small oscillations around a reference frequency f_s. The rotor electrical angle of the generator however can be written in the form (3-23) and repeated below for convenience:

$$\theta_e(t) = 2\pi f_s t + \delta_e(t)$$
$$\delta_e(t) = \delta_e(0) + \int_0^t [\omega_e(\tau) - 2\pi f_s]d\tau = \delta_e(0) + \int_0^t \Delta\omega_e(\tau)d\tau \quad (3\text{-}36)$$

For stable operation of the generator, $\delta_e(t)$ should be bounded and hence frequency fluctuations $\Delta\omega_e(\tau)$ should have zero mean. Consider generator terminal voltage be given by the following

relations: **(From now on time dependency of phasors will not be indicated explicitly for simplicity)**

$$\mathbf{v}_{abc} = \begin{bmatrix} v_a \\ v_b \\ v_c \end{bmatrix} = \sqrt{2}V_g \begin{bmatrix} \sin(2\pi f_s t + \alpha) \\ \sin\left(2\pi f_s t - \frac{2\pi}{3} + \alpha\right) \\ \sin\left(2\pi f_s t + \frac{2\pi}{3} + \alpha\right) \end{bmatrix}$$

Applying the Park's transform $\mathbf{P}(\theta_e(t))$ to generator terminal voltage will result:

$$\mathbf{v}_{0dq} = \begin{bmatrix} v_0 \\ v_d \\ v_q \end{bmatrix} = \sqrt{3}V_g \begin{bmatrix} 0 \\ \sin(-\delta + \alpha) \\ \cos(-\delta + \alpha) \end{bmatrix} \tag{3-37}$$

It's desirable to be able to write $\underline{V_{abc}} = V_g e^{j\alpha} = V_g\cos\alpha + \mathbf{j}\, V_g\sin\alpha$ (which is the phasor of $\mathbf{v}_{abc}$ in the system reference frame (complex plane)) in terms of v_d and v_q. The quantities $V_g\cos\alpha$ and $V_g\sin\alpha$ can be found in terms of v_d and v_q from (3-37):

$$\begin{bmatrix} V_g\cos\alpha \\ V_g\sin\alpha \end{bmatrix} = \underbrace{\begin{bmatrix} \cos\delta_e & -\sin\delta_e \\ \sin\delta_e & \cos\delta_e \end{bmatrix}}_{\mathbf{T}} \begin{bmatrix} V_g\cos(-\delta_e + \alpha) \\ V_g\sin(-\delta_e + \alpha) \end{bmatrix} = \mathbf{T} \begin{bmatrix} v_q/\sqrt{3} \\ v_d/\sqrt{3} \end{bmatrix} \tag{3-38}$$

The matrix T in (3-38) is a phase shift operator which rotates any point in the complex plane around the origin with an angle δ_e. Note that this is different from the unitary matrix defined by the equation (3.121) in (Machowski, 2008). Regarding (3-38), the phasor $\underline{V_{abc}}$ in the system reference frame (complex plane) can be considered as the complex number $v_q/\sqrt{3} + jv_d/\sqrt{3}$ which is rotated around the origin with an angle δ_e. In other words:

$$\underline{V_{abc}} = e^{j\delta_e}\left(v_q/\sqrt{3} + jv_d/\sqrt{3}\right) \tag{3-39}$$

The phasor for terminal currents of the generator can be found in terms of the quantities i_q and i_d in a similar way.

Regarding (3-39) it's customary to divide d_axis and q_axis variables in (3-27), (3-31), (3-32), (3-34) and (3-35) by $\sqrt{3}$ and denote them by capital letters to emphasize that these variables are real or imaginary part of a phasor.

Application and usefulness of the concept presented in this section will be shown later in Section 0, but first summary of the generator models will be given in next section.

3.1.11 Summary Generator Models

Summary of generator models presented in Section 3.1.9 will be gathered here for convenience. According the discussion in the previous section, d_axis and q_axis variables in (3-27), (3-31), (3-32), (3-34) and (3-35) will be divided by $\sqrt{3}$ and denoted by capital letters to emphasize that these variables are real or imaginary part of a phasor.

Generator Model in the Steady State: This is the simplest model that neglects transient phenomena after a disturbance in the currents and voltages of generator. This model can also be used to find the steady-state operating point of the generator in the network if the swing equation also be considered in the steady state condition. The model is given in Table (3-1).

Table (3-1) Generator Model with the Steady State Voltage-Current Relationship

$$\begin{bmatrix} V_d \\ V_q \end{bmatrix} = -\begin{bmatrix} r & x_q \\ -x_d & r \end{bmatrix}\begin{bmatrix} I_d \\ I_q \end{bmatrix} + \begin{bmatrix} E_d \\ E_q \end{bmatrix}$$

where

$E_d = 0 \quad , \quad E_q = E_f = e_q/\sqrt{3} = \omega_s k M_F v_F/\left(\sqrt{3} r_F\right) \quad , \quad x_d = \omega_s L_d \quad , \quad x_q = \omega_s L_q$

$\underline{V_t} = e^{j\delta_e}(V_q + jV_d)$ (Phasor of terminal voltage in the system reference frame)

$\underline{I_t} = e^{j\delta_e}(I_q + jI_d)$ (Phasor of output current in the system reference frame)

$P_{out} = 3(V_d I_{d+} V_q I_q)$ (From (3-20), assuming $v_o = i_o = 0$ and considering that $V_d = v_d/\sqrt{3}$ and the same is true for the other currents and voltages)

The Swing Equation:

$$J\omega_m \frac{d\omega_m}{dt} = \eta_g \eta_t \rho g H_t Q_t - P_{out} \ , \qquad \omega_e = \frac{n_P}{2}\omega_m \ , \qquad \Delta\omega_e = \omega_e - \omega_s = \frac{d\delta_e}{dt}$$

The Swing Equation in the Steady-State:

$P_{out} = \eta_g \eta_t \rho g H_t Q_t \ \ , \ \ \delta_e = \text{constant}$

Generator Model in the Transient State: This model takes the transient phenomenon in the field windings into account. This model is the same as the one used in Heffron-Phillips formulation (Andersson, 2010). The model is given in Table (3-2).

Table (3-2) Generator Model in the Transient State

$$T'_{do} \frac{dE'_q}{dt} = -E'_q + E_q + (x_d - x'_d) I_d$$

$T'_{do} = L_F/r_F$, $E'_q = \left(\frac{1}{\sqrt{3}}\right)\omega_s (kM_F/L_F)\Psi_F$

$E_q = E_f = \left(\frac{1}{\sqrt{3}}\right)\omega_s k M_F v_F / r_F$, $x_d = \omega_s L_d$, $x'_d = \omega_s L'_d$, $L'_d = L_d - k^2 M_F^2/L_F$

$$\begin{bmatrix} V_d \\ V_q \end{bmatrix} = -\begin{bmatrix} r & x'_q \\ -x'_d & r \end{bmatrix}\begin{bmatrix} I_d \\ I_q \end{bmatrix} + \begin{bmatrix} E'_d \\ E'_q \end{bmatrix}$$

where $x'_q = x_q = \omega_s L_q$ and $E'_d = 0$

(in (Machowski, 2008) E'_d is not 0 because there a third damper winding "g" has been considered which as stated before does not apply to salient pole machines)

$\underline{V_t} = e^{j\delta_e}(V_q + jV_d)$ (Phasor of terminal voltage in the system reference frame)

$\underline{I_t} = e^{j\delta_e}(I_q + jI_d)$ (Phasor of output current in the system reference frame)

$P_{out} = 3(V_d I_{d+} V_q I_q)$ (From (3-20), assuming $v_o = i_o = 0$ and considering that $V_d = v_d/\sqrt{3}$ and the same is true for the other currents and voltages)

The Swing Equation:

$$J\omega_m \frac{d\omega_m}{dt} = \eta_g \eta_t \rho g H_t Q_t - P_{out} \ , \qquad \omega_e = \frac{n_P}{2}\omega_m \ , \qquad \Delta\omega_e = \omega_e - \omega_s = \frac{d\delta_e}{dt}$$

Generator Model in the Subtransient State: This model takes the subtransient phenomenon in the damper windings "D" and "Q" into account. This model is the most complete one. The model is given in Table (3-3).

Table (3-3) Generator Model in the Subtransient State

$$T''_{do} \frac{dE''_q}{dt} = E'_q - E''_q + I_d(x'_d - x''_d)$$

$$T''_{qo} \frac{dE''_d}{dt} = E'_d - E''_d - I_q(x'_q - x''_q)$$

Where

$$T''_{do} = (L_D - M_R^2/L_F)/r_D \ , \ T''_{qo} = L_Q/r_Q \ , \ x''_q = \omega_s L''_q \ , \ L''_q = L_q - \frac{kM_Q}{L_Q} \ , \ x''_d = \omega_s L''_d$$

$$L''_d = L_d - k^2\left(\frac{L_D M_F^2 + L_F M_D^2 - 2M_R M_D M_F}{L_F L_D - M_R^2}\right)$$

$$x'_q = x_q = \omega_s L_q \ , \ x'_d = \omega_s L'_d \ , \ L'_d = L_d - k^2 M_F^2/L_F$$

$E'_d = 0$ (in (Machowski, 2008) E'_d is not 0 because there a third damper winding "g" has been considered which as stated before does not apply to salient pole machines)

$$T'_{do} \frac{dE'_q}{dt} = -E'_q + E_q + (x_d - x'_d)I_d$$

$T'_{do} = L_F/r_F$, $E_q = E_f = \left(\frac{1}{\sqrt{3}}\right)\omega_s k M_F v_F/r_F$ and $x_d = \omega_s L_d$

$$\begin{bmatrix} V_d \\ V_q \end{bmatrix} = -\begin{bmatrix} r & x''_q \\ -x''_d & r \end{bmatrix}\begin{bmatrix} I_d \\ I_q \end{bmatrix} + \begin{bmatrix} E''_d \\ E''_q \end{bmatrix}$$

$\underline{V_t} = e^{j\delta_e}(V_q + jV_d)$ (Phasor of terminal voltage in the system reference frame)

$\underline{I_t} = e^{j\delta_e}(I_q + jI_d)$ (Phasor of output current in the system reference frame)

$P_{out} = 3(V_d I_{d+} V_q I_q)$ (From (3-20), assuming $v_o = i_o = 0$ and considering that $V_d = v_d/\sqrt{3}$ and the same is true for the other currents and voltages)

The Swing Equation:

$$J\omega_m \frac{d\omega_m}{dt} = \eta_g \eta_t \rho g H_t Q_t - P_{out} \ , \qquad \omega_e = \frac{n_P}{2}\omega_m \ , \qquad \Delta\omega_e = \omega_e - \omega_s = \frac{d\delta_e}{dt}$$

All the above models assume that resistive losses in armature windings are included in the generator efficiency η_g. If this is not the case, then these losses can be added to P_{out}:

$$P_{out} = 3\left[V_d I_d + V_q I_q + r\left(I_d^2 + I_q^2\right)\right] \tag{3-40}$$

By evaluating the above formula for different Voltage-Current relationships for the three models the following relations can be concluded:

$$\begin{aligned} P_{out} &= 3\left[E_d I_d + E_q I_q + \left(x_d - x_q\right) I_d I_q\right] && \text{(For the Model in Table (3-1))} \\ P_{out} &= 3\left[E'_d I_d + E'_q I_q + \left(x'_d - x'_q\right) I_d I_q\right] && \text{(For the Model in Table (3-2))} \\ P_{out} &= 3\left[E''_d I_d + E''_q I_q + \left(x''_d - x''_q\right) I_d I_q\right] && \text{(For the Model in Table (3-3))} \end{aligned} \tag{3-41}$$

3.1.12 Simulation of Generator connected to an Infinite Bus

Figure (3-15) shows the generator which is connected to an infinite bus. Equivalent impedance $r_e + j\,x_e$ is assumed between the generator and the bus (Demiroren, 2002). This impedance could be for example the transformer impedance or equivalent impedance of a transmission line

(Machowski, 2008). The system reference frame (Section 0) can be considered to be the bus in which case the phasor of the bus voltage will be the positive real number V_s. A transient model for the generator (Table (3-2)) will be assumed. An exciter which controls the voltage across the field winding with following transfer function will be assumed (Demiroren, 2002):

$$E_q = E_f = \frac{K_E}{1 + sT_E}(V_{tr} - V_t - V_{stabilizer})$$
$$V_{stabilizer} = \frac{sK_F}{1 + sT_{FE}} \tag{3-42}$$

Limiters can also be considered for the $E_q(= E_f)$. V_{tr} is the voltage reference set point for the exciter. In (Demiroren, 2002) it's been shown how to determine the net mechanical power delivered to generator by turbine and V_{tr} in exciter so that at the steady-state condition a certain amount of active and reactive power (with controlled proportion) be injected into the network (infinite bus).

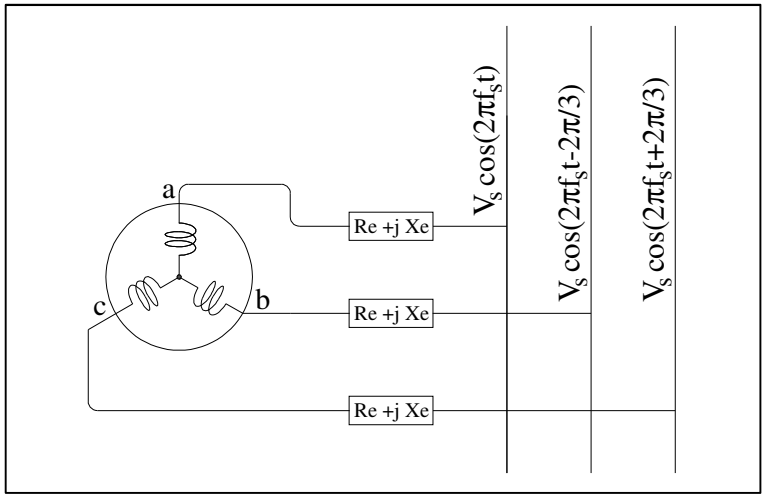

Figure (3-15) Generator on Infinite Bus

Steady-State Operation, Requirements and Determining V_{tr} (Reference Voltage) and P_{mo} (Net Turbine Output Power): It is of interest to find suitable values for V_{tr} and P_{mo} so that at the steady state condition an active power equal to P_o and a reactive

power equal to Q_o be delivered to the infinite bus. The bus voltage is constant and equal to V_s and bus frequency is constant and equal to f_s. Table (3-1) can be used for relationships in the steady-state. The procedure will be as follows (In the following the subscript "o" denotes the steady state or operating point): (Demiroren, 2002)

I_{do} and I_{qo}:

$$I_{to} = \frac{\sqrt{P_o^2 + Q_o^2}}{3V_s}, \qquad \varphi_o = \arctan\frac{Q_o}{P_o}, \qquad \underline{I_{to}} = I_{to}e^{-j\varphi_o} \tag{3-43}$$

Where

I_{to} = RMS value of terminal phase current at steady state [A]

$\underline{I_{to}}$ = Phasor of output current of generator at steady state [A]

Substituting for $\underline{I_{to}}$ from Table (3-1) will result:

$$I_{to}e^{-j\varphi_o} = e^{j\delta_{eo}}(I_{qo} + jI_{do})$$

Which in turn will give the relations for I_{do} and I_{qo}:

$$I_{do} = -I_{to}\sin(\varphi_o + \delta_{eo}) \text{ and } I_{qo} = I_{to}\cos(\varphi_o + \delta_{eo}) \tag{3-44}$$

I_{do} and I_{qo} can be determined if δ_{eo} is known. An independent relation for δ_{eo} will be given in (3-50) below.

RMS value of the Terminal Voltage:

The relationship between bus voltages and generator terminal voltages and currents in the system reference frame can be written as follows:

$$\underline{V_{to}} = \underline{V_s} + \underline{I_{to}}(r_e + j\,x_e) \tag{3-45}$$

Where

$\underline{V_s}$ = Phasor of bus voltage [V]

$\underline{V_{to}}$ = Phasor of terminal voltage of generator at steady state [V]

As mentioned $\mathbf{V_s}$ is equal to real number V_s**.** By substituting for $\mathbf{I_{to}}$ from (3-43)**,** RMS value of terminal voltage can then be found as follows:

$$V_{to} = \sqrt{\underline{V_{to}}\,\underline{V_{to}^*}} \qquad (\text{“*” denotes for complex conjugate}) \tag{3-46}$$

$\boldsymbol{\delta_o}$**:**

Substituting for $\underline{V_{to}}$ and $\underline{I_{to}}$ from Table (3-1) will result:

$$V_s = e^{j\delta_{eo}}\left(V_{qo} + jV_{do}\right) - e^{j\delta_{eo}}(I_{qo} + jI_{do})(r_e + j\,x_e)$$

Separating the real and imaginary parts of the above equation will result in the following set of equations:

$$\begin{bmatrix} V_{do} \\ V_{qo} \end{bmatrix} = \begin{bmatrix} r_e & x_e \\ -x_e & r_e \end{bmatrix}\begin{bmatrix} I_{do} \\ I_{qo} \end{bmatrix} + \begin{bmatrix} -V_s \sin\delta_{eo} \\ V_s \cos\delta_{eo} \end{bmatrix} \tag{3-47}$$

A relation for $\begin{bmatrix} V_{do} \\ V_{qo} \end{bmatrix}$ can also be found from Table (3-1):

$$\left(\begin{bmatrix} V_{do} \\ V_{qo} \end{bmatrix} = -\begin{bmatrix} r & x_q \\ -x_d & r \end{bmatrix}\begin{bmatrix} I_{do} \\ I_{qo} \end{bmatrix} + \begin{bmatrix} E_{do} \\ E_{qo} \end{bmatrix} \;\text{ where }\; E_{do} = 0\right) \Rightarrow\; V_{do} = -r\,I_{do} - x_q I_{qo} \tag{3-48}$$

Eliminating V_{do} from the first equation in (3-47) and the resultant relation in (3-48) will give:

$$V_s \sin\delta_{eo} = (r + r_e)\,I_{do} + (x_q + x_e)I_{qo} \tag{3-49}$$

Substitution from (3-44) into (3-49) and solving for δ_o will result in the following relation:

$$\delta_{eo} = \arctan \frac{I_{to}(x_q + x_e)\cos\varphi_o - I_{to}(r + r_e)\sin\varphi_o}{V_s + I_{to}(r + r_e)\cos\varphi_o + I_{to}(x_q + x_e)\sin\varphi_o} \quad (3\text{-}50)$$

$\mathbf{E_{fo}(= E_{qo})}$:

Can be found by eliminating V_{qo} from (3-47) and (3-48):

$$E_{fo} = V_s \cos\delta_{eo} + (r + r_e)\, I_{qo} - (x_d + x_e) I_{do} \quad (3\text{-}51)$$

$\mathbf{P_{mo}}$:

P_{mo} can be set equal to the air gap power as first relation in (3-41). This way the resistive losses in the armature windings are accounted for but other losses within the generator are neglected. If efficiency of the generator is available, it can be applied in here:

$P_{mo} = 3\left[E_{do}I_{do} + E_{qo}I_{qo} + (x_d - x_q)I_{do}I_{qo}\right]$ (Only armature resistive losses are accounted for)

Or

$P_{mo} = \frac{3}{\eta_g}\left[V_d I_d + V_q I_q\right]$ (If η_g accounts for all the losses within the generator)

Or

$P_{mo} = P_{mo} = \frac{3}{\eta_g}\left[V_d I_d + V_q I_q\right] + 3r\left(I_d^2 + I_q^2\right)$ (If η_g accounts for all the losses except for the armature resistive losses)

And finally $\mathbf{V_{tr}}$:

V_{tr} can be found from (3-42) in the steady state:

$$V_{tr} = V_{t0} + \frac{E_{fo}}{K_E} \quad (3\text{-}52)$$

Dynamic Equations:

The dynamic equations for transient operation will be the ones in the Table (3-2) plus the alternative active power relations (3-40) and (3-41) (whichever is applicable) and also (3-47) which is applicable in the transient operation of generator also:

$$\begin{bmatrix} V_d \\ V_q \end{bmatrix} = \begin{bmatrix} r_e & x_e \\ -x_e & r_e \end{bmatrix} \begin{bmatrix} I_d \\ I_q \end{bmatrix} + \begin{bmatrix} -V_s \sin\delta_e \\ V_s \cos\delta_e \end{bmatrix} \tag{3-53}$$

By eliminating $\begin{bmatrix} V_d \\ V_q \end{bmatrix}$ from the above relation and the voltage-current relation in Table (3-2), $\begin{bmatrix} I_d \\ I_q \end{bmatrix}$ can be found:

$$\begin{bmatrix} V_d \\ V_q \end{bmatrix} = \begin{bmatrix} r_e & x_e \\ -x_e & r_e \end{bmatrix} \begin{bmatrix} I_d \\ I_q \end{bmatrix} + \begin{bmatrix} -V_s \sin\delta_e \\ V_s \cos\delta_e \end{bmatrix} = -\begin{bmatrix} r & x'_q \\ -x'_d & r \end{bmatrix} \begin{bmatrix} I_d \\ I_q \end{bmatrix} + \begin{bmatrix} E'_d \\ E'_q \end{bmatrix} \tag{3-54}$$

$$\begin{bmatrix} r_e + r & x_e + x'_q \\ -(x_e + x'_d) & r_e + r \end{bmatrix} \begin{bmatrix} I_d \\ I_q \end{bmatrix} = \begin{bmatrix} V_s \sin\delta_e \\ -V_s \cos\delta_e \end{bmatrix} + \begin{bmatrix} E'_d \\ E'_q \end{bmatrix} \tag{3-55}$$

Simulations: In this part the generator is simulated along with the waterway with inelastic penstock and the transient droop controller introduced in Chapter 2. The generator is connected to an infinite bus so it is supposed that rotor electrical frequency do not alter much from the bus frequency. The simulation is done for a guide vane opening change at the time t=200 sec. Parameters for simulation are given in Appendix III part D in the Main_parameters.m and InitializeGenerator.m.

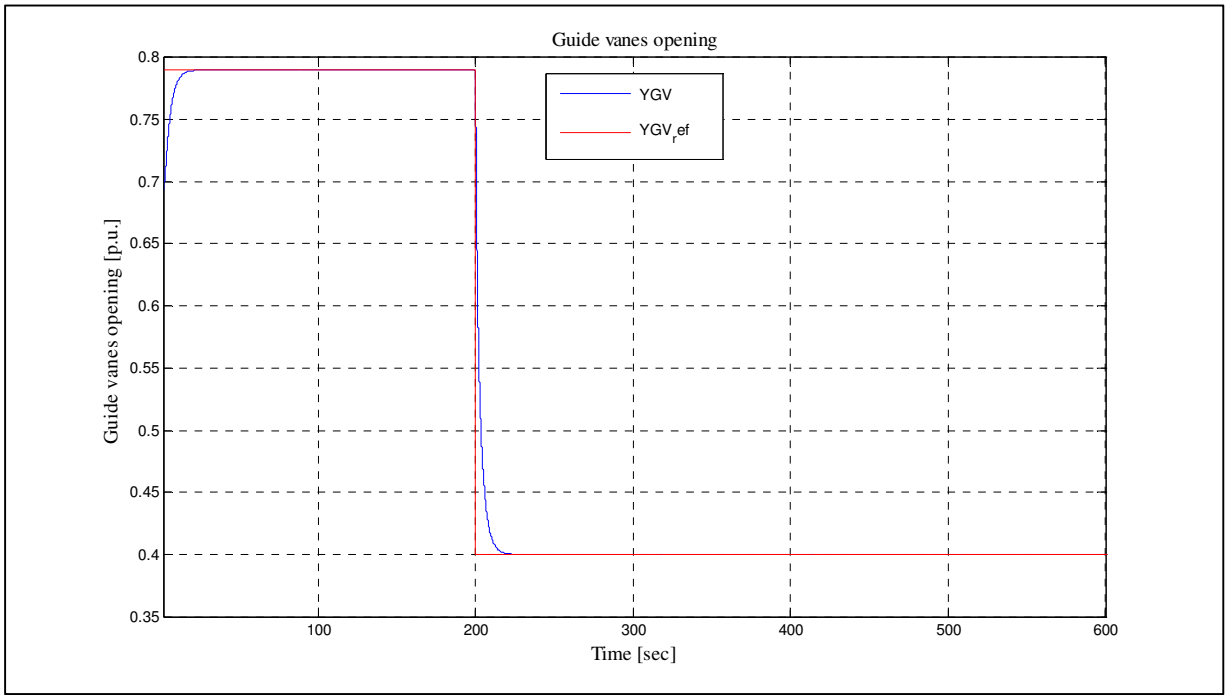

Figure (3-16) Simulation of generator connected to an infinite bus (guide vane closes at t=200 sec)

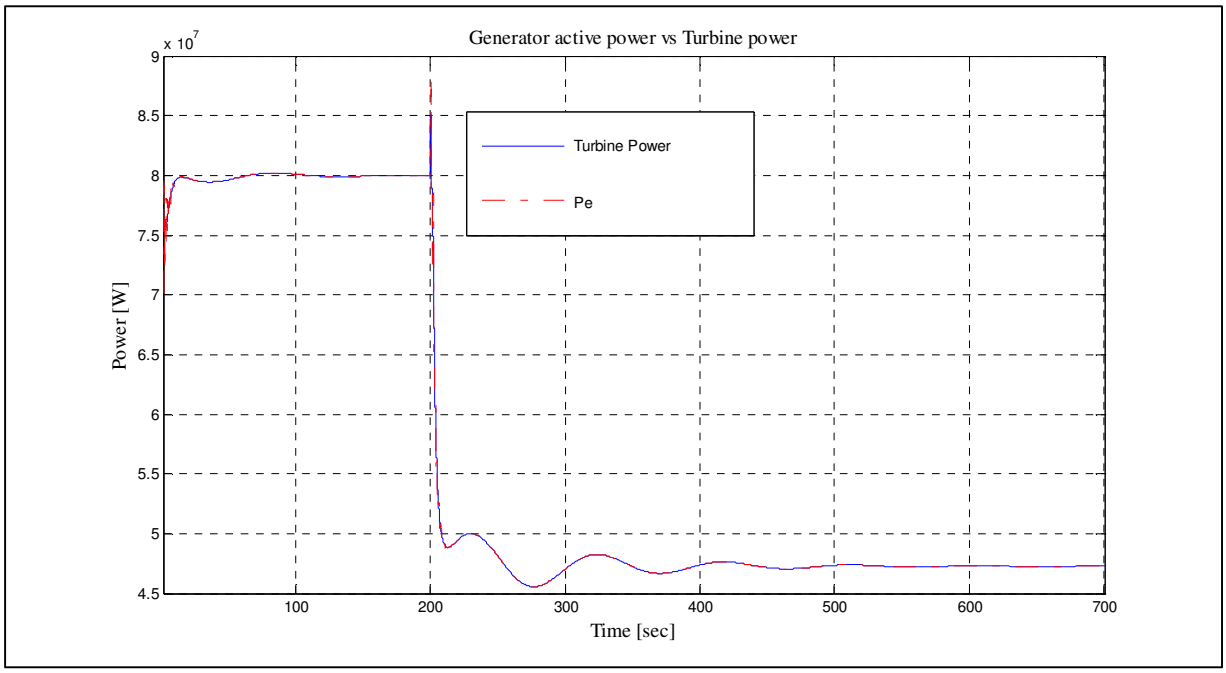

Figure (3-17) Simulation of generator connected to an infinite bus (Since frequency cannot change much, due to droop relation guide vane opening and hence the powers of turbine and generator follow the guide vane reference)

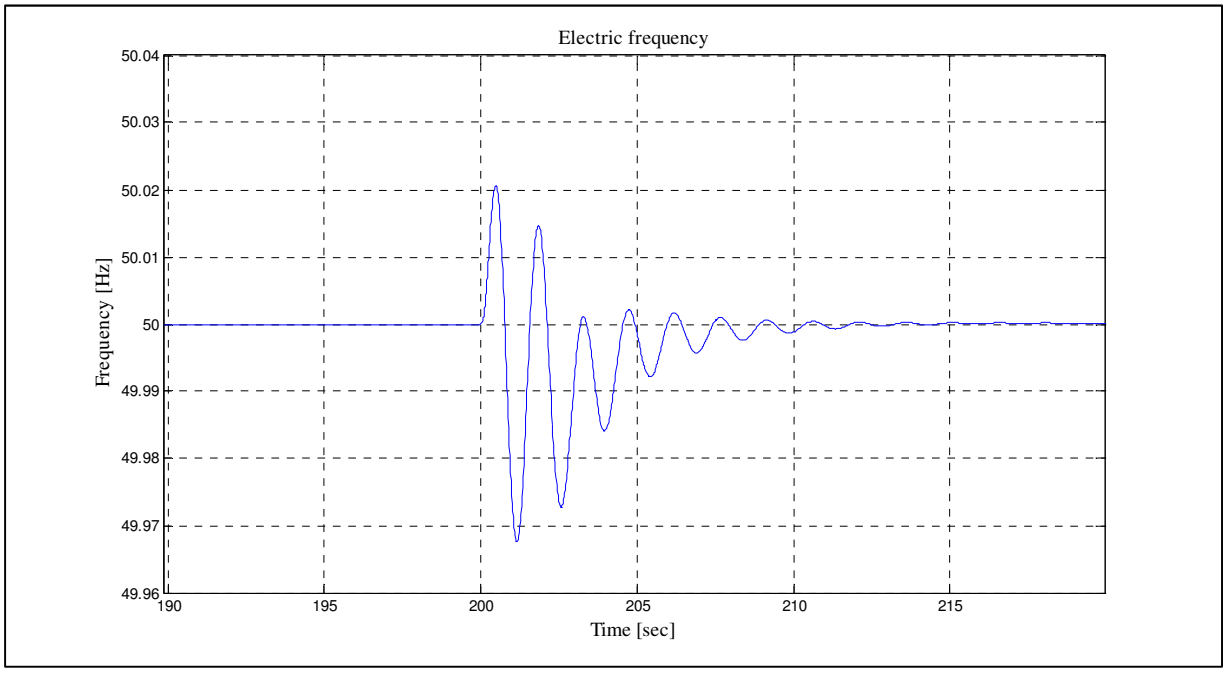

Figure (3-18) Frequency disturbance at the time of guide vanes closing

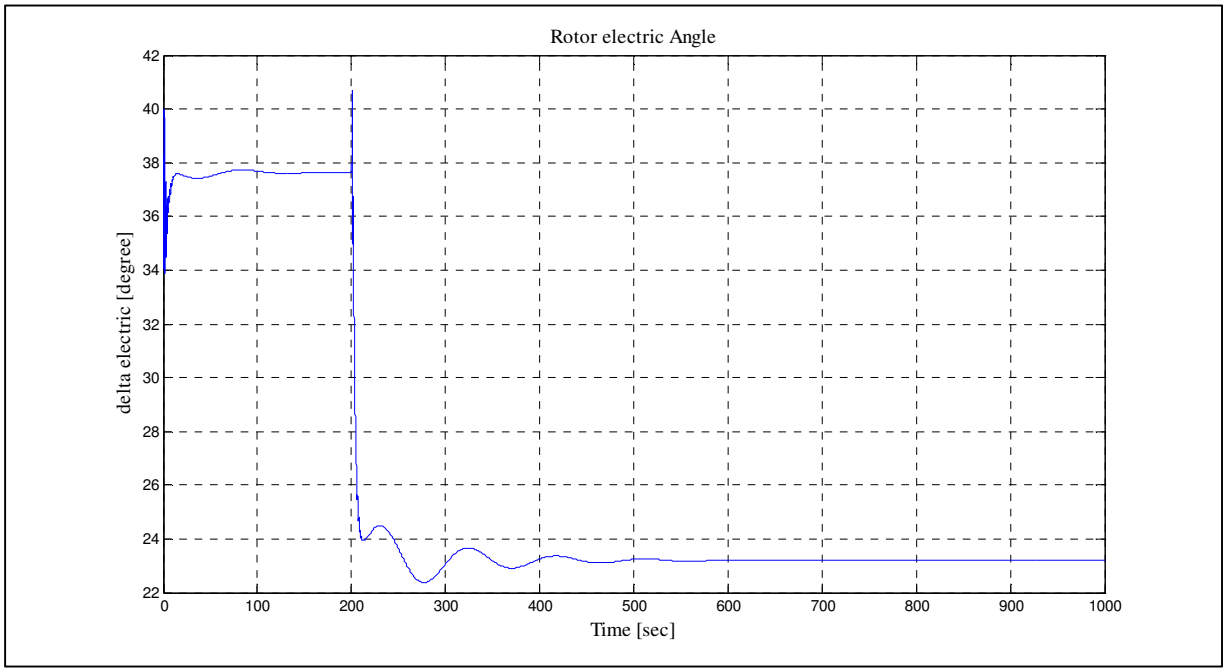

Figure (3-19) Simulation of generator connected to an infinite bus (by decreasing power, rotor electrical angle reduces to maintain the reactive power and hence the terminal voltage almost constant)

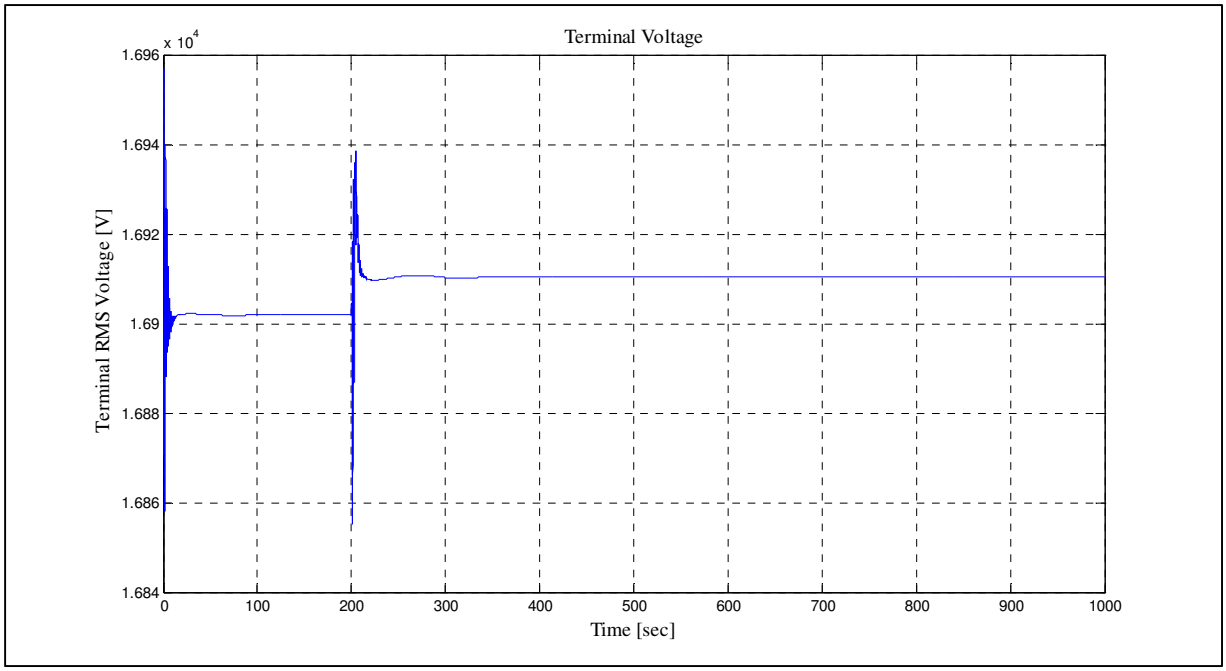

Figure (3-20) Simulation of generator connected to an infinite bus (disturbance in terminal voltage due to guide vanes closing)

Chapter 4 Conclusion

Modeling of a high-head hydropower generation unit was considered in this work. It's been shown how to use the "Finite Volume Method" and MATLAB to simulate the behavior of a penstock when elasticity of the penstock walls and compressibility of the water is taken into account. "Staggered grid" is used for spatial discretization of the variables along the penstock. This way a set of ODEs as a model for the penstock can be obtained. The "ode15s" ODE solver in MATLAB was used for solving this set of equation. It was shown that under default options, especially the default relative tolerance, the solution will have some numerical errors which will distort the solution completely.

The model introduced for the elastic penstock was validated in a classic penstock-valve problem with uniform valve closing. The responses of the model for different conditions were compared to Allievi charts (Warnick, 1984). It was found that except for high water velocities (higher than one or two m/s) the results almost agree. It was doubted that the value considered as Fanning friction factor (0.04) is more than usual for a penstock. However an illustrative value for penstock was not available.

It was shown how to enter Francis turbine efficiency data from its hill chart into MATLAB to create a suitable interpolation function. It was shown that the "square root of head" criteria for the discharge of turbine under constant guide vanes opening might not be accurate enough and the reason was guessed to be the motoring head of the turbine which varies for different heads (at least for the head ranges between %65 and %125 of design head)

Available models for the other parts of the waterway (inelastic) were extended to include an interface to the elastic penstock model.

The whole waterway model (with both elastic and inelastic penstock sub-models) was simulated in MATLAB using a classic transient droop controller for a given time-varying active-power-consuming turbine load. No significant difference between the responses of the two models was observed.

Simulation was also carried out with constant turbine load and time varying reference signal for the guide vanes opening. This time some effect of the moving waves could be observed in the

surge-shaft downstream pressure. However due to the controller action and more importantly due to the sluggish behavior of the guide vanes actuator the observed effects were not significant either.

Simplified synchronous generator models available in the literature were studied and applied to the whole hydropower generation unit considering the inelastic penstock model. Synchronous operation of the hydropower generation unit was then simulated when generator connected to an infinite bus. The difference in the feature of the response in this case compared to the case when turbine was connected to the active load was studied. Without a dynamic generator model this was impossible.

Simplified models of the generator are used for two reasons:

- Variations of Δf_e is much less than f_e (like 50Hz against 0.01 Hz). See Figure (3-17).
- The phenomena within generator and power network are described using these simplified models in almost all the literature like (Machowski, 2008).

Future Work:

- The methods described in this report can be extended to the units working in parallel.
- If enough data from real plants become available, the methods can be validated against real data
- Operation of an advanced controller can be simulated using the models introduced in this report
- No significant diversion between the responses of the elastic and inelastic models (when operating in the closed loop) was observed in this work. This needs more investigation.

Bibliography

Selecting Hydraulic Reaction Turbines. (1976). Retrieved 06 2011, from Unite States Department of interior: http://www.usbr.gov/pmts/hydraulics_lab/pubs/EM/EM20.pdf

Andersson, G. (2010). Dynamics and Control of Electric Power Systems. Swiss Federal Institute of Technology Zurich.

Chapman, S. J. (2005). *Electric Machinery Fundamentals, Fourth Edition.* McGraw-Hill Higher Education.

Chung, T. J. (2002). *Computational Fluid Dynamics.* Cambridge University Press.

Demiroren, A. (2002). Modelling and Simulation of Synchronous Machine Transient Analysis using SIMULINK. *International Journal of Electrical Engineering Education Vol.39/4*, 337-346.

Farell, C. (1987). Hydromechanics of Variable Speed Turbines. *Journal of Energy Engineering 113:1(1).*

IEEE. (1992). Hydraulic Turbine and Turbine Control Models for System Dynamin Studies. *IEEE transaction on Power Systems Vol. 7, No 1.*

Johansson, L. (2009). *Dynamisk simulering och modellering av vattenkraftverk.* Lunds University.

Kishor, N. (2007). A review on hydropower plant models and control. *Renewable and Sustainable Energy Reviews*, 776–796.

Kjølle, A. (2001). *HYdropower in Norway Mechanical Equipment.* Trondheim: Norwegian University of Science and Technology.

Lie, B. (2011). *Hydro Power Stations from a Control Engineering Perspective (In Progress).* Porsgrunn: Telemark University College.

Machowski, J. (2008). *Power System Dynamics: Stability and Control (2nd edition).* John Wiley & Sons, Ltd.

Modelon. (2010). *Hydro Plant Library Version 2.0 User's Guide.* Modelon AB.

Parmakian, J. (1963). *Waterhammer Analysis (2nd edition).* New York: Dover Publications, Inc.

Schavemaker, P. (2009). *Electrical Power System Essentials.* John Wiley & Sons, Ltd.

Shresta, S. K. (2010). *Modeling of the Sundsbarm Hydroplant.* Porsgrunn: Telemark University College.

Thoresen, H. (2010). *Modeling and Optimization of Deviation in Hydropower Plants (Project Report).* Porsgrunn: Telemark University College.

US Army Corps of Engineers. (1998). *Water Hammer and Mass Oscillation (WHAMO) 3.0 User's Manual.* US Army Corps of Engineers: Construction Engineering Research Laboratories.

Versteeg, H. K., & Malalasekera, W. (1995). *An Introduction to Computational Fluid Dynamics: The Finite Volume Method.* Longman.

Warnick, C. (1984). *Hydropower Engineering.* Prentice-Hall.

WHAMO. (1998). *Water Hammer and Mass Oscillation (WHAMO) 3.0 User's Manual.* US Army Corps of Engineers: Construction Engineering Research Laboratories.

Appendices

Appendix I THESIS TASK DESCRIPTION

Appendix II TURBINE EFFICIENCY DATA

Appendix III MATLAB CODES

Appendix I THESIS TASK DESCRIPTION

FMH606 Master Thesis

Title: Modeling For Control of Hydropower Systems

Student: Behzad Rahimi Sharefi

Supervisor: Bernt Lie, PhD, Professor, HiT

Co-supervisor:

Task description:

The following tasks should be carried out:

1. An overview of hydropower systems is to be given, with special emphasis on storage based systems.
2. Description of a model library for simulation of storage type hydropower systems with Francis turbine should be given, with models suitable for prediction and control of the various units.
3. Parameters for an illustrative hydropower plant (e.g. Sundsbarm) with grid are to be given.
4. A model for the chosen hydropower plant is to be implemented in MATLAB and the simulation model is to be validated.
5. If there is time, a control structure is to be developed for the simulated system, and the suggested structure is to be compared with a standard control structure for such systems.
6. The work is to be reported in a thesis.

Task background:

A hydropower system of storage type consists of a reservoir, a waterway, turbine gate + turbine, generator, transmission lines/grid, and consumer loads. The inlet tunnel from the reservoir to the penstock typically has a varying cross sectional area. In fact: several inlet tunnels may be joined in manifolds. Surge volumes of different types may be present. The system may have manifolds with several penstocks to several turbines, and the water may exhibit compressibility in the penstock + the penstock walls may exhibit elasticity. Governors of various types may be used to control the turbine gate operation. Salient-pole synchronous generators with a different number of pole pairs may be used. Several generators connected to a grid have restrictions on the frequency, etc. It is of interest to give as complete a description in the form of a dynamic model as possible of the various units in a hydropower system. As the various models may operate on different time scales, it is of interest to rationally develop simplified models that are suitable on the chosen time scale. As an example, simplified models of generators are needed, and it is useful with a rational development of simplified models in the time domain based on standard generator models from Kirchhoff's laws, etc.
The developed models are meant for controller design/operational analysis, and illustrative realistic parameters should be chosen.

Practical information (where, how, available equipment etc.):
The work will be carried out at Telemark University College.

Formal acceptance by the student (with ultimate task description as stated above):

Student's signature and date:

Supervisor's signature and date:

Appendix II TURBINE EFFICIENCY DATA

#	YGV	H	η
1	0,3	65,0	70,0
2	0,3	66,0	71,0
3	0,3	68,0	72,0
4	0,3	70,0	73,0
5	0,3	70,5	74,0
6	0,3	71,5	75,0
7	0,3	73,5	76,0
8	0,3	76,0	77,0
9	0,3	80,0	78,0
10	0,3	83,0	79,0
11	0,3	86,0	80,0
12	0,3	92,0	81,0
13	0,3	114,0	81,0
14	0,3	121,0	80,0
15	0,3	125,0	79,5
16	0,4	65,0	75,0
17	0,4	66,0	76,0
18	0,4	67,0	77,0
19	0,4	68,5	78,0
20	0,4	70,5	79,0
21	0,4	71,0	80,0
22	0,4	73,0	81,0
23	0,4	74,5	82,0
24	0,4	77,0	83,0
25	0,4	78,5	84,0
26	0,4	81,5	85,0
27	0,4	84,5	86,0
28	0,4	90,0	87,0
29	0,4	116,0	87,0
30	0,4	121,0	86,0

#	YGV	H	η
31	0,4	125,0	85,0
32	0,5	65,0	80,0
33	0,5	65,5	81,0
34	0,5	66,5	82,0
35	0,5	68,0	83,0
36	0,5	69,0	84,0
37	0,5	70,5	85,0
38	0,5	72,5	86,0
39	0,5	75,0	87,0
40	0,5	79,0	88,0
41	0,5	82,0	89,0
42	0,5	87,0	90,0
43	0,5	100,0	91,0
44	0,5	109,0	91,0
45	0,5	120,5	90,0
46	0,5	125,0	89,0
47	0,6	65,0	84,0
48	0,6	66,0	85,0
49	0,6	67,0	86,0
50	0,6	69,5	87,0
51	0,6	72,0	88,0
52	0,6	75,0	89,0
53	0,6	79,0	90,0
54	0,6	84,0	91,0
55	0,6	90,5	92,0
56	0,6	113,0	92,0
57	0,6	121,0	91,0
58	0,7	66,0	86,0
59	0,7	68,0	87,0
60	0,7	70,5	88,0

#	YGV	H	η
61	0,7	73,0	89,0
62	0,7	78,0	90,0
63	0,7	83,5	91,0
64	0,7	91,0	92,0
65	0,7	110,0	92,0
66	0,7	118,0	91,0
67	0,8	67,5	86,0
68	0,8	70,0	87,0
69	0,8	74,5	88,0
70	0,8	78,0	89,0
71	0,8	84,0	90,0
72	0,8	92,5	91,0
73	0,8	108,5	91,0
74	0,8	121,0	90,0
75	0,8	125,0	89,0
76	0,9	65,0	85,0
77	0,9	70,0	86,0
78	0,9	74,0	87,0
79	0,9	82,0	88,0
80	0,9	88,0	89,0
81	0,9	111,0	89,0
82	0,9	118,0	88,0
83	0,9	123,0	87,0
84	0,9	125,0	86,0
85	1,0	70,0	85,0
86	1,0	73,0	86,0
87	1,0	78,0	87,0
88	1,0	113,0	87,0
89	1,0	117,0	86,0
90	1,0	118,5	85,0

Appendix III MATLAB CODES

A. Simulation of turbine

```
% TurbineData.m
% This program determines necessary data to be used by the functions
% H_Turb and Eff_Turb for interpolation of turbine head and turbine
% efficiency.

YGV=   [ 0.2;   0.3;  0.4;  0.5;  0.6;  0.7;  0.8;  0.9;  1.0];
Theta=[ 10.09; 8.16; 6.76; 5.30; 3.30; 2.56; 1.50; 0.64; 0];

global YGV_PP;
YGV_PP=spline(YGV,Theta);

figure(1)
YGVI=0.2:0.01:1;
ThetaI=ppval(YGV_PP,YGVI);
grid on;
plot(YGV,Theta,'o',YGVI,ThetaI);
grid;xlabel('YGV');ylabel('Theta');

Turb_Data_Table3=[
0.3  65.0   70.0;
0.3  66.0   71.0;
0.3  68.0   72.0;
0.3  70.0   73.0;
0.3  70.5   74.0;
0.3  71.5   75.0;
0.3  73.5   76.0;
0.3  76.0   77.0;
0.3  80.0   78.0;
0.3  83.0   79.0;
0.3  86.0   80.0;
0.3  92.0   81.0;
0.3  114.0  81.0;
0.3  121.0  80.0;
0.3  125.0  79.5];

Turb_Data_Table4=[
0.4  65.0   75.0;
0.4  66.0   76.0;
0.4  67.0   77.0;
0.4  68.5   78.0;
0.4  70.5   79.0;
0.4  71.0   80.0;
0.4  73.0   81.0;
0.4  74.5   82.0;
0.4  77.0   83.0;
0.4  78.5   84.0;
0.4  81.5   85.0;
0.4  84.5   86.0;
```

```
0.4  90.0   87.0;
0.4  116.0  87.0;
0.4  121.0  86.0;
0.4  125.0  85.0];

Turb_Data_Table5=[
0.5  65.0   80.0;
0.5  65.5   81.0;
0.5  66.5   82.0;
0.5  68.0   83.0;
0.5  69.0   84.0;
0.5  70.5   85.0;
0.5  72.5   86.0;
0.5  75.0   87.0;
0.5  79.0   88.0;
0.5  82.0   89.0;
0.5  87.0   90.0;
0.5  100.0  91.0;
0.5  109.0  91.0;
0.5  120.5  90.0;
0.5  125.0  89.0];

Turb_Data_Table6=[
0.6  65.0   84.0;
0.6  66.0   85.0;
0.6  67.0   86.0;
0.6  69.5   87.0;
0.6  72.0   88.0;
0.6  75.0   89.0;
0.6  79.0   90.0;
0.6  84.0   91.0;
0.6  90.5   92.0;
0.6  113.0  92.0;
0.6  121.0  91.0];

Turb_Data_Table7=[
0.7  66.0   86.0;
0.7  68.0   87.0;
0.7  70.5   88.0;
0.7  73.0   89.0;
0.7  78.0   90.0;
0.7  83.5   91.0;
0.7  91.0   92.0;
0.7  110.0  92.0;
0.7  118.0  91.0];

Turb_Data_Table8=[
0.8  67.5   86.0;
0.8  70.0   87.0;
0.8  74.5   88.0;
0.8  78.0   89.0;
0.8  84.0   90.0;
0.8  92.5   91.0;
0.8  108.5  91.0;
0.8  121.0  90.0;
0.8  125.0  89.0;
```

```
];

Turb_Data_Table9=[
0.9  65.0   85.0;
0.9  70.0   86.0;
0.9  74.0   87.0;
0.9  82.0   88.0;
0.9  88.0   89.0;
0.9  111.0  89.0;
0.9  118.0  88.0;
0.9  123.0  87.0;
0.9  125.0  86.0];

Turb_Data_Table10=[
1.0  70.0   85.0;
1.0  73.0   86.0;
1.0  78.0   87.0;
1.0  100.0  88.0;
1.0  112.0  87.0;
1.0  116.5  86.0;
1.0  118.5  85.0];


Y1=0.3:0.1:1.0;
H1=(65:5:125)';
[qY1,qH1] = meshgrid(Y1,H1);
V1=zeros(size(qY1));
V1(:,1)=interp1(Turb_Data_Table3(:,2),Turb_Data_Table3(:,3),H1,'spline');
V1(:,2)=interp1(Turb_Data_Table4(:,2),Turb_Data_Table4(:,3),H1,'spline');
V1(:,3)=interp1(Turb_Data_Table5(:,2),Turb_Data_Table5(:,3),H1,'spline');
V1(:,4)=interp1(Turb_Data_Table6(:,2),Turb_Data_Table6(:,3),H1,'spline');
V1(:,5)=interp1(Turb_Data_Table7(:,2),Turb_Data_Table7(:,3),H1,'spline');
V1(:,6)=interp1(Turb_Data_Table8(:,2),Turb_Data_Table8(:,3),H1,'spline');
V1(:,7)=interp1(Turb_Data_Table9(:,2),Turb_Data_Table9(:,3),H1,'spline');
V1(:,8)=interp1(Turb_Data_Table10(:,2),Turb_Data_Table10(:,3),H1,'spline');

Y2=0.3:0.01:1.0;
H2=(65:1:125)';
global Grid_Turb_YGV Grid_Turb_Head Efficiency_Turb_Interpolant;
[Grid_Turb_YGV,Grid_Turb_Head] = meshgrid(Y2,H2);
Efficiency_Turb_Interpolant =
INTERP2(qY1,qH1,V1,Grid_Turb_YGV,Grid_Turb_Head,'cubic');

figure(2);
grid on;
contour(Grid_Turb_YGV, Grid_Turb_Head, Efficiency_Turb_Interpolant);
grid;xlabel('YGV');ylabel('Head');

figure(3);
mesh(Grid_Turb_YGV, Grid_Turb_Head, Efficiency_Turb_Interpolant);
xlabel('YGV');ylabel('Head');zlabel('Efficiency');


%%%%%%%%%%%%%%%%%%%%%%%%%%%%%%%%%%%%%%%%%%%%%%
```

```
function H=H_Turb(YGV,Q)

global YGV_PP;

Theta=ppval(YGV_PP,YGV);

Theta1=(72.04+Theta)*pi/180;

H=(70/134)*((Q+32.2)*tan(Theta1)-331.6+60*134/70);
```

%%

```
function Efficiency=Eff_Turb(YGV,H)

global Grid_Turb_YGV Grid_Turb_Head Efficiency_Turb_Interpolant;

if H>125
    H=125;
elseif H<65
    H=65;
end

Efficiency=interp2(Grid_Turb_YGV,Grid_Turb_Head,Efficiency_Turb_Interpolant,Y
GV,H,'cubic');
```

%%

B. Simulation of elastic penstock + valve

```
%test.m main program for simulation of penstock-valve problem. Valve
%closure is determined by the function valveCV.m as a function of time.
clc
close all
clear all

tic;
```

```
% Quick Simulation Parameters:
LP=1000; %Penstock Length  [m]
VT=1; %Valve closure time [sec]
ho=100; %Gross head  [m]
vo=1; %Initial Water Velocity [m/sec]
hHW=0; %Reservoir height [m]
a=1000; %Sound Velocity [m/sec]

global CONSTANTS;
CONSTANTS=[];
CONSTANTS.rho_atm=1000; %Water density at atmospheric pressure [Kg/m3]
CONSTANTS.g=9.8;        %gravity acceleration [m/sec2]
CONSTANTS.p_atm=1e5;    %Atmospheric pressure [Pa]
CONSTANTS.beta=4.5e-10; %compressibility of water [1/Pa]

global PPENSTOCK; %Parameters for  penstock
PPENSTOCK=[];
PPENSTOCK.LP=LP;     %Penstock length [m]
PPENSTOCK.AP=7;      %Penstock cross-section area [m2]
PPENSTOCK.ThetaP=asin((ho-hHW)/LP);  %Penstock slope [radians]
PPENSTOCK.fP=0.00;    %Fanning friction factor for the penstock
PPENSTOCK.N=50;       %No of deltax length along the penstock
PPENSTOCK.beta_eq=1/(CONSTANTS.rho_atm*a^2)-CONSTANTS.beta; %penstock wall
elasticity

global PHEADWATER; %Parameters for head water system
PHEADWATER=[];
PHEADWATER.ho=ho;      %Gross head [m]
PHEADWATER.hR=hHW;      %Head water reservoir water level [m]

global PTAILWATER; %Parameters for tail water system
PTAILWATER=[];
PTAILWATER.VT=VT; %Valve closure time [sec]
PTAILWATER.vo=vo; %Initial Water Velocity [m/sec]

% Initial conditions:
N=PPENSTOCK.N;
rho_atm=CONSTANTS.rho_atm;
g=CONSTANTS.g;
p_atm=CONSTANTS.p_atm;
AP=PPENSTOCK.AP;

p1=p_atm+rho_atm*g*hHW; %pressure at the entrance of penstock (in head water)
deltap=rho_atm*g*(ho-hHW)/N;
P0=(p1+deltap:deltap:p1+(N-1)*deltap)';
mdot0=rho_atm*AP*vo*ones(N-2,1);
X0=[rho_atm*AP*vo;rho_atm*AP*vo;P0;mdot0];


tspan=[0 100];
options=odeset('MaxOrder',1,'RelTol',1e-6,'AbsTol',1e-6);
[T,X] = ode15s(@overall,tspan,X0,options);

% [T,X] = ode45(@overall,tspan,X0);
```

```
toc;

lT=length(T);
UV=zeros(1,lT);
for i=1:lT
    [~,UV(i)]=valveCV(T(i));
end

figure(1);grid on; plot(T,UV);axis([0,100,-0.1,1.1]);
title('Cv of the valve [p.u]');grid;

figure(2);grid on; plot(T,X(:,N+1));xlabel('Time [sec]');
title('pressure before the valve [Pa]');grid;

figure(3);grid on;plot(T,X(:,2*N-1));xlabel('Time [sec]');
title('Mass flow rate at the valve [Kg/sec]');grid;

subplot(221);grid on; plot(T,X(:,2+floor(N/4)));xlabel('Time [sec]');
title('pressure at 1/4 length from head water [Pa]');grid;

subplot(222);grid on;plot(T,X(:,2+floor(N/4)+N-1));xlabel('Time [sec]');
title('Mass flow rate at 1/4 length from head water [Kg/sec]');grid;

subplot(223);grid on; plot(T,X(:,3));xlabel('Time [sec]');
title('pressure at the head water interface [Pa]');grid;

subplot(224);grid on;plot(T,X(:,N+2));xlabel('Time [sec]');
title('Mass flow rate at the head water interface [Kg/sec]');grid;
```

%%%%%%%%%%%%%%%%%%%%%%%%%%%%%%%%%%%%%%

```
function dXdt=overall(t,X)

global PPENSTOCK CONSTANTS PHEADWATER;
LP=PPENSTOCK.LP;      %Penstock length [m]
AP=PPENSTOCK.AP;       %Penstock cross-section area [m2]
ThetaP=PPENSTOCK.ThetaP;  %Penstock slope [radians]
N=PPENSTOCK.N;        %No of deltax length along the penstock
deltax=LP/N;



rho_atm=CONSTANTS.rho_atm;
g=CONSTANTS.g;
p_atm=CONSTANTS.p_atm;

hHW=PHEADWATER.hR;       %Head water reservoir water level [m]

xR=X(1);
xV=X(2);
S=X(3:2*N-1);
pHWI=S(1);pTWI=S(N-1);
```

```
pHWO=p_atm+rho_atm*g*hHW;
dxRdt=deltax\(AP*(pHWO-pHWI)+rho_atm*g*deltax*AP*sin(ThetaP));

deltap_valve=xV*abs(xV)/(rho_atm^2*valveCV(t)^2);
pTWO=p_atm+deltap_valve;
dxVdt=deltax\(-AP*(pTWO-pTWI)+rho_atm*g*deltax*AP*sin(ThetaP));

dSdt=penstock(S,xR,xV);

dXdt=[dxRdt;dxVdt;dSdt];
```

%%%%%%%%%%%%%%%%%%%%%%%%%%%%%%%%%%%%%%%

```
function dSdt=penstock(S,mdotHWI,mdotTWI)

global CONSTANTS;

rho_a=  CONSTANTS.rho_atm; %Water density at atmospheric pressure [Kg/m3]
g=      CONSTANTS.g;       %gravity acceleration [m/sec2]
Pa=     CONSTANTS.p_atm;   %Atmospheric pressure [Pa]
beta=   CONSTANTS.beta;    %compressibility of water [1/Pa]

global   PPENSTOCK; %Parameters for  penstock
Aa=      PPENSTOCK.AP;      %Penstock cross-section area [m2]
theta=   PPENSTOCK.ThetaP;  %Penstock slope [radians]
fP=       PPENSTOCK.fP;      %Fanning friction factor for the penstock
N=       PPENSTOCK.N;       %No of deltax length along the penstock
deltax=  PPENSTOCK.LP/PPENSTOCK.N;
beta_eq= PPENSTOCK.beta_eq; %penstock wall elasticity

beta_tot=beta+beta_eq;

p=S(1:N-1);
mdot=S(N:2*N-3);

mdot_ext=[mdotHWI;mdot;mdotTWI];

dpdt=(mdot_ext(1:N-1)-mdot_ext(2:N))/(Aa*rho_a*deltax*beta_tot);

Fp=Aa*rho_a*(ones(N-1,1)+beta_tot*(p-Pa*ones(N-1,1)));
Fmdot=(Fp(1:N-2)+Fp(2:N-1))/2;
Fmdot_ext=[Aa*rho_a;Fmdot;Aa*rho_a];

vmdot_ext=mdot_ext./Fmdot_ext;
```

%%%%%%%%%%%%%%%%%%%%%%%%%%%%%%%%%%%%%%%

```
function coef=velocitycoef(mdot_2n_ext,kthi_2n)
%This function calculates the coefficients of the velocity variables in the
%momentum equation using upwind discretization:
```

```
global PPENSTOCK;
N=PPENSTOCK.N;        %No of deltax length along the penstock

coef=zeros(N-2,3);

for i=1:N-2
    t1=(mdot_2n_ext(i)+mdot_2n_ext(i+1))/2;
    t2=(mdot_2n_ext(i+1)+mdot_2n_ext(i+2))/2;
    t3=(mdot_2n_ext(i+2)-mdot_2n_ext(i))/2;

    if         t1>=0,
               coef(i,1)=t1+t3-kthi_2n(i);
               coef(i,2)=t1;
               coef(i,3)=0;
    elseif     t2<=0,
               coef(i,1)=-t2+t3-kthi_2n(i);
               coef(i,2)=0;
               coef(i,3)=-t2;
    else
               coef(i,1)=-kthi_2n(i);
               coef(i,2)=0;
               coef(i,3)=0;
    end

end
```

%%

```
function [y,uv]=valveCV(t)


global CONSTANTS PPENSTOCK PTAILWATER PHEADWATER;

rho_atm=CONSTANTS.rho_atm; %Water density at atmospheric pressure [Kg/m3]
g=CONSTANTS.g;          %gravity acceleration [m/sec2]

AP=PPENSTOCK.AP;        %Penstock cross-section area [m2]

ho=PHEADWATER.ho;        %Gross head [m]

VT=PTAILWATER.VT; %Valve closure time [sec]
vo=PTAILWATER.vo; %Initial Water Velocity [m/sec]

Max_VolumetricFlowRate=AP*vo;
Max_DiffPressure=rho_atm*g*ho;



if t<50,
   uv=1;
```

```
else

    uv=max(0.9,1-VT\(t-50));
end

y=uv*Max_VolumetricFlowRate/sqrt(Max_DiffPressure);
```

%%

C. Simulation of waterway, turbine and controller (with and without Compressibility and Elasticity Effects) and with a Torque Disturbance on Turbine Consuming Constant Active Power

```
% main program for simulation of inelastic and elastic models of the plant
% with transient droop controller and disturbance as torque on turbine
% consuming constant active power

clc
clear all
close all
Main_parameters %run to define parameters
TurbineData %run to generate turbine data

%initial state vector for inelastic system:
% lS=x_ie(1);     %Length of water column in the surge shaft
% mdotC=x_ie(2); %Mass flow rate of water in the conduit
% mdotP=x_ie(3); %Mass flow rate of water in the penstock
% YGV=x_ie(4);    %guide vane openning
% xr=x_ie(5);     %transient droop state
% u=x_ie(6);      %pilot servomotor output
% wm=x_ie(7);     %angular speed [rad/sec]
x_ie0=[55;28000;28000;0.7;0;0;500*2*pi/60];

%initial state vector for elastic system:
% YGV=x(1);    %guide vane openning
% xr=x(2);     %transient droop state
% u=x(3);      %pilot servomotor output
% wm=x(4);     %angular speed [rad/sec]
% lS=x(5);     %Length of water column in the surge shaft
% mdotC=x(6); %Mass flow rate of water in the conduit
% mdotHWDO=x(7); %Mass flow rate of water in the penstock interface at HW
% mdotTWUO=x(8); %Mass flow rate of water in the penstock interface at TW
% S=x(9:2*N+5);  %Penstock state vector
LP=PPENSTOCK.LP;
N=PPENSTOCK.N;
deltax=LP/N;
p0=(5+28/N:28/N:5+28-28/N)'*1e5;
mdot0=28000*ones(N-2,1);
x0=[0.7;0;0;500*2*pi/60;55;28000;28000;28000;p0;mdot0];
```

```
tspan=[0 500];
options=odeset('MaxOrder',5,'RelTol',1e-9,'AbsTol',1e-9);
[T_ie,X_ie] = ode15s(@ODEWaterwayInelastic,tspan,x_ie0,options);
[T,X] = ode15s(@ODEWaterway,tspan,x0,options);


lT=length(T_ie);
X_ie2=zeros(lT,6);
for i=1:lT
    t=T_ie(i);
    xi=X_ie(i,1:3);
    Ygvi=X_ie(i,4);
    wmi=X_ie(i,7);
    PowerDemandi=ActivePowerDemand(t);
    [~,pHWDOi,pTWUOi,Hti,EFFti,Pti]=WaterwayInelasticOutputs(xi,Ygvi,wmi);
    X_ie2(i,:)=[pHWDOi pTWUOi Hti EFFti Pti PowerDemandi];
end


lT=length(T);
X2=zeros(lT,6);
for i=1:lT
    t=T(i);
    xi=X(i,:);
    YGV=xi(1);   %guide vane openning
    wm=xi(4);    %angular speed [rad/sec]
    xHW=xi(5:7);
    mdotTWUO=xi(8); %Mass flow rate of water in the penstock interface at TW
    S=xi(9:2*N+5);  %Penstock state vector
    pTWUI=S(N-1);
    pHWDI=S(1);
    PowerDemandi=ActivePowerDemand(t);
    [~,pTWUOi,Hti,EFFti,Pti]=TailWaterOutputs(mdotTWUO,pTWUI,YGV,wm,deltax);
    [~,pHWDO]=HeadWaterOutputs(xHW,pHWDI,deltax);
    X2(i,:)=[pHWDO pTWUOi Hti EFFti Pti PowerDemandi];
end

figure(1);grid on;
plot(T, sin(PHEADWATER.ThetaS)\X(:,5),'b-');hold on;
plot(T_ie, sin(PHEADWATER.ThetaS)\X_ie(:,1),'r-.');hold off;
grid;xlabel('Time [sec]');ylabel('Height [m]');
title('Water column height in the surge shaft');
legend('Elastic Penstock','Inelastic Penstock');

figure(2);grid on;
plot(T, X(:,6),'-b');hold on;plot(T_ie, X_ie(:,2),'-.r');hold off;
grid;xlabel('Time [sec]');ylabel('Flow rate [Kg/sec]');
title('Water mass flow rate in the conduit');
legend('Elastic Penstock','Inelastic Penstock');

figure(3);grid on;
plot(T, X(:,8),'-b');hold on;plot(T_ie, X_ie(:,3),'-.r');
grid;xlabel('Time [sec]');ylabel('Flow rate [Kg/sec]');
title('Water mass flow rate in the turbine');
```

```
legend('Elastic Penstock','Inelastic Penstock');

figure(4);grid on;
plot(T, X(:,1),'-b');hold on;plot(T_ie, X_ie(:,4),'-.r');hold off;
grid;xlabel('Time [sec]');ylabel('Guide vanes opening [p.u.]');
title('Guide vanes opening');
legend('Elastic Penstock','Inelastic Penstock');

figure(5);grid on;
plot(T, X(:,4)*50/PTURBINE.wm_design,'-b');hold on;
plot(T_ie, X_ie(:,7)*50/PTURBINE.wm_design,'-.r');
grid;xlabel('Time [sec]');ylabel('Frequency [Hz]');
title('Electric frequency');
legend('Elastic Penstock','Inelastic Penstock');

figure(6);grid on;
plot(T, X2(:,1),'-b');hold on;plot(T_ie, X_ie2(:,1),'-.r');hold off;
grid;xlabel('Time [sec]');ylabel('Pressure [Pa]');
title('Pressure at the surge shaft junction');
legend('Elastic Penstock','Inelastic Penstock');

figure(7);grid on;
plot(T, X2(:,2),'-b');hold on;plot(T_ie, X_ie2(:,2),'-.r');hold off;
grid;xlabel('Time [sec]');ylabel('Pressure [Pa]');
title('Pressure at the turbine inlet');
legend('Elastic Penstock','Inelastic Penstock');

figure(8);grid on;
plot(T, X2(:,3),'-b');hold on;plot(T_ie, X_ie2(:,3),'-.r');hold off;
grid;xlabel('Time [sec]');ylabel('Head [m]');
title('Turbine head');
legend('Elastic Penstock','Inelastic Penstock');

figure(9);grid on;
plot(T, X2(:,4),'-b');hold on;plot(T_ie, X_ie2(:,4),'-.r');hold off;
grid;xlabel('Time [sec]');ylabel('efficiency [%]');
title('Turbine efficiency');
legend('Elastic Penstock','Inelastic Penstock');

figure(10);grid on;
plot(T, X2(:,5),'- b',T,X2(:,6),'-.b');hold on;
plot(T_ie, X_ie2(:,5),'-.r');hold off;
grid;xlabel('Time [sec]');ylabel('Power [W]');
title('Active power demand vs Turbine power');
legend('Elastic Penstock','Demand','Inelastic Penstock');
```

%%%%%%%%%%%%%%%%%%%%%%%%%%%%%%%%%%%%%%

```
% Main_parameters.m
% defines parameters for simulation of plant with inelastic and elastic
% models with transient droop controller and a disturbance torque
% on turbine which consumes constant active power
```

```
global CONSTANTS;
CONSTANTS=[];
CONSTANTS.rho_atm=1000; %Water density at atmospheric pressure [Kg/m3]
CONSTANTS.g=9.8;        %gravity acceleration [m/sec2]
CONSTANTS.p_atm=1e5;    %Atmospheric pressure [Pa]
CONSTANTS.beta=4.5e-10; %water compressibility

global PTURBINE; %Turbine parameters
PTURBINE=[];
PTURBINE.Qrated=36;             %Rated descharge [m3/sec]
PTURBINE.Hdesign=330;           %Design head [m]
PTURBINE.wm_design=500*2*pi/60; %Design angular speed

global PCONTROLLER; %Controller Parameters
PCONTROLLER=[];
PCONTROLLER.J=850000; %Generator rotor and turbine moment of inertia

% PCONTROLLER.YGV_ref=0.6; %Operating point openning for guide vane [p.u]

PCONTROLLER.Tp=0.04; %pilot servomotor time constant [sec]
PCONTROLLER.Tg=0.2;  %main servomotor integration time [sec]
PCONTROLLER.Tr=1.75;  %transient droop time constant [sec]
PCONTROLLER.delta=0.04; %transient droop
PCONTROLLER.droop=0.10; %droop [p.u.]
PCONTROLLER.YGVMax=1;   %Max guide vane opening [p.u.]
PCONTROLLER.YGVMin=0.3; %Min guide vane openning [p.u]
PCONTROLLER.YGVdotMax=0.05;   %Max guide vane opening rare [1/sec]
PCONTROLLER.YGVdotMin=0.2; %Max guide vane closing rate [1/sec]

global PHEADWATER; %Parameters for head water system
PHEADWATER=[];
PHEADWATER.hR=40;      %Head water reservoir water level [m]
PHEADWATER.LC=4500;    %Conduit length [m]
PHEADWATER.AC=25;      %Condit cross-section area [m2]
PHEADWATER.ThetaC=0.2*pi/180; %Conduit slope [radians]
PHEADWATER.fC=0.04;    %Fanning friction factor for the conduit
PHEADWATER.AS=10;      %Surge shaft cross-section area [m2]
PHEADWATER.ThetaS=60*pi/180;  %Surge shaft slope [radians]
PHEADWATER.fS=0.04;    %Fanning friction factor for the surge shaft

global PPENSTOCKINTERFACE %Penstock interface (head water and tail water)
parameters
PPENSTOCKINTERFACE=[];
PPENSTOCKINTERFACE.A2=7;      %Penstock cross-section area head water [m2]
PPENSTOCKINTERFACE.A2N=7;      %Penstock cross-section area tail water [m2]
PPENSTOCKINTERFACE.ThetaP=45*pi/180;  %Penstock slope [radians]
PPENSTOCKINTERFACE.fP=0.04;    %Fanning friction factor for the penstock

global PPENSTOCK; %Parameters for  penstock
PPENSTOCK=[];
PPENSTOCK.LP=400;     %Penstock length [m]
PPENSTOCK.AP=7;      %Penstock cross-section area [m2]
PPENSTOCK.ThetaP=45*pi/180;  %Penstock slope [radians]
PPENSTOCK.fP=0.04;    %Fanning friction factor for the penstock
```

```
% PPENSTOCK.N=50;        %No of deltax length along the penstock
PPENSTOCK.N=25;        %No of deltax length along the penstock

PPENSTOCK.beta_eq=2.04e-9; %penstock wall elasticity

global PTAILWATER; %Parameters for tail water system
PTAILWATER=[];
PTAILWATER.hDT=5;       %Draft tube height [m]
PTAILWATER.LTWT=300;    %Tail water tunnel length [m]
PTAILWATER.ATWT=25;     %Tail water tunnel cross-section area [m2]
PTAILWATER.ThetaTWT=0.5*pi/180;%Tail water tunnel slope [radians]
PTAILWATER.fTWT=0.04;    %Fanning friction factor for Tail water tunnel
PTAILWATER.hTW=10;       %Tail water reservoir water level [m]
```

%%%%%%%%%%%%%%%%%%%%%%%%%%%%%%%%%%%%%%%

```
function dxdt=ODEWaterwayInelastic(t,x)

% This function calculates time derivatives for all of the states in
% waterway, controller and the swing.
% inputs are the time and the state vector x consisting of:
% lS=x(1);     %Length of water column in the surge shaft
% mdotC=x(2); %Mass flow rate of water in the conduit
% mdotP=x(3); %Mass flow rate of water in the penstock
% YGV=x(4);   %guide vane openning
% xr=x(5);    %transient droop state
% u=x(6);     %pilot servomotor output
% wm=x(7);    %angular speed [rad/sec]

global PCONTROLLER;

YGV=x(4);    %guide vane openning
wm=x(7);     %angular speed [rad/sec]

J=PCONTROLLER.J; %Generator rotor and turbine moment of inertia
% YGV_ref=PCONTROLLER.YGV_ref;
YGV_ref=YGVREFERENCE(t);


[dxWWdt,~,~,~,~,Pt]=WaterwayInelasticOutputs(x(1:3),YGV,wm);
dxCONdt=ControllerOutputs(x(4:6),wm,YGV_ref);
dwmdt=(J*wm)\(Pt-ActivePowerDemand(t));

dxdt=[dxWWdt;dxCONdt;dwmdt];
```

%%%%%%%%%%%%%%%%%%%%%%%%%%%%%%%%%%%%%%%

```
function [dxdt,pHWDO,pTWUO,Ht,EFFt,Pt]=WaterwayInelasticOutputs(x,YGV,wm)
%This function returns time derivative of the parameters of a waterway with
%inelastic penstock.Inputs are:
```

```
%state vector x:
% lS=x(1);    %Length of water column in the surge shaft
% mdotC=x(2); %Mass flow rate of water in the conduit
% mdotP=x(3); %Mass flow rate of water in the penstock
% guide vane opening YGV [p.u.]
% angular speed of turbine wm [rad/sec]
% outputs are
% time derivative of the state vector
% pressure at conduit-surgeshaft-penstock junction pHWDO [Pa]
% pressure at turbine inlet pTWUO [Pa]
% Turbine head [m]
% Turbine efficiency
% Turbine power [Watt]

%State variables:
lS=x(1);    %Length of water column in the surge shaft
mdotC=x(2); %Mass flow rate of water in the conduit
mdotP=x(3); %Mass flow rate of water in the penstock

%Parameters and constants:
global PHEADWATER PPENSTOCK PTAILWATER CONSTANTS PTURBINE;

hR=PHEADWATER.hR;            %Head water reservoir water level [m]
LC=PHEADWATER.LC;            %Conduit length [m]
AC=PHEADWATER.AC;            %Condit cross-section area [m2]
ThetaC=PHEADWATER.ThetaC;    %Conduit slope [degrees]
fC=PHEADWATER.fC;            %Fanning friction factor for the conduit
AS=PHEADWATER.AS;            %Surge shaft cross-section area [m2]
ThetaS=PHEADWATER.ThetaS;    %Surge shaft slope [degrees]
fS=PHEADWATER.fS;            %Fanning friction factor for the surge shaft

LP=PPENSTOCK.LP;            %Penstock length [m]
AP=PPENSTOCK.AP;            %Penstock cross-section area [m2]
ThetaP=PPENSTOCK.ThetaP;    %Penstock slope [degrees]
fP=PPENSTOCK.fP;            %Fanning friction factor for the penstock

hDT=PTAILWATER.hDT;          %Draft tube height [m]
LTWT=PTAILWATER.LTWT;        %Tail water tunnel length [m]
ATWT=PTAILWATER.ATWT;         %Tail water tunnel cross-section area [m2]
ThetaTWT=PTAILWATER.ThetaTWT; %Tail water tunnel slope [degrees]
fTWT=PTAILWATER.fTWT;         %Fanning friction factor for Tail water tunnel
hTW=PTAILWATER.hTW;           %Tail water reservoir water level [m]

rho_atm=CONSTANTS.rho_atm;  %Water density at atmospheric pressure [Kg/m3]
g=CONSTANTS.g;              %gravity acceleration [m/sec2]
p_atm=CONSTANTS.p_atm;      %Atmospheric pressure [Pa]

Qrated=PTURBINE.Qrated;             %Rated descharge [m3/sec]
Hdesign=PTURBINE.Hdesign;           %Design head [m]
wm_design=PTURBINE.wm_design; %Design angular speed

PC=2*sqrt(pi*AC);   %Perimeter of conduit (circular cross-section) [m]
PS=2*sqrt(pi*AS);   %Perimeter of surge shaft [m]
PP=2*sqrt(pi*AP);   %Perimeter of penstock [m]
PTWT=2*sqrt(pi*ATWT);   %Perimeter of tail water tunnel [m]
```

```
%K coefficients as defined in the text
KC=fC*LC*PC*sign(mdotC)/(2*AC^2*rho_atm);
KS=fS*lS*PS*sign(mdotP-mdotC)/(2*AS^2*rho_atm)+1/(AS*rho_atm);
KP=fP*LP*PP*sign(mdotP)/(2*AP^2*rho_atm);
KTWT=fTWT*LTWT*PTWT*sign(mdotP)/(2*ATWT^2*rho_atm);

pCI=p_atm+rho_atm*g*hR;
pTWTX=p_atm+rho_atm*g*hTW;

Qt=mdotP/rho_atm; %turbine volumetric flow rate [m3/sec]
Qt_percent=Qt*100/Qrated; %turbine volumetric flow rate [% rated flow]
Qt_eq=Qt_percent*wm_design/wm; %equivalent turbine volumetric flow rate [%
rated flow] in design speed
Ht_eq=H_Turb(YGV,Qt_eq);       %equivalent turbine head [% design head] in
design speed
Ht=Ht_eq*(Hdesign/100)*(wm^2/wm_design^2); %turbine head [m] at wm
EFFt=Eff_Turb(YGV,Ht_eq); %Turbine efficiency [%]
Pt=rho_atm*g*(EFFt/100)*Ht*Qt; %Turbine power [Watt]

c1=AC/LC+AS/lS;
c2=AP/LP;
c3=LC\AC*pCI+lS\AS*p_atm...
    +rho_atm*g*(AC*sin(ThetaC)-AP*sin(ThetaP)+AS*sin(ThetaS))...
    -LC\KC*mdotC^2-lS\KS*(mdotP-mdotC)^2+LP\KP*mdotP^2;
c4=AP*LTWT/(ATWT*LP);
c5=rho_atm*g*(Ht-hDT)+pTWTX...
    +rho_atm*g*LTWT*(sin(ThetaTWT)+sin(ThetaP)*AP/ATWT)...
    +(KTWT-KP*LTWT/LP)*mdotP^2/ATWT;

pTWUO=(c3*c4+c1*c5+c2*c5)/(c1+c2+c1*c4);
pHWDO=(c3+c3*c4+c2*c5)/(c1+c2+c1*c4);

dlSdt=(AS*rho_atm)\(mdotC-mdotP);
dmdotCdt=LC\(-AC*(pHWDO-pCI)+rho_atm*g*LC*AC*sin(ThetaC)-KC*mdotC^2);
dmdotPdt=LP\(-AP*(pTWUO-pHWDO)+rho_atm*g*LP*AP*sin(ThetaP)-KP*mdotP^2);

dxdt=[dlSdt;dmdotCdt;dmdotPdt];
%%%%%%%%%%%%%%%%%%%%%%%%%%%%%%%%%%%%%%%%%%%%%%



function dxdt=ControllerOutputs(x,wm,YGV_ref)
%calculates time derivatives of transient droop controller

global PTURBINE;
wm_design=PTURBINE.wm_design;

global PCONTROLLER;
Tp=PCONTROLLER.Tp; %pilot servomotor time constant [sec]
Tg=PCONTROLLER.Tg;  %main servomotor integration time [sec]
Tr=PCONTROLLER.Tr;  %transient droop time constant [sec]
delta=PCONTROLLER.delta; %transient droop
droop=PCONTROLLER.droop; %droop [p.u.]
```

```
YGVMax=PCONTROLLER.YGVMax;   %Max guide vane opening [p.u.]
YGVMin=PCONTROLLER.YGVMin; %Min guide vane openning [p.u]
YGVdotMax=PCONTROLLER.YGVdotMax;   %Max guide vane opening rare [1/sec]
YGVdotMin=PCONTROLLER.YGVdotMin; %Max guide vane closing rate [1/sec]

%state variables;
YGV=x(1);   %guide vane openning
xr=x(2);    %transient droop state
u=x(3);     %pilot servomotor output

d=delta*YGV-xr;
e=droop*(YGV_ref-YGV)-(wm/wm_design-1)-d;


if (YGV<=YGVMin)&&(u<0)
    dYGVdt=0;
elseif (YGV>=YGVMax)&&(u>0)
    dYGVdt=0;
elseif (u/Tg)>=YGVdotMax
    dYGVdt=YGVdotMax;
elseif (u/Tg)<=-YGVdotMin
    dYGVdt=-YGVdotMin;
else
    dYGVdt=u/Tg;
end
dxrdt=Tr\d;
dudt=Tp\(e-u);

dxdt=[dYGVdt;dxrdt;dudt];
```

%%

```
function y=ActivePowerDemand(t)

%This function simulates a time varying active load which can be used as
%load disturbance.

ybase=100e6;
t1=2;
t2=2;
y1=0.8*ybase;
y2=0.5*ybase;
y3=0.8*ybase;

if t<500,
    y=y1;
elseif (t>=500)&&(t<=500+t1)
    y=y1+t1\(t-500)*(y2-y1);
elseif (t>=500+t1)&&(t<=1000)
    y=y2;
elseif (t>=1000)&&(t<=1000+t2)
    y=y2+t2\(t-1000)*(y3-y2);
```

```
else
    y=y3;
end
%%%%%%%%%%%%%%%%%%%%%%%%%%%%%%%%%%%%%%%%



function y=YGVREFERENCE(t)

if t<300
    y=0.6;
else
    y=0.4;
end



%%%%%%%%%%%%%%%%%%%%%%%%%%%%%%%%%%%%%%



function dxdt=ODEWaterway(t,x)

% This function calculates time derivatives for all of the states in
% waterway, controller and the swing.
% inputs are the time and the state vector x consisting of:
% YGV=x(1);   %guide vane openning
% xr=x(2);    %transient droop state
% u=x(3);     %pilot servomotor output
% wm=x(4);    %angular speed [rad/sec]
% lS=x(5);    %Length of water column in the surge shaft
% mdotC=x(6); %Mass flow rate of water in the conduit
% mdotHWDO=x(7); %Mass flow rate of water in the penstock interface at HW
% mdotTWUO=x(8); %Mass flow rate of water in the penstock interface at TW
% S=x(9:2*N+5);  %Penstock state vector

global PCONTROLLER PPENSTOCK;
LP=PPENSTOCK.LP;      %Penstock length [m]
N=PPENSTOCK.N;        %No of deltax length along the penstock
deltax=LP/N;

YGV=x(1);   %guide vane openning
wm=x(4);    %angular speed [rad/sec]
xHW=x(5:7);
mdotTWUO=x(8); %Mass flow rate of water in the penstock interface at TW
S=x(9:2*N+5);  %Penstock state vector
pHWDI=S(1);
pTWUI=S(N-1);
mdotHWI=xHW(3);
mdotTWI=mdotTWUO;

J=PCONTROLLER.J; %Generator rotor and turbine moment of inertia
% YGV_ref=PCONTROLLER.YGV_ref;
YGV_ref=YGVREFERENCE(t);
```

```
[dxHWdt,~]=HeadWaterOutputs(xHW,pHWDI,deltax);
[dmdotTWUOdt,~,~,~,Pt]=TailWaterOutputs(mdotTWUO,pTWUI,YGV,wm,deltax);
dSdt=penstock(S,mdotHWI,mdotTWI);

dxCONdt=ControllerOutputs(x(1:3),wm,YGV_ref);
dwmdt=(J*wm)\(Pt-ActivePowerDemand(t));

dxdt=[dxCONdt;dwmdt;dxHWdt;dmdotTWUOdt;dSdt];
```

%%%%%%%%%%%%%%%%%%%%%%%%%%%%%%%%%%%%%%

```
function [dxHWdt,pHWDO]=HeadWaterOutputs(xHW,pHWDI,deltax)
% This function calculates time derivative of the state vector (xHW) and
% pressure at the junction of the conduit,
% surge shaft and penstock interface/penstock (pHWDO).
% The inputs are:
% the state vector of the head water system (xHW)
% the pressure at downstream of the penstock interface/penstock (pHWDI)
% the length of the penstock interface (deltax)

%State variables:
lS=xHW(1);     %Length of water column in the surge shaft
mdotC=xHW(2); %Mass flow rate of water in the conduit
mdotHWDO=xHW(3); %Mass flow rate of water in the penstock interface/penstock

% parameters and constants:
global PHEADWATER CONSTANTS PPENSTOCKINTERFACE;

rho_atm=CONSTANTS.rho_atm;  %Water density at atmospheric pressure [Kg/m3]
g=CONSTANTS.g;              %gravity acceleration [m/sec2]
p_atm=CONSTANTS.p_atm;      %Atmospheric pressure [Pa]

hR=PHEADWATER.hR;            %Head water reservoir water level [m]
LC=PHEADWATER.LC;            %Conduit length [m]
AC=PHEADWATER.AC;            %Condit cross-section area [m2]
ThetaC=PHEADWATER.ThetaC;    %Conduit slope [degrees]
fC=PHEADWATER.fC;            %Fanning friction factor for the conduit
AS=PHEADWATER.AS;            %Surge shaft cross-section area [m2]
ThetaS=PHEADWATER.ThetaS;    %Surge shaft slope [degrees]
fS=PHEADWATER.fS;            %Fanning friction factor for the surge shaft

A2=PPENSTOCKINTERFACE.A2;          %Penstock cross-section area [m2]
ThetaP=PPENSTOCKINTERFACE.ThetaP; %Penstock slope [degrees]
fP=PPENSTOCKINTERFACE.fP;          %Fanning friction factor for the penstock

PC=2*sqrt(pi*AC);   %Perimeter of conduit (circular cross-section) [m]
PS=2*sqrt(pi*AS);   %Perimeter of surge shaft [m]
P2=2*sqrt(pi*A2);   %Perimeter of penstock [m]

KC=fC*LC*PC*sign(mdotC)/(2*AC^2*rho_atm);
```

```
KS=fS*lS*PS*sign(mdotHWDO-mdotC)/(2*AS^2*rho_atm)+1/(AS*rho_atm);
KHW=fP*deltax*P2*sign(mdotHWDO)/(2*A2^2*rho_atm);

pCI=p_atm+rho_atm*g*hR;
pHWDO=(AC/LC+A2/deltax+AS/lS)\((LC\AC*pCI+deltax\A2*pHWDI+lS\AS*p_atm)+...
rho_atm*g*(AC*sin(ThetaC)-A2*sin(ThetaP)+AS*sin(ThetaS))-...
LC\KC*mdotC^2-lS\KS*(mdotHWDO-mdotC)^2+deltax\KHW*mdotHWDO^2);

dlSdt=(AS*rho_atm)\(mdotC-mdotHWDO);
dmdotCdt=LC\(-AC*(pHWDO-pCI)+rho_atm*g*LC*AC*sin(ThetaC)-KC*mdotC^2);
dmdotHWDOdt=deltax\(-A2*(pHWDI-pHWDO)+rho_atm*g*deltax*A2*sin(ThetaP)...
            -KHW*mdotHWDO^2);
dxHWdt=[dlSdt;dmdotCdt;dmdotHWDOdt];
```

%%

```
function
[dmdotTWUOdt,pTWUO,Ht,EFFt,Pt]=TailWaterOutputs(mdotTWUO,pTWUI,YGV,wm,deltax)
% This function calculates pressure at the turbine inlet (pTWUO),
% turbine head, efficiency and power and time derivative of the state
% variable mdotTWUO . The inputs are:
% the state variable (mdotTWUO)
% the pressure at upstream of the penstock interface(pTWUI)
% the length of the penstock interface (deltax)
% turbine angular speed (wm)
% guide vane opening (YGV)

% parameters and constants:
global PTAILWATER CONSTANTS PPENSTOCKINTERFACE PTURBINE;

rho_atm=CONSTANTS.rho_atm;  %Water density at atmospheric pressure [Kg/m3]
g=CONSTANTS.g;              %gravity acceleration [m/sec2]
p_atm=CONSTANTS.p_atm;      %Atmospheric pressure [Pa]

hDT=PTAILWATER.hDT;            %Draft tube height [m]
LTWT=PTAILWATER.LTWT;          %Tail water tunnel length [m]
ATWT=PTAILWATER.ATWT;          %Tail water tunnel cross-section area [m2]
ThetaTWT=PTAILWATER.ThetaTWT;  %Tail water tunnel slope [degrees]
fTWT=PTAILWATER.fTWT;          %Fanning friction factor for Tail water tunnel
hTW=PTAILWATER.hTW;            %Tail water reservoir water level [m]

A2N=PPENSTOCKINTERFACE.A2N;          %Penstock cross-section area [m2]
ThetaP=PPENSTOCKINTERFACE.ThetaP; %Penstock slope [degrees]
fP=PPENSTOCKINTERFACE.fP;         %Fanning friction factor for the penstock

Qrated=PTURBINE.Qrated;              %Rated descharge [m3/sec]
Hdesign=PTURBINE.Hdesign;            %Design head [m]
wm_design=PTURBINE.wm_design; %Design angular speed

P2N=2*sqrt(pi*A2N);   %Perimeter of penstock [m]
PTWT=2*sqrt(pi*ATWT);   %Perimeter of tail water tunnel [m]

KTW=fP*deltax*P2N*sign(mdotTWUO)/(2*A2N^2*rho_atm);
```

```
KTWT=fTWT*LTWT*PTWT*sign(mdotTWUO)/(2*ATWT^2*rho_atm);

pTWTX=p_atm+rho_atm*g*hTW;

Qt=mdotTWUO/rho_atm; %turbine volumetric flow rate [m3/sec]
Qt_percent=Qt*100/Qrated; %turbine volumetric flow rate [% rated flow]
Qt_eq=Qt_percent*wm_design/wm; %equivalent turbine volumetric flow rate [%
rated flow] in design speed
Ht_eq=H_Turb(YGV,Qt_eq);       %equivalent turbine head [% design head] in
design speed
Ht=Ht_eq*(Hdesign/100)*(wm^2/wm_design^2); %turbine head [m] at wm
EFFt=Eff_Turb(YGV,Ht_eq); %Turbine efficiency [%]
Pt=rho_atm*g*(EFFt/100)*Ht*Qt; %Turbine power [Watt]

pTWUO=(1+LTWT*A2N/(deltax*ATWT))\(rho_atm*g*(Ht-hDT)...
      +pTWTX+pTWUI*LTWT*A2N/(deltax*ATWT)...
      +rho_atm*g*LTWT*(sin(ThetaTWT)+sin(ThetaP)*A2N/ATWT)...
      +(KTWT-KTW*LTWT/deltax)*mdotTWUO^2/ATWT);

dmdotTWUOdt=deltax\(-A2N*(pTWUO-pTWUI)+rho_atm*g*deltax*A2N*sin(ThetaP)...
            -KTW*mdotTWUO^2);
```

%%%%%%%%%%%%%%%%%%%%%%%%%%%%%%%%%%%

D. Simulation of inelastic waterway with generator connected to the infinite bus

```
%main program for simulation of inelastic model of the plant with
%transient droop controller and generator connected to an infinite bus


clc
% clear all
close all
Main_parameters %run to define parameters
TurbineData %run to generate turbine data

InitializeGenerator; %returns generator state-vector initial values
% and determines Vtr
%Generator state vector:
% XG0(1)=EEd_op;   %E'd
% XG0(2)=EEq_op;   %E'q
% XG0(3)=DELTA_op; %Electrical rotor angle
% XG0(4)=Ef_op;    %Ef
% XG0(5)=Vstabilizer_op;

%initial state vector for inelastic system:
% lS=x_ie(1);    %Length of water column in the surge shaft
% mdotC=x_ie(2); %Mass flow rate of water in the conduit
% mdotP=x_ie(3); %Mass flow rate of water in the penstock
% YGV=x_ie(4);   %guide vane openning
% xr=x_ie(5);    %transient droop state
```

```
% u=x_ie(6);     %pilot servomotor output
% wm=x_ie(7);    %angular speed [rad/sec]
x_ie0=[55;28000;28000;0.79;0;0;500*2*pi/60];

X0=[x_ie0;XG0];

tspan=[0 1000];
options=odeset('MaxOrder',5,'RelTol',1e-7,'AbsTol',1e-7);
[T_ie,X_ie] = ode15s(@ODEWaterwayInelastic,tspan,X0,options);

lT=length(T_ie);
X_ie2=zeros(lT,11);

for i=1:lT
    t=T_ie(i);
    xi=X_ie(i,1:3);
    xG=X_ie(i,8:12);
    Ygvi=X_ie(i,4);
    wmi=X_ie(i,7);
    YGVRefi=YGVREFERENCE(t);
    [~,pHWDOi,pTWUOi,Hti,EFFti,Pti]=WaterwayInelasticOutputs(xi,Ygvi,wmi);
    [Pe,Qe,Vt,It,~]=ODEGenerator(t,xG,wmi);
    X_ie2(i,:)=[pHWDOi pTWUOi Hti EFFti Pti 0 YGVRefi Pe Qe Vt It];
end

figure(1);grid on;plot(T_ie, sin(PHEADWATER.ThetaS)\X_ie(:,1));grid;
xlabel('Time [sec]');ylabel('Height [m]');
title('Water column height in the surge shaft');

figure(2);grid on;plot(T_ie, X_ie(:,2));grid;xlabel('Time [sec]');
ylabel('Flow rate [Kg/sec]');title('Water mass flow rate in the conduit');


figure(3);grid on;plot(T_ie, X_ie(:,3));grid;xlabel('Time [sec]');
ylabel('Flow rate [Kg/sec]');title('Water mass flow rate in the penstock');


figure(4);grid on;plot(T_ie, X_ie(:,4),'-b',T_ie, X_ie2(:,7),'-
r');grid;xlabel('Time [sec]');
ylabel('Guide vanes opening [p.u.]');title('Guide vanes opening');
legend('YGV','YGV_ref');

figure(5);grid on;plot(T_ie,
X_ie(:,7)*50/PTURBINE.wm_design);grid;xlabel('Time [sec]');
ylabel('Frequency [Hz]');title('Electric frequency');

figure(6);grid on;plot(T_ie, X_ie2(:,1));grid;
xlabel('Time [sec]');ylabel('Pressure [Pa]');
title('Pressure at the surge shaft junction');

figure(7);grid on;plot(T_ie, X_ie2(:,2));grid;
xlabel('Time [sec]');ylabel('Pressure [Pa]');
title('Pressure at the turbine inlet');
```

```
figure(8);grid on;plot(T_ie, X_ie2(:,3));grid;
xlabel('Time [sec]');ylabel('Head [m]');
title('Turbine head');

figure(9);grid on;plot(T_ie, X_ie2(:,4));grid;
xlabel('Time [sec]');ylabel('efficiency [%]');
title('Turbine efficiency');

figure(10);grid on;plot(T_ie, X_ie2(:,5),'- b',T_ie,X_ie2(:,8),'-.r');grid;
xlabel('Time [sec]');ylabel('Power [W]');
title('Generator active power vs Turbine power');
Legend('Turbine Power', 'Pe');

figure(11);grid on;plot(T_ie, X_ie(:,10)*180/pi);grid;xlabel('Time [sec]');
ylabel('delta electric [degree]');title('Rotor electric Angle');

figure(12);grid on;plot(T_ie, X_ie2(:,9));grid;xlabel('Time [sec]');
ylabel('Reactive Power [VAR]');title('Reactive Power');

figure(13);grid on;plot(T_ie, X_ie2(:,10));grid;xlabel('Time [sec]');
ylabel('Terminal RMS Voltage [V]');title('Terminal Voltage');
```

%%

```
% Main_parameters.m
% defines parameters for simulation of plant with inelastic
% models with transient droop controller and generator connected to the
% infinite bus

global CONSTANTS;
CONSTANTS=[];
CONSTANTS.rho_atm=1000; %Water density at atmospheric pressure [Kg/m3]
CONSTANTS.g=9.8;        %gravity acceleration [m/sec2]
CONSTANTS.p_atm=1e5;    %Atmospheric pressure [Pa]
CONSTANTS.beta=4.5e-10; %water compressibility

global PTURBINE; %Turbine parameters
PTURBINE=[];
PTURBINE.Qrated=36;             %Rated descharge [m3/sec]
PTURBINE.Hdesign=330;           %Design head [m]
PTURBINE.wm_design=500*2*pi/60; %Design angular speed

global PCONTROLLER; %Controller Parameters
PCONTROLLER=[];
PCONTROLLER.J=850000; %Generator rotor and turbine moment of inertia

% PCONTROLLER.YGV_ref=0.6; %Operating point openning for guide vane [p.u]

PCONTROLLER.Tp=0.04; %pilot servomotor time constant [sec]
PCONTROLLER.Tg=0.2;  %main servomotor integration time [sec]
PCONTROLLER.Tr=1.75;  %transient droop time constant [sec]
PCONTROLLER.delta=0.04; %transient droop
PCONTROLLER.droop=0.10; %droop [p.u.]
PCONTROLLER.YGVMax=1;   %Max guide vane opening [p.u.]
PCONTROLLER.YGVMin=0.3; %Min guide vane openning [p.u]
```

```
PCONTROLLER.YGVdotMax=0.05;   %Max guide vane opening rare [1/sec]
PCONTROLLER.YGVdotMin=0.2; %Max guide vane closing rate [1/sec]

global PHEADWATER; %Parameters for head water system
PHEADWATER=[];
PHEADWATER.hR=40;       %Head water reservoir water level [m]
PHEADWATER.LC=4500;     %Conduit length [m]
PHEADWATER.AC=25;       %Condit cross-section area [m2]
PHEADWATER.ThetaC=0.2*pi/180; %Conduit slope [radians]
PHEADWATER.fC=0.04;     %Fanning friction factor for the conduit
PHEADWATER.AS=10;       %Surge shaft cross-section area [m2]
PHEADWATER.ThetaS=60*pi/180;  %Surge shaft slope [radians]
PHEADWATER.fS=0.04;     %Fanning friction factor for the surge shaft

global PPENSTOCKINTERFACE %Penstock interface (head water and tail water)
parameters
PPENSTOCKINTERFACE=[];
PPENSTOCKINTERFACE.A2=7;       %Penstock cross-section area head water [m2]
PPENSTOCKINTERFACE.A2N=7;       %Penstock cross-section area tail water [m2]
PPENSTOCKINTERFACE.ThetaP=45*pi/180;  %Penstock slope [radians]
PPENSTOCKINTERFACE.fP=0.04;    %Fanning friction factor for the penstock

global PPENSTOCK; %Parameters for  penstock
PPENSTOCK=[];
PPENSTOCK.LP=400;      %Penstock length [m]
PPENSTOCK.AP=7;       %Penstock cross-section area [m2]
PPENSTOCK.ThetaP=45*pi/180;  %Penstock slope [radians]
PPENSTOCK.fP=0.04;     %Fanning friction factor for the penstock

% PPENSTOCK.N=50;        %No of deltax length along the penstock
PPENSTOCK.N=25;        %No of deltax length along the penstock

PPENSTOCK.beta_eq=2.04e-9; %penstock wall elasticity

global PTAILWATER; %Parameters for tail water system
PTAILWATER=[];
PTAILWATER.hDT=5;       %Draft tube height [m]
PTAILWATER.LTWT=300;    %Tail water tunnel length [m]
PTAILWATER.ATWT=25;     %Tail water tunnel cross-section area [m2]
PTAILWATER.ThetaTWT=0.5*pi/180;%Tail water tunnel slope [radians]
PTAILWATER.fTWT=0.04;    %Fanning friction factor for Tail water tunnel
PTAILWATER.hTW=10;       %Tail water reservoir water level [m]


global PGENERATOR PNETWORK;

PGENERATOR=[];
PGENERATOR.Ra=0.01; %Phase winding resistance [Ohms]
PGENERATOR.Re=0.1;      %Equivalent network resistance [Ohms]
PGENERATOR.xd=12;       %d_axis reactance [Ohms]
PGENERATOR.xq=12;      %q_axis reactance [Ohms]
PGENERATOR.xxd=1.7;    %d_axis transient reactance [Ohms]
PGENERATOR.xxq=1.7;    %q_axis transient reactance [Ohms]
PGENERATOR.xe=1.4;       %Equivalent network reactance [Ohms]
PGENERATOR.TTdo=6;     %d_axis transient open-circuit time constant [sec]
```

```
PGENERATOR.TTqo=0.1;  %q_axis transient open-circuit time constant [sec]
PGENERATOR.KE=400;      %Excitation system gain
PGENERATOR.Efmin=50000; %Min field voltage [V]
PGENERATOR.Efmax=50000;  %Max field voltage [V]
PGENERATOR.TE=0.05;     %Excitation system time constant [sec]
PGENERATOR.KF=0.025;    %Stablizer gain
PGENERATOR.TFE=1;       %Stablizer time constant [sec]
PGENERATOR.Vtr=0;     %Terminal Voltage Reference [V]  (Will be assigned
% value during initialization)
PGENERATOR.np=12;
PGENERATOR.Wm_op=100*pi/6;
PGENERATOR.M=170000;
PGENERATOR.D=0;

PNETWORK.Vs=15000;        %Network rms voltage [V]
```

%%%

```
%InitializeGenerator.m

P_op=80e6; %Active power drawn from generator at SS operating condition
Q_op=50e6;  %Reactive power drawn from generator at SS operating condition

PHI_op=atan(Q_op/P_op); %Power angle at steady_state [radian]

I_op=(3*PNETWORK.Vs)\sqrt(P_op^2+Q_op^2); %RMS current (per phase) of
generator

DELTA_op=atan((I_op*(PGENERATOR.xq+PGENERATOR.xe)*cos(PHI_op)-I_op*...
    (PGENERATOR.Ra+PGENERATOR.Re)*sin(PHI_op))/...
    (PNETWORK.Vs+I_op*(PGENERATOR.Ra+PGENERATOR.Re)*cos(PHI_op)+...
    I_op*(PGENERATOR.xq+PGENERATOR.xe)*sin(PHI_op)));

Id_op=-I_op*sin(DELTA_op+PHI_op);
Iq_op=I_op*cos(DELTA_op+PHI_op);

Ef_op=PNETWORK.Vs*cos(DELTA_op)+(PGENERATOR.Ra+PGENERATOR.Re)*Iq_op-...
    (PGENERATOR.xd+PGENERATOR.xe)*Id_op;

Vt_op=sqrt((PNETWORK.Vs+I_op*PGENERATOR.Re*cos(PHI_op)+...
    I_op*PGENERATOR.xe*sin(PHI_op))^2+...
    (I_op*PGENERATOR.xe*cos(PHI_op)-I_op*PGENERATOR.Re*sin(PHI_op))^2);

PGENERATOR.Vtr=PGENERATOR.KE\Ef_op+Vt_op;

Vstabilizer_op=0;

EEd_op=(PGENERATOR.xxd-PGENERATOR.xq)*Iq_op;

EEq_op=Ef_op+(PGENERATOR.xd-PGENERATOR.xxd)*Id_op;

XG0=zeros(5,1);
XG0(1)=EEd_op;
```

```
XG0(2)=EEq_op;
XG0(3)=DELTA_op;
XG0(4)=Ef_op;
XG0(5)=Vstabilizer_op;
```

%%%%%%%%%%%%%%%%%%%%%%%%%%%%%%%%%%%

```
function dxdt=ODEWaterwayInelastic(t,x)

% This function calculates time derivatives for all of the states in
% waterway, controller , the swing and generator.
% inputs are the time and the state vector x consisting of:
% lS=x(1);     %Length of water column in the surge shaft
% mdotC=x(2); %Mass flow rate of water in the conduit
% mdotP=x(3); %Mass flow rate of water in the penstock
% YGV=x(4);   %guide vane openning
% xr=x(5);     %transient droop state
% u=x(6);      %pilot servomotor output
% wm=x(7);     %angular speed [rad/sec]
%Generator state vector:
% x(8)=EEd_op;    %E'd
% x(9)=EEq_op;    %E'q
% x(10)=DELTA_op; %Electrical rotor angle
% x(11)=Ef_op;     %Ef
% x(12))=Vstabilizer_op;


global PCONTROLLER;

YGV=x(4);   %guide vane openning
wm=x(7);    %angular speed [rad/sec]
XG=x(8:12);

J=PCONTROLLER.J; %Generator rotor and turbine moment of inertia
% YGV_ref=PCONTROLLER.YGV_ref;
YGV_ref=YGVREFERENCE(t);


[dxWWdt,~,~,~,~,Pt]=WaterwayInelasticOutputs(x(1:3),YGV,wm);
dxCONdt=ControllerOutputs(x(4:6),wm,YGV_ref);

[Pe,~,~,~,dXGdt]=ODEGenerator(t,XG,wm);

dwmdt=(J*wm)\(Pt-Pe);

dxdt=[dxWWdt;dxCONdt;dwmdt;dXGdt];
```

%%%%%%%%%%%%%%%%%%%%%%%%%%%%%%%%%%%%%

```
function [Pe,Qe,Vt,It,dXdt]=ODEGenerator(t,X,W)

global PGENERATOR PNETWORK;
```

```
EEd=    X(1);
EEq=    X(2);
DELTA=  X(3);
Ef=     X(4);
Vstabilizer= X(5);

    Temp=[PGENERATOR.Ra+PGENERATOR.Re PGENERATOR.xxd+PGENERATOR.xe;-
PGENERATOR.xxd-PGENERATOR.xe PGENERATOR.Ra+PGENERATOR.Re];
    Idq=Temp\[EEd+PNETWORK.Vs*sin(DELTA);EEq-PNETWORK.Vs*cos(DELTA)];
    Id=Idq(1);Iq=Idq(2);
    Vt=sqrt((EEd-PGENERATOR.Ra*Id-PGENERATOR.xxd*Iq)^2+(EEq-
PGENERATOR.Ra*Iq+PGENERATOR.xxd*Id)^2);


It=sqrt(Id^2+Iq^2);

Pe=3*(EEd*Id+EEq*Iq);

Qe=sqrt(9*Vt^2*It^2-Pe^2);

dEEd=PGENERATOR.TTqo\(-EEd+(PGENERATOR.xxd-PGENERATOR.xq)*Iq);

dEEq=PGENERATOR.TTdo\(-EEq+(PGENERATOR.xd-PGENERATOR.xxd)*Id+Ef);

dDELTA=(W-PGENERATOR.Wm_op)*PGENERATOR.np/2;

dEf=PGENERATOR.TE\(-Ef+PGENERATOR.KE*(PGENERATOR.Vtr-Vt-Vstabilizer));
if ((Ef>=PGENERATOR.Efmax)&&(dEf>0))
    dEf=0;
elseif ((Ef<-PGENERATOR.Efmin)&&(dEf<0))
    dEf=0;
end

dVstabilizer=PGENERATOR.TFE\(-Vstabilizer+PGENERATOR.KF*dEf);

dXdt=[
dEEd;
dEEq;
dDELTA;
dEf;
dVstabilizer;
];
```

%%%%%%%%%%%%%%%%%%%%%%%%%%%%%%%%%

```
function y=YGVREFERENCE(t)

% y=.79;
if t<200
    y=0.79;
```

```
else
    y=0.4;
end
```